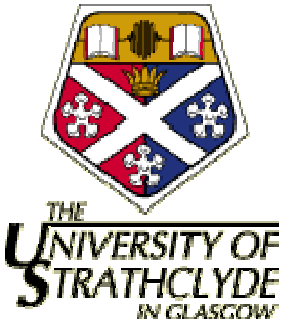

IN THE WAKE OF A MARINE CURRENT TURBINE

Thesis submitted in partial fulfilment of the requirement leading to the award of a Master of Science degree in Sustainable Engineering: Energy Systems and the Environment

By

Francis Akwensivie, BSc

Energy Systems Research Unit
Department of Mechanical Engineering
Faculty of Engineering
University of Strathclyde

ABSTRACT

Renewable energy sources, most notably, wind energy, solar energy and small scale hydro power schemes have undergone major development, however their intermittency and weather dependency poses a challenge. One other form of renewable energy which has attracted great interest in recent times is marine current or tidal stream energy. This energy resource has a great potential to be exploited on a large scale because of its predictability and intensity. It is most likely to be the new clean energy alternative for the 21st century.

The environmental impacts of marine current energy have been branded as benign even though no detailed Environmental Impact Assessment (EIA) studies have been conducted yet. This is crucial especially for those impacts that are unique to marine current developments most notably the influence of the energy extraction on coastal processes, tidal flows, seabed scouring and sediment transport.

This is what this project seeks to do. The flow around the turbine in a channel has been modelled. Investigations were carried out to determine the influence of the depth of deployment of the rotor blades and changing velocity of the currents on the flow downstream of the turbine.

The study has shown that locating the rotor blades closer to the free surface for the purposes of maximising output leads to a greater distortion of the velocity profile downstream. This may have a greater impact on adjacent ecosystems depending on the level of exploitation of the resource. There is also increased upwelling of the flow directly below the rotor blades resulting in scouring and increased turbidity levels. Locating the turbine blades about quarter depth (10 m in this case) below the free surface is most likely to result in minimal environmental impact downstream of the units.

ACKNOWLEDGEMENT

My appreciation goes to the innumerable people who contributed to the success of this project.

Dr Nick Kelly, you were a wealth of knowledge, support and direction. Thank you.

Dr Andy Grant, your advice during the initial stages of the project was great, thank you.

Dr Tom Scanlon, thank you for the tips on using FLUENT and for providing me with the tutorial materials.

Mrs Jennifer Dudgeon, I am grateful for the tips and review of the write up on the environmental impacts.

Dr Peter Fraenkel and Dr Jeremy Thakes of Marine Current Turbine Ltd, thank you for responding to my enquiries, I am grateful.

A big thank you also to Prof Joe Clark, Lecturers and other staff of the Department of Mechanical Engineering especially Mrs Janet Harbidge.

Lastly to my family, friends and countless others who lent their support in diverse ways when the going was tough. Thank you.

Francis Akwensivie

Table of Contents

Table of Figures

CHAPTER ONE - INTRODUCTION

1.0 Background

The world's population is estimated to double by the year 2050 and the world's energy demand is also estimated to increase by at least 70 % over the next 30 years (Jennings, 1996). These estimates may be inaccurate however, as society increases at an ever-accelerating rate, the need for energy also increases. Currently most of the world's energy demand is met by fossil fuels with their attended devastating effects on the environment, most notably the emission of carbon dioxide (CO_2) leading to climate change. According to the most authoritative body, the *International Panel on Climate Change* (IPCC), atmospheric concentrations of CO_2 resulting from burning of fossil fuels and deforestation have increased by more than one third in the past 150 years and are at the highest levels for at least the past 420,000 years (Singer 2003). Fossil fuels that took 200,000 years to be formed by geological processes are now being burned in one year. Efforts must therefore being made to meet present and future energy demands cleanly and efficiently. As a result renewable energy issues have become a top global agenda.

Renewable energy sources, most notably, wind energy, solar energy and small scale hydro power schemes have undergone major development. Their potential to meet the world's energy demand for the 21st century and beyond, cleanly, safely and economically is high. However the intermittency and weather dependency of most of them still poses a challenge and calls for extensive and diligent research and development effort. One other form of renewable energy which has attracted great interest is marine current or tidal stream energy. This energy resource has a great potential to be exploited on a large scale because of its predictability and intensity. It is most likely to be the new clean energy alternative for the 21st century.

1.2 Marine Current Resource

Marine currents or tidal streams are large movement of seawater driven mostly by the tides and magnified by underwater topography. A few completed resource assessment studies indicate that marine currents have the potential to supply a significant fraction of future electricity needs. The European Commission (EC) sponsored project "*The Exploitation of Tidal Marine Currents*" identified 106

European locations with strong marine currents. These sites if exploited were estimated to supply some 48 TWh of electricity per annum to the European grid. The DTI sponsored "*Tidal Stream Energy Review*" also assessed UK sites of which the eight largest may have an aggregate electrical energy output in the order of 62 TWh per annum (about 20 % of the UK's electricity needs). Indeed this resource is potentially enormous, however in most sea areas the velocities, and hence the energy densities, are too low for economic exploitation (Fraenkel 2004). Areas with favourable seabed topographies as well as straits resulting in fast currents are most desirable. It so happens that the UK and Scotland in particular is well endowed with such locations.

1.3 Marine Current Technology

The basic physical principles for extracting energy from marine currents are virtually identical to those of wind. Just as wind turbines, lift dependent devices have been found to be most efficient enough to be cost effective. Hence, there are three main lift-based mechanisms currently being promoted, evaluated and tested; the axial flow rotor which is favoured generally for wind turbines, the cross flow or Darrieus rotor and also devices which reciprocate across the current. Most of these devices are at the prototype stage. As with all new technologies there are bound to be challenges. Maintenance requirements in the hash marine environment are of paramount importance. Moreover issues like cavitation, turbulence levels, packing density needs attention. As prototypes are now being tested in the real marine environment enough knowledge and experience will be gathered to tackle these problems.

1.4 Environmental Impacts

Any system that results in the production of electricity needs to be assessed in its entirety to pinpoint any energy, environmental, social or economic implications. The environmental impacts of marine current energy have been branded as benign even though no detailed Environmental Impact Assessment (EIA) studies have been conducted yet. Past studies have identified likely impacts, however they need quantification to make informed judgments. This is crucial especially for those impacts that are unique to marine current developments most notably the influence of the energy extraction on coastal processes, tidal flows, seabed scouring and sediment

transport. Experience in other offshore installations especially offshore wind energy may prove vital with regards to impacts which are common to them like cabling, construction and noise.

1.5 Aims of this Project

The overall objective of this project is to support the development process of marine current energy by investigating the interaction between a marine current turbine and the marine environment. Specific objectives are to:

- Model a 3D channel and marine current turbine
- Model the wake behind the turbine
- Investigate effects on the flow around and downstream of the turbine by changing the depth of deployment of the rotor blades.
- Investigate the effect of changing velocity of the currents on the flow round and downstream of the turbine
- Investigate the environmental impact downstream of the turbine

1.6 Structure of the report

This report is made up of six chapters. A brief description of the content of each chapter is as follows:

Chapter one gives a background to marine current energy. The need to meet increasing energy demand cleanly and safely was highlighted. The marine current resource, the technology status and challenges as well as the need for environmental impact studies were briefly discussed resulting in the definition of objectives of this project.

Chapter two looks at more detailed explanation of the marine current resource dynamics and estimation making reference to past studies. The modes of operation of the technologies were then highlighted with particular reference to marine current turbines. Prototypes undergoing testing and refinement were also discussed, enumerating the engineering challenges facing most of them. This is followed by a summary of the environmental impacts of these developments and a discussion on

the importance of three physical factors of the marine environment which are likely to be affected. An overview of Computational Fluid Dynamics (CFD) followed by examples from the wind industry which may serve as a look-on concluded the chapter.

Chapter three is made of the theoretical concepts underlying the study. These include the theories of vertical velocity profiles in open channels, energy extraction and turbulence modelling. Emphasis was placed on the k-e turbulence model employed in FLUENT.

Chapter four enumerates the method employed in the study. A brief description of the modelling and simulation procedure using GAMBIT and FLUENT was provided. The inputs as well as assumptions made and a validation of the model using a simple analytical method have also been included.

Chapter five presents the results and discussion of the simulation. In this case results for three current velocities were presented. For each velocity three sets of results are presented; Resource, Turbine 1 and Turbine 2. For each the flow has been analysed in three views; plan, front and side.

Chapter six provides the conclusion and future work.

CHAPTER TWO - LITERATURE REVIEW

2.0 Introduction

Tidal currents are recognised as a resource to be exploited for the sustainable generation of electrical energy. As with all energy generation developments they have to be considered and analysed in entirety; energy, economics and environmental concerns. This chapter looks at the nature of the marine current resource and the technology required to exploit it. Prototypes which have been developed and undergoing testing have been highlighted as well as possible environmental impacts. Focus was placed on three physical factors of the aquatic environment which are likely to be affected. This is followed by an overview of an important analysis technique; Computational Fluid Dynamics (CFD) which is likely to play an important role in understanding the possible interaction of the device with each other and the marine environment and also inform the device design. Lastly examples of the use of this technique in the wind industry which may serve as a look-on have been discussed.

2.1 Marine Current Energy Resource

The operation of most renewable energy technologies are closely related to the nature of the resource. A basic understanding of the resource dynamics is therefore one of the first steps to be considered before exploiting it. This section seeks to address that as well as the resource distribution and estimates for energy production.

2.1.1 Resource Basics

The global marine current energy resource is mostly driven by the tides and to a lesser extent by thermal and density effects. The tides cause water to flow inwards twice each day (flood tide) and seawards twice each day (ebb tide) with a period of approximately 12 hours and 24 minutes (a semi-diurnal tide), or once both inwards and seawards in approximately 24 hours and 48 minutes (a diurnal tide). In most locations the tides are a combination of the semi-diurnal and diurnal effects, with the tide being named after the most dominant type.

Tides are generated by gravitational forces of the sun and moon on the ocean waters of the rotating earth. The proximity of the moon and sun relative to Earth has a

significant effect on the tides. The magnitude of the tide-generating force is about 68% moon and 32% sun due to their respective masses and distance from Earth (Open University, 1989). The sun's and moon's gravitational forces create two "bulges" in the earth's ocean waters: one directly under or closest to the moon and other on the opposite side of the earth. These "bulges" are the two tides a day observed in many places in the world. Unfortunately, this simple concept is complicated by the fact that the earth's axis is tilted at 23.5 degrees to the moon's orbit; the two bulges in the ocean are not equal unless the moon is over the equator. This difference in tidal height between the two daily tides is called the diurnal inequality or declinational tides and they repeat on a 14 day cycle as the moon rotates around the earth.

Where the semi-diurnal tide is dominant, the largest marine currents occur at new moon and full moon (spring tides), which is when the sun and moon's gravitational pull is aligned as shown in *Figure2.1*.The lowest, occurs at the first and third quarters of the moon (neap tides), where the sun and moon's gravitational pull are 90 degrees out of phase.

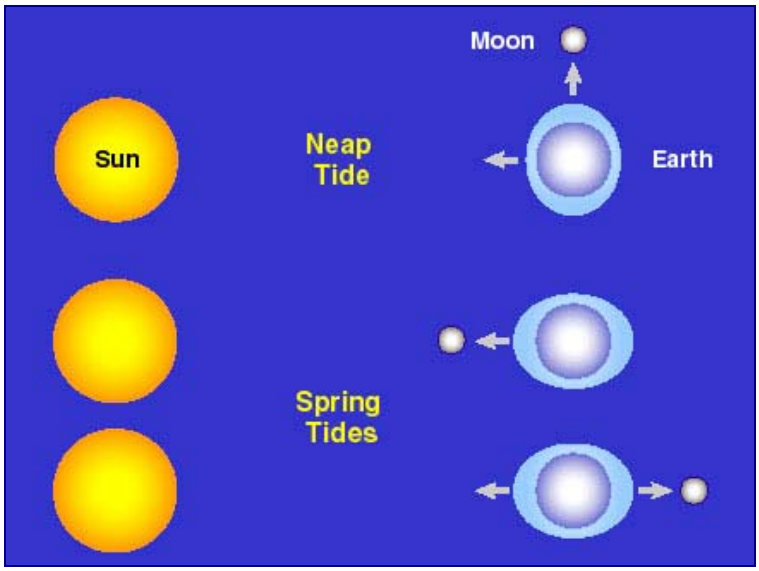

Figure 2.1 Spring and neap tides

With diurnal tides, the current strength varies with the declination. The largest currents occur at the extreme declination of the moon and lowest currents at zero declination. Therefore differences in currents occur due to changes between the

distances of the moon and sun from Earth, their relative positions with reference to Earth and varying angles of declination. These occur with a periodicity of two weeks, one month, one year or longer, and are entirely predictable. This means that the strength of the marine currents generated by the tide varies, depending on the position of the site on the earth. Other factors such as the shape of the coastline and the bathymetry (shape of the sea bed) also affect the strength of marine currents. Along straight coastlines and in the middle of deep oceans, the tidal range and marine currents are typically low. Another factor that impacts the magnitude of marine currents is the presence of narrow passages or straits between islands and around headlands. These passages result in a narrowing and concentration of tidal flow. However the flow through a passage is constrained by the loss of energy due to friction. Entrances to lochs, bays and large harbours often also have high marine current flows (Fraenkel 2004).

Generally, but not always, the strength of the currents is directly related to the tidal height of the location. It is worth noting that large marine currents do not necessarily require a large tidal range or height. In land-locked seas such as the Mediterranean, where the tidal range is small, some sizeable marine currents exist (BC Hydro, 2002). Some of the largest tidal flows in the world occur between the islands on the east side of the Philippines where the tidal range is small. The tide is high in the Pacific at the same time that the tide is low within the Philippine Islands. The result is very large tidal currents.

Generally the marine current resource follows an approximate sinusoidal pattern with the largest currents generated during the mid-tide. The flood tide often has slightly larger currents than the ebb tide. The flood and ebb flows are generally 180 degrees out of face with no flow at the turn of the tide (slack tide). However there are some locations where the water flows continuously in one direction only, the strength being largely independent of the moon's phase. These currents are dependent on large thermal movements and run generally from the equator to cooler areas. A not too far fetching example is the Gulf Stream, which moves approximately 80 million cubic metres of water per second (BC Hydro, 2002). Another example is the Strait of Gibraltar where in the upper layer, a constant flow of water passes into the

Mediterranean basin from the Atlantic and a constant outflow in the lower layer. (BC Hydro. 2002)

2.1.2 Resource Estimates

There are many sites world-wide with velocities of 2.5 m/s and greater. Countries with an exceptionally high resource include the UK, Ireland, Philippines, Japan and parts of the United States. Few studies have been carried out to determine the total global marine current resource, although it is estimated to exceed 450 GW (Blue Energy, 2000). The EC sponsored project "*The Exploitation of Tidal Marine Currents*" analysed 106 locations in European waters with certain pre-defined characteristics to make them suitable for energy exploitation, and the aggregate capacity of this selection of sites amounted to 12,000 MW installed capacity, capable of yielding some 48 TWh of electrical energy per annum.

Source: MEG report 2004

Figure 2.2 Leading potential UK tidal sites

Indeed this resource is potentially enormous, however in most sea areas the velocities, and hence the energy densities, are too low for economic exploitation (Fraenkel 2004). Areas with favourable seabed topographies as well as straits resulting in fast currents are most desirable. It so happens that the UK and Scotland in particular is well endowed with such locations. *Figure 2.2* shows the UK tidal sites with the greatest potential. Scotland's significant resources are clustered around the Pentland Firth, Orkney, Shetland and the western coast of mainland Scotland. According to the DTI sponsored "*Tidal Stream Energy Review*" the eight largest of these sites if fully developed may have an aggregate energy capacity in the order of 62 TWh of electricity per year (about 20 % of the UK's energy needs).

It is worth noting these studies used approximate methods to arrive at their results on the basis of sparse and barely adequate data. However, if they are not accurate in their predictions, they at least indicate a huge potential resource. The hash marine environment with strong currents is partly to blame for the inadequate data. Newly developed technologies such as the Acoustic Doppler Current Profiler (ADCP) will provide accurate data leading to rapid improvement of the knowledge and understanding of this resource. For instance a boat mounted ADCP can gather more accurate and detailed velocity profiles in a few hours compared to mechanical flow meters which will take months. Computer-based flow modelling also offers a valuable relatively new tool for identifying promising sites and rapidly assessing their energy potential.

2.2 Marine Current Energy Extraction Technologies

The oldest technology to harness tidal power for the generation of electricity involves building a dam, known as a barrage across a bay or estuary that has large differences in elevation between high and low tides. Water retained behind the dam at high tides generates a power head sufficient to generate electricity as the tide ebbs and water released from within the dams turns conventional turbines. See Crumpton (2004) for a more detailed description of the mode of operation.

The first commercial scale tidal generating barrage rated at 250 MW was built in La Rance, France in 1960.This plant continues to operate today just as another smaller

plant constructed in 1984 in Nova Scotia, Canada rated at 20 MW. These first-generation tidal power plants have all withstood the hash marine environment and been in continuous emission-free operation for many years. But due to the very high capital and environmental problems from accumulation of silt within the catchments area of the dam (which requires regular, expensive dredging), barrage-style tidal power is no longer feasible for energy generation, instead they have developed two new concepts.

The first and most favoured and advanced, adapted from the wind energy industry can be considered as an underwater turbine. It can be subdivided into Horizontal and Vertical axis models, depending on the orientation of the rotating shaft that turns a gearbox on one end and linked to slow-moving rotor blades on the other. The second, adapted from the oil industry, is a system of oscillating hydroplanes linked to a hydraulic motor and generator arrangement. Currently these concepts are undergoing prototype testing and refinement prior to commercialisation. Other interesting variants of these concepts, particularly the horizontal axis configuration, are also emerging. Most of them are in the experimental stages. More focus is therefore placed on the horizontal axis concept in the discussion that follows.

2.2.1 Mode of Operation

Underwater Turbines use similar principles, as wind turbines, to harness the kinetic energy in moving water. Basically three steps are involved in the energy transformation as in *Figure 2.3*:

The turbine rotor is driven by the current. This converts the energy of the current into rotational energy of the shaft. The power is optimised by adjusting the angle between the rotor blades and the current vector (pitch control).

The gearbox converts the low rotational speed of the turbine shaft to the desired higher speed of the generator shaft.

The generator converts its shaft energy to electric energy which is transmitted to the shore via a cable on the sea bed.

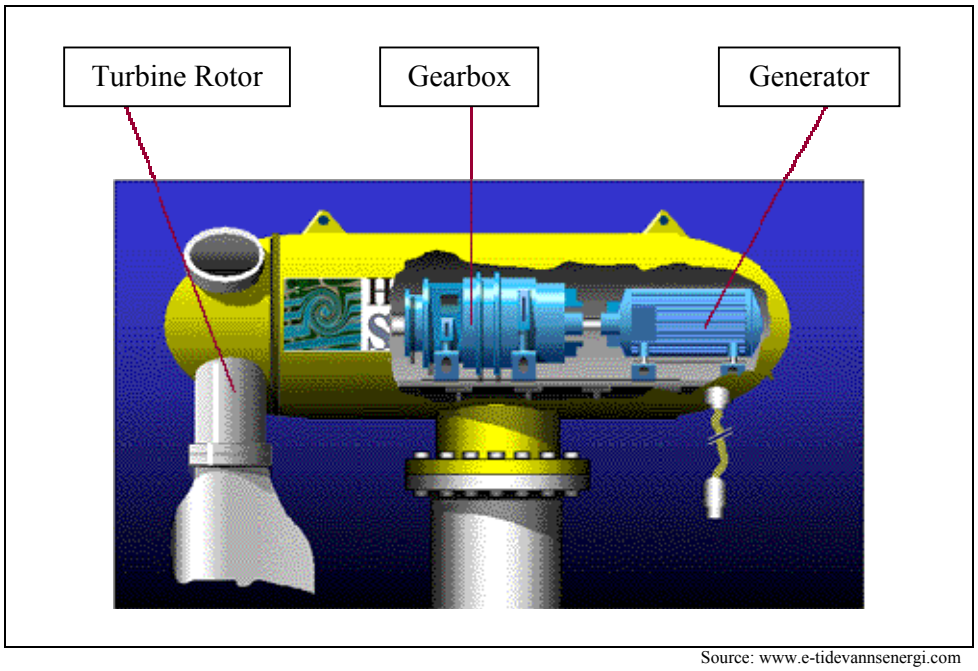

Source: www.e-tidevannsenergi.com

Figure 2.3 Principal components of a horizontal axis marine current turbine

2.2.2 Support Structure Concepts

A key requirement for the turbines is to hold them reliably in place taking into consideration the harsh marine environment. Currently there are three options, as shown in *Figure 2.4*, under consideration.

Gravity Structures are substantial steel or concrete mass attached to the base of the units to achieve stability by their own inertia.

Piled Structures are pinned to the seabed by one or more steel or concrete beams. The beams or piles are fixed to the seabed by hammering if the ground conditions are sufficiently soft or by pre-drilling, positioning and grouting if the rock is harder (EU-JOULE II). The simplest form of piled structures is a single pile penetrating the seabed with the turbine fixed to the pile at the desired depth of deployment. The pile may stick out on the water surface or below.

Floating Structures provide a more credible solution for deep water locations. In this case the turbine unit is attached to a downward pointing vertical beam rigidly fixed to a barge. The barge is then moored to the seabed by chains or wire or synthetic

ropes which may be fixed to the seabed by drag, piled or gravity anchors, depending on the seabed condition.

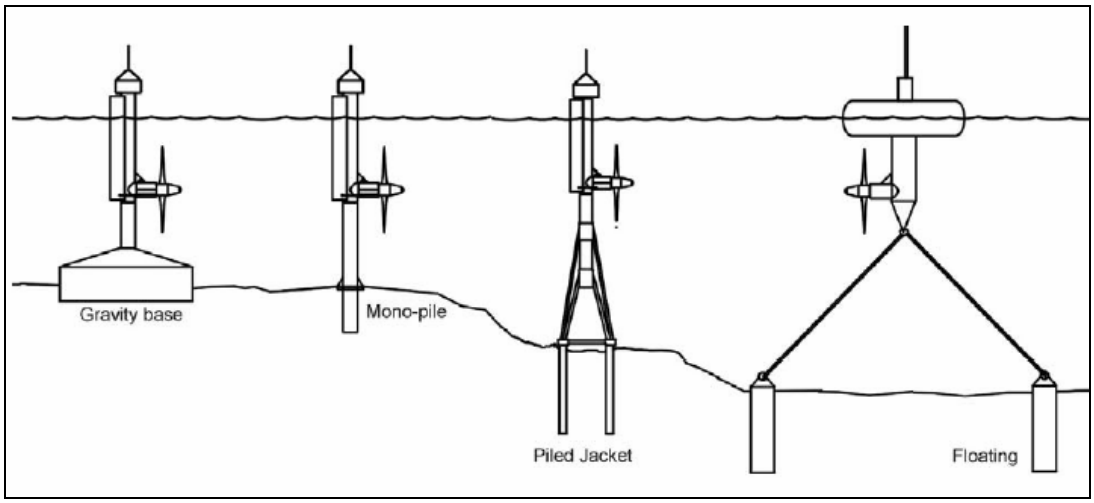

Figure 2.4 Support structure concepts

Monopile installation is an already established technique and seems to be the most favoured option. However this is currently limited to depths less than 50 m considering the capabilities of available jack-up barges (Fraenkel, 2004).

2.2.3 Prototypes

In general technology development in the marine current energy sector has been slow worldwide. The high costs coupled with the hash nature of the marine environment have been the main reasons. For instance in 1993 the then UK Department of Energy (DEn), decided not to support any proposals for funding marine current energy schemes from the UK Renewable Energy Programme (Fraenkel 2004). This was based on the findings of a review of the opportunities for obtaining energy from marine currents around the UK which concluded that although the UK resource is large, the unit costs of extracting such energy would be relatively high. The project was administered by ETSU on behalf of DEn and carried out by Engineering & Power Development Consultants Ltd, with support from Sir Robert McAlpine & Sons Ltd, Binnie & Partners and IT Power Ltd. Recent advances in offshore installations and innovation have translated into real prototypes or field trial models. However, these technologies are not expected to come into full commercialisation for several years, most likely post 2010 (Creswell 2004). The focus now is to prove

that the technologies can be made to work reliably. Below are the most promising ones. It is worth noting that most of these technologies are being developed as commercial ventures and therefore there is some reluctance to release information for fear of competitive advantage.

2.2.3.1 Seaflow

The first "full-size" marine current turbine known as "Seaflow" was installed during May 2003 on the North Devon Coast, UK. It was built by an industrial consortium consisting of Marine Current Turbines Ltd. (owners of the IPR), IT Power Ltd. (consultants), Bendalls Engineering (part of Carrs Milling plc, and steel fabrication specialists) and Corus (major national metal supplier) in the UK together with German organisations ISET – Institut fur Solare Energieversorgungstechnik (specialists in fluid dynamics and electrical power and control systems) and Jahnell Kestermann GmbH (manufacturer of wind turbine and marine gearboxes). The UK Department of Trade and Industry, the European Commission and German government provided financial support.

The technology consists of a two-bladed rotor mounted on a steel pile (tubular steel column) set into a socket drilled in the seabed. The rotor is made from composite materials and is 11 m in diameter with full span pitch control thereby making it capable of generating power for both directions of flow. However, it is currently operating in one direction of flow and a dump load is being used instead of grid connection due to economic reasons. The power train consists of an epicyclic gearbox and an induction generator. These form an integral, sealed, watertight unit. The system operates at variable speed and the control system and power conditioning, together with the dump load ballast are located in the housing above the pile, which also carries the statutory navigation lights and a fog horn. A key feature of this technology is that the rotor and drive train (i.e. gearbox and generator) can be raised completely above the surface as shown in *Figure 2.5*. In this position maintenance or repair procedures can be readily carried out.

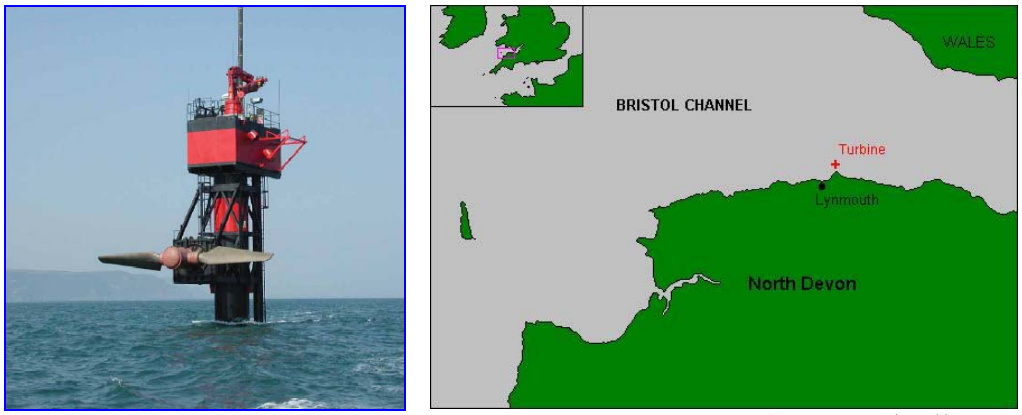

Source: www.marineturbines.com

Figure 2.5 Seaflow in position for maintenance and location in Bristol Channel, UK

The prototype experimental unit, installed between the channel between Foreland Ledge and Foreland Point on the North Devon coast, 3 km to the North-East of Lynmouth, UK, is rated at a power output of 300 kW in a current speed of 2.7 m/s. The choice of Foreland Point was made due to favourable tidal stream speeds and characteristics as well as suitable seabed geology. According to Coastal Research, an independent consultancy in marine environmental science, this location has tidal streams in excess of 2.5 m/s during spring tides.

2.2.3.2 Tidal Stream Turbine

Hammerfest Strøm AS, a Norwegian company, in collaboration with *ABB*, *Rolls Royce* and *Sintef* as well as *Statoil* developed the first grid connected marine turbine. The 300 kW turbine was installed on 17 September, 2003 in the Kval Sound (north coast of Norway). The prototype is expected to supply 700 MWhr per year, corresponding to electricity consumption by 35 Norwegian homes[1]. The submerged structure weighs 120 tonnes and is gravity mounted with gravity footings of 200 tonnes. Its three-bladed turbine have been made in glassfibre-reinforced plastic and measure 10 metres from hub to tip. By rotating the blades around their own axis by 180 degrees at slack water, the machine is ready for the reversing current keeping.

[1] www.e-tidevannsenergi.com

Source: www.e-tidevannsenergi.com

Figure 2.6 Deployment of the first grid connected tidal turbine in Kval Sound, Norway

The average current velocity at this location is 1.8 m/s. The strait has a width of 400 m at its narrowest cross section and a maximum depth of 50 m allowing a sailing depth of 19 m.

2.2.3.3 Tidal Fence (Davis Hydro Turbine)

Blue Energy has over two decades developed a floating vertical axis turbine known as Davis Hydro Turbine. It is technically very similar to straight blade vertical axis wind turbine.

The turbine is mounted in a durable concrete marine caisson which anchors the unit to the ocean floor, directs the water flow through the turbine and supports the coupler, gearbox, and generator above. The four fixed unidirectional hydrofoil blades employ the hydrodynamic lift principle. Prototypes ranging form 4 kW to 100 kW have been tested mostly in rivers. For large-scale power production, multiple Davis Hydro Turbines are to be linked in series to form a tidal fence across an ocean passage, estuary or inlet. Referred to as the Blue Energy Power System, these structures can be made many kilometres long, and may operate in depths up to 70 meters.

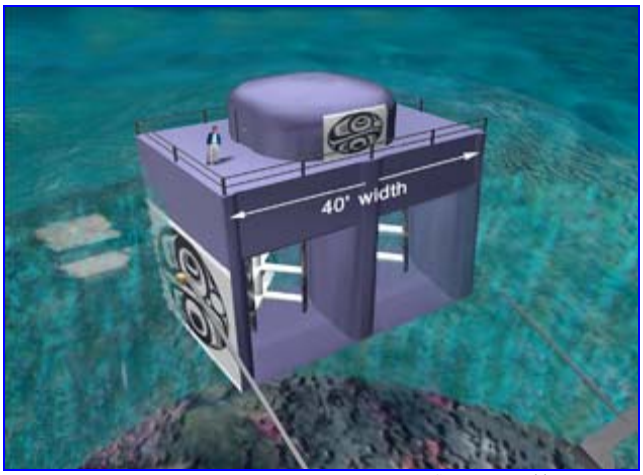

Source: www.bluenergy.com

Figure 2.7 Computer rendering of the twin (2 x 250 kW) floating units

Blue Energy is currently pursuing the development of a 500kW pre-commercial demonstration project off the coast of British Columbia, Canada. The project is comprised of two floating 250kW units as shown in *Figure 2.7*. The unit will be viable in ocean currents of 1.75 m/s. The Company has also proposed the development of a four-kilometer long tidal fence between the islands of Samar and Dalupiri in the San Bernardino Strait in the Philippines.

2.2.3.4 The Stingray Tidal Stream Generator

The stingray generator transforms the kinetic energy of moving water into hydraulic power, which turns an electrical generator by means of a hydraulic motor. It consists of a parallel linkage holding a stack of large hydroplanes. The hydroplanes have their attack angle relative to the approaching water stream varied by a simple mechanism. The combination of lift and drag force causes the arm to oscillate vertically. A hydraulic cylinder attached to the main arm is forced to alternately extend and retract, producing high-pressure oil, which is delivered to the hydraulic motor driving the generator, thus producing electricity. The whole structure is fully submerged and is fixed rigidly onto the sea bed. This concept was produced by *Engineering Business Limited* with support from the *DTI*.

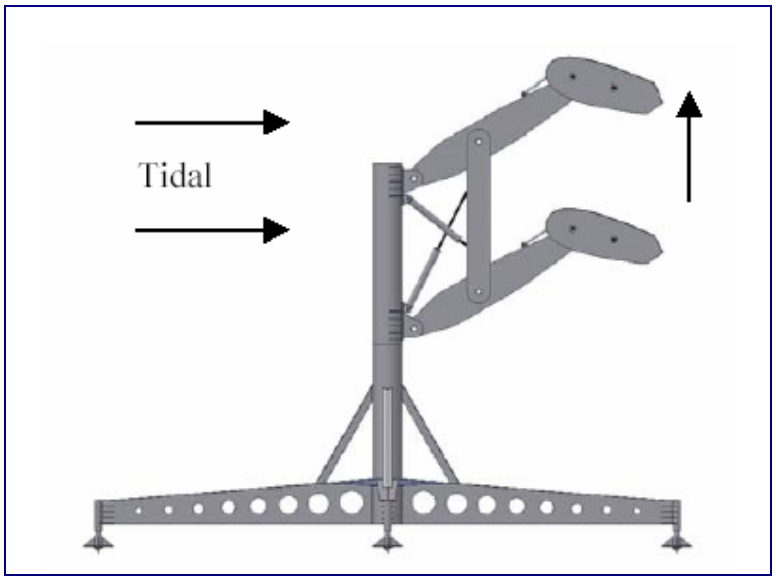

Figure 2.8 Principle of operation of the Stingray Generator

On Friday September 13th 2002, a 150 kW prototype was successfully deployed for the first time in Yell Sound, Shetland Island. Very simple power cycles were completed in a range of tide speeds and significant power output were said to be was observed. The testing continued in September with data being gathered, prior to recovery and decommissioning. According to Engineering Business[2] initial power cycles completed with 'manual' control of the hydroplane angle produced a peak hydraulic power of 250kW and a time averaged electrical power output of 90kW in a 1.5 m/s measured current.

Source: www.engb.com

Figure 2.9 Deployment of Stingray in Yell Sound, Scotland

[2] www.engb.com

2.2.4 Emerging Technologies

There are a couple of additional concept variants currently in development. Some of them are worth noting as they may emerge as strong options for future.

2.2.4.1 TidEI Tidal Stream Generator

The TidEI concept, under development by *SMD Hydrovision*, a subsea equipment manufacturer, is a pair of contra-rotating turbines, mounted together on a single crossbeam. The complete assembly is buoyant and tethered to the seabed by a series of mooring chains. The mooring system allows the turbines to align themselves in the direction of the tide automatically, i.e. following the tide backwards and forwards as it changes direction. During slack water, the turbines float in a vertical position. This position also allows for easy access for maintenance and repair works. The turbine blades are fixed pitch and variable speed operated.

Source: www.smdhydrovision.com

Figure 2.10 1/10th scale TidEI tidal stream generator

A commercial size, 1000 kW (2 x 500 kW), prototype with 15 m diameter is at the development stage for offshore testing to be carried out in 2005 and 2006. It is likely to be tested in an offshore environment with peak tidal speed of 2.5 m/s or more and a water depth of 30 m. This will help to prove its viability and numerous perceived advantages. Meanwhile a 1:10 scale system (Figure 2.10), partly funded by DTI, has undergone a seven week trial program at the New and Renewable Energy Centre (NaREC) in Blyth.

2.2.4.2 Lunar system

This technology being developed by *Lunar Energy* features a ducted turbine, fixed to the seabed by a gravity foundation. The blades are bi-directional rather than variable-pitch, and there is no yaw mechanism as the venturi-effect of the ducting is said to help maximise the energy from the water flow, even when flow is not parallel to the turbine axis. This reduction in complexity allows for improved reliability. Moreover it is likely to be deployed in deep waters without impacting shipping traffic. A 1/20th model was tested in April 2004 in the Department of Naval Architecture and Marine Engineering test tank, University of Strathclyde. A 1MW prototype is expected soon, with commercial launch following.

2.2.5 Technology Challenges

As with all new technologies challenges are bound to be faced. This section looks at some of the most pressing ones. As prototypes are being tested and the technology matures most of them, if not all, are bound to be addressed. Though some of them may be unique to certain technologies, most of them are common to most if not all the technologies under development.

***Installation, Foundation and Moorings*:** The installation of marine current machines will present their own unique difficulties. Constructing foundations and installation during water movement will be challenging. Only a few minutes of slack water can be expected each day. Scouring around the base of temporary support structures, such as jack-up barges, can be significant even over very short periods. The construction of bridges in tidal stream areas (such as the Severn bridges in the UK) has been successful and similar construction techniques may be applicable to marine current devices. Most devices will have similar installation, foundation and mooring problems and so there is scope for generic research in this area.

***Maintenance Requirements*:** It is important to have access to the unit for maintenance. Two concepts have been proposed. The first is a hoist system based on a hydraulic unit, similar to the system used to raise marine platform legs. The other is a semi-submersible system which allows the rotor and power train to float on the water surface for access.

The size and shape of the assembly is likely to make removal and replacement a difficult operation requiring calm sea conditions which may be hard to find. For economic reasons it may be necessary to design the turbines such that it only requires minimum level of maintenance.

***Cavitation*:** Relatively high velocities at the tips of the rotor blades are likely to lead to formation of cavities which may be difficult to avoid at all points along the blade. Eventhough design to avoid cavitation in hydraulic pumps and propellers is well understood a different approach may be necessary for marine current turbines because of its larger plane or rotor area (EU-JOULE II). Cavitation is also sensitive to water depth and so some cavitation problems can be avoided by placing units in deeper water at potential cavitation sites. Research is therefore required to understand the problems of cavitation and whether informed choices of blade profiles and materials can be made to avoid cavitation efficiency loss and damage problems.

***Packing Density*:** A good understanding of how many devices and of what size cause a significant effect on the marine environment and flow pattern can be used to suggest design guidelines for the sizing and placing of schemes. Some of the factors to be taken into consideration include seabed structure and depth, flow pattern and available area. This will help developers find suitable sites, and planners to understand the implications of these farms.

***Turbulence*:** The velocity of the flow at a given location can vary greatly across the actuator area. This could lead to significant variations in loading across the actuator and associated fatigue and vibration problems. Understanding the turbulence levels is important not only to the sitting of individual units (e.g. avoiding areas with strongly stratified flow) but can also inform the device design. The turbulent structure of the flow field is another important design driver affecting the design of components to resist fatigue. Design codes for marine current devices may therefore refer to the likely design turbulence levels. Understanding what these levels will be is important to setting realistic limits to design. Prototype testing will play a major role in determining the importance of these issues. Turbulence measurements should also

form part of resource assessments so that such measurements are taken at many sites and representative values obtained (Fraenkel 2004).

***Biofouling*:** Many devices installed in the sea become artificial reefs, attracting a wide variety of marine organisms (EU-JOULE II). These cover the structures and can cause significant fouling. Fouling of moving parts could affect the performance of devices (Bahaj and Myers 2003). Several methods for preventing fouling have been proposed. These include the use of antifouling paints and sonic and ultra sonic systems. Both methods have their challenges and drawbacks calling for further research.

2.3 Environmental Impacts of Marine Current Development

Renewable energy by it nature is taught to be environmentally benign. This is not true since most, if not all of the renewable energy resources developed have some adverse impact on the environment to some degree. Currently no detailed Environmental Impact Assessment (EIA) has been carried out on any marine current device. However a few studies (DTI 2001[3], 2002[4]) have identified the possible and likely environmental impacts. These impacts can be grouped into two main categories namely:

(i) Effects common to other construction projects (e.g. offshore wind)

- Visual impact
- Noise and construction
- Installation of cables
- Onshore power lines and substations
- Land access for construction and maintenance
- Pollution (e.g. oil spillage)

[3] *Commercial prospects of tidal stream power* (2001), Binnie Black and Veatch, IT Power, Published by ETSU for DTI (T/02/00209/REP)
[4] *A scoping study for an environmental impact field programme in tidal energy,* (2002) Centre for Environmental Engineering and Sustainable Energy, RGU, Published by ETSU for DTI (T/04/00213/REP)

(ii) Effects unique to marine current power schemes

- Physical Impacts- The influence of tidal energy extraction on coastal processes, tidal flows, seabed scouring and sediment transport
- Ecological Impacts- Possible interaction between moving submerged rotor blades and marine creatures
- Antifouling- The need to have moving parts within the seawater environment is likely to lead to a need for regular maintenance action or the use of antifouling paints

EIA experience in coastal and marine installations (e.g. oil and offshore wind) with regards to the first group of effects can prove vital. The latter, which is unique to marine current power installations, is therefore the outstanding issue requiring urgent attention. The purpose of this section is therefore to overview the four main physical characteristics (salinity, temperature, sediment transport and turbidity) of the marine environment which are likely to be affected and their importance.

2.3.1 The Marine Environment

Many benefits of aquatic ecosystems can only be maintained if the ecosystems are protected from degradation. Aquatic ecosystems comprise a body of water, biological community (animals, plants and micro-organisms), and the physical and chemical characteristics and climatic regime with which they interact. It is predominantly the physical characteristics (e.g. temperature, salinity, light, flow) and chemical characteristics (e.g. organic and inorganic carbon, oxygen, nutrients) of an ecosystem that determine what lives and breeds in it, and therefore the structure of the food web.

Economic exploitation of marine current energy is likely to be in areas of high current speeds, typically with peak speeds at spring tides of 2 to 3 m/s or more (Fraenkel 2004). These areas include narrow straits, between islands and around headlands. By reversing four times a day tidal currents cause the mixing of waters of different salinity, temperature and nutrients. They also cause eddies that separate bodies of water and they help distribute phyto- and zooplankton. Eventough fishes are known to avoid these high current areas (ref), they influence marine life in other

areas. For example the strength of the currents determines the salinity distribution in estuaries and river mouths where the diversity of the biological community can not be overemphasised. The discussion of the physical characteristics therefore makes reference to adjacent water bodies and in particular estuaries.

2.3.3 Salinity

Salinity is a measure of the salt content of water. The principal elements that contribute to the ocean's salinity are chlorine (55 %) and sodium (31 %), which combine to produce table salt. Salinity levels fluctuate with the penetration of tidal flows, and with mixing of fresh water and marine water by wind and currents. In estuaries overall salinity levels decline in the spring when snowmelt and rain produce elevated freshwater discharges from streams and groundwater. Salinity levels therefore grade from fresh (< 1 ppt) to almost oceanic (> 30 ppt), as freshwater entering from rivers and streams gradually mixes with seawater. Seawater has a global average salinity of 35 kg/m^3 or 35 ppt (parts per thousand).

2.3.3.1 Salinity Profiles

Generally salinity levels in the ocean tend to vary vertically (high saline water is denser than low saline water) but due to the penetration of tidal currents in estuaries horizontal variation is common there. The degree of vertical and horizontal variation depends on the strength of the marine current. Moreover the distance up to which the tidal effect is felt depends on amongst others, the slope of the channel, the tidal range, the volume of fresh water discharge and the configuration of the river. This leads to three different salinity regimes as in *Figure 2.11*.

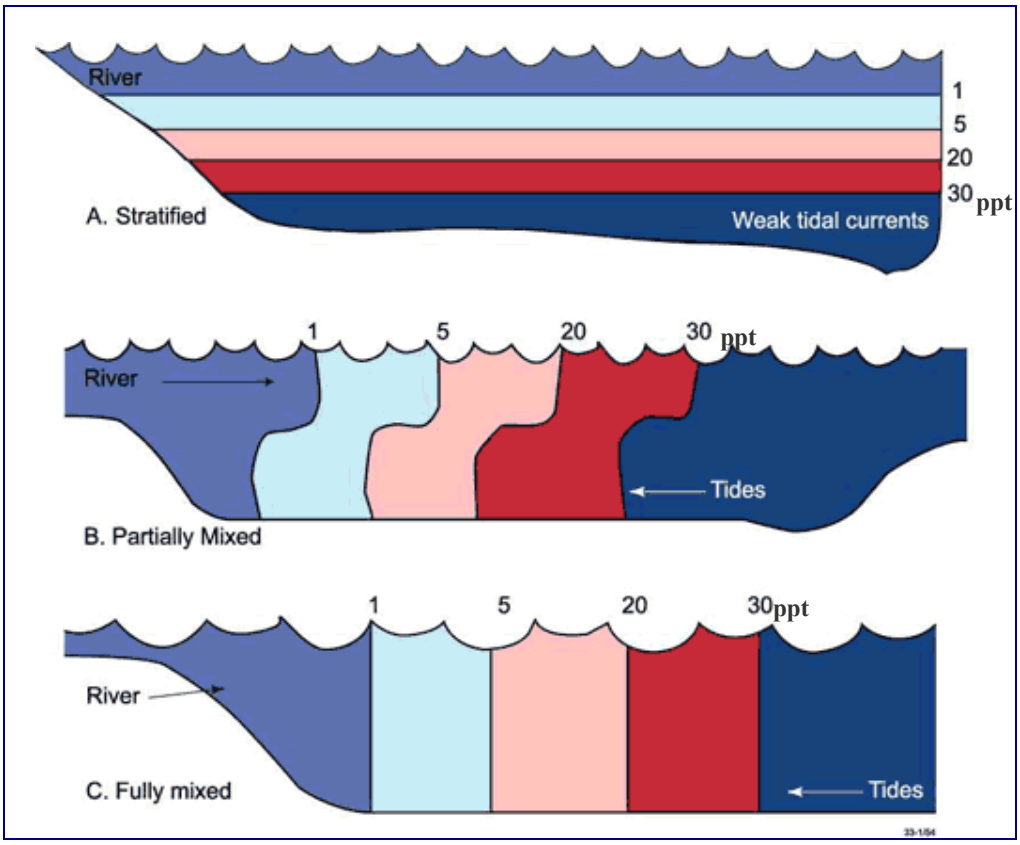

Figure 2.11 Salinity regimes (unit is ppt)

Stratified Conditions is characterised by a distinct increase in salinity with water depth. It occurs when river flow is sufficient to produce a plume of low-density freshwater (1000 kg/m^3 at 20^{o}C) which can flow over higher-density seawater (1025 kg/m^3 at 20^{o}C), and where marine currents and waves are not strong enough to mix the water column (e.g. in wave-dominated estuaries). Such conditions can lead to bottom waters being isolated from dissolved oxygen enriching processes, including gas exchange across the water surface and photosynthesis by plants in shallow water.

Partially mixed condition results as marine currents generate turbulence which promotes vertical mixing, however, the tidal currents are of insufficient strength to fully mix the water column, and salinity varies both vertically and horizontally.

Fully mixed conditions occur in coastal waterways in cases where tide, river or wave energy produces enough turbulence to mix the water column (*Figure 2.1C*). In this

case, salinity is uniform through the water column, but varies between the riverine and oceanic ends.

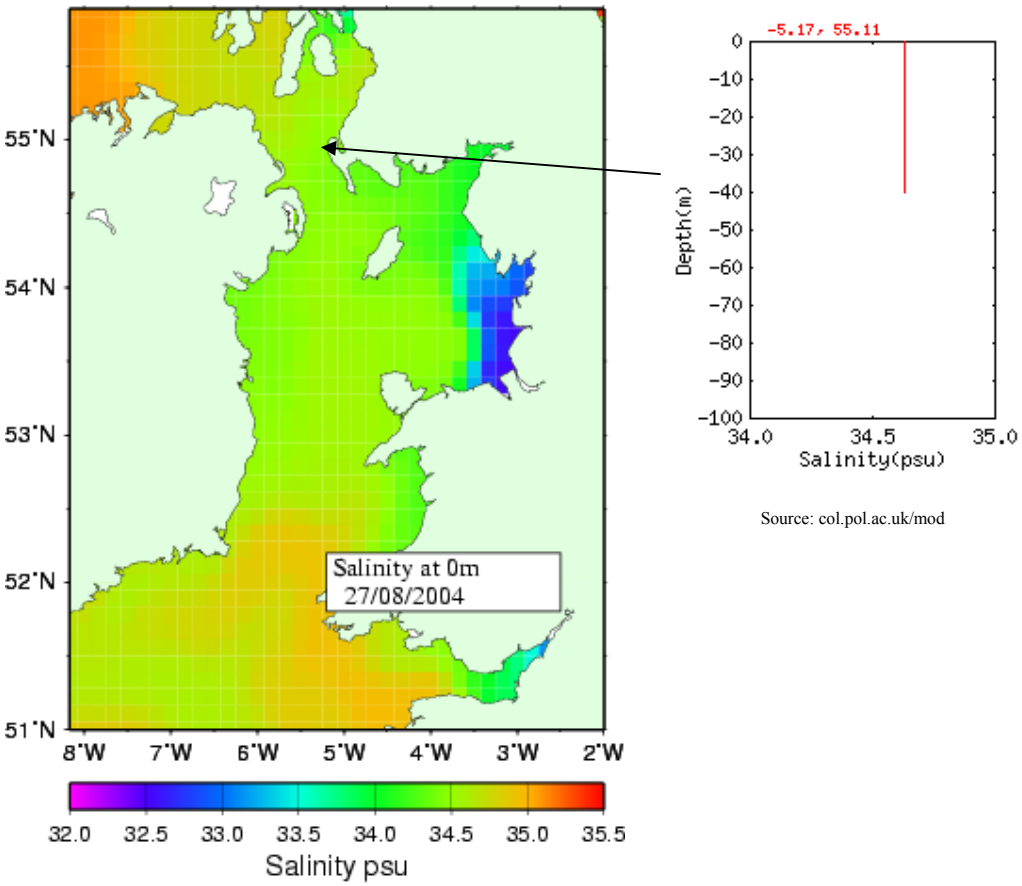

Source: col.pol.ac.uk/mod

Figure 2.12 Vertical and horizontal salinity variation in the Irish Sea

Measurements by *Coastal Laboratory, Liverpool Bay*, in the Irish Sea have shown that there is little or no vertical variation in salinity in high current areas as shown in *Figure 2.12*. This may be due to the high turbulence levels experienced there. These measurements were made with instruments based on land, at sea and from space.

2.3.3.2 Importance of Salinity

Most aquatic organisms function optimally within a narrow range of salinity. When salinity changes to above or below this range, an organism may lose the ability to regulate its internal ion concentration. As a result the organism may succumb to biotic pressures such as predation, competition, disease or parasitism. For example, most bottom-dwelling (benthic) organisms are able to tolerate changing salinities, but

salinities outside an acceptable range will affect their growth and reproduction (Alber 2002). This is also true for rooted vegetation (*e.g.* seagrasses). The salinity level is also an important factor in the successful recruitment of larval and juvenile fish (Whitefield 1994). A difference of only 3 degrees can double or halve their metabolic rate. Notwithstanding, some organisms can thrive between full strength seawater and upstream freshwater. Variations in salinity therefore results in changes in species composition, distribution and abundance.

Salinity also affects chemical conditions especially within an estuary, particularly dissolved oxygen levels. It is known that the amount of dissolved oxygen in water decreases with increasing salinity. For example the solubility of oxygen in seawater is about 20 % less than in freshwater of the same temperature.

2.3.4 Water Temperature

Water temperature is a measure of the heat (or kinetic energy) in water. Unnatural changes in water temperature are a suggested indicator of water quality and the state of the environment. It is therefore a critical factor in determining where marine organisms live and how well they thrive there. Water temperature in coastal areas changes naturally, as part of daily and seasonal cycles, with variations in air temperature, currents and local hydrodynamics.

2.3.4.1 Temperature Profile

Most of the solar radiation (light and heat) that hits the ocean is absorbed in the first few tens of meters of water. Waves and turbulence mix this heat downward quickly leading to a gradual decrease in temperature followed by a sharp decrease in the thermocline region and a gradual decrease in the deep zone. Generally as the depth increases the variation in temperature decreases as shown in *Figure 2.2*

Measurements by Coastal Laboratory, Liverpool Bay, in the Irish Sea have shown little departure of the trend in channels, however the temperature difference is small (1 degree for the graph shown in *Figure 2.14*). These levels are nonetheless variable in both time and space, partly due to the seasonal and daily variations in the tides and solar radiation.

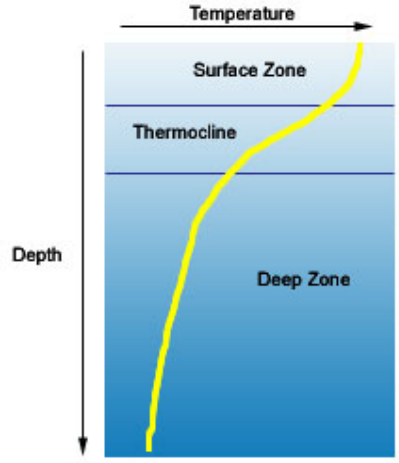

Figure 2.13 Typical temperature profile of the sea

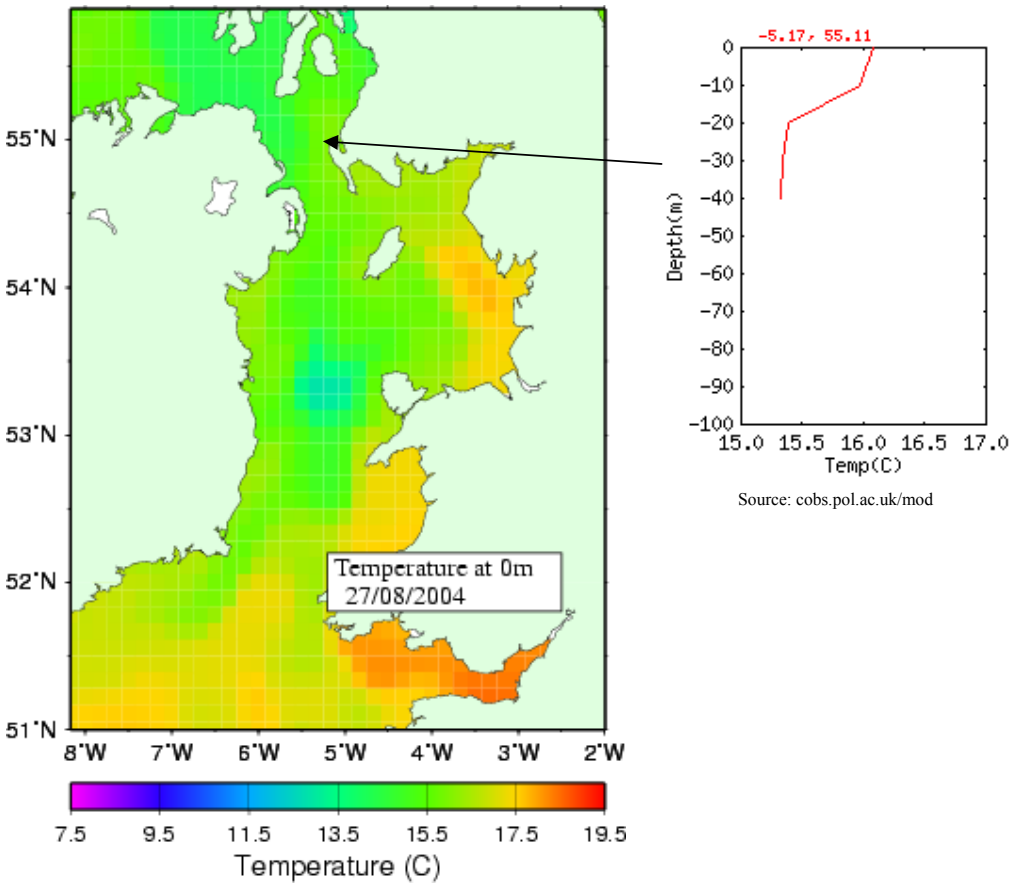

Source: cobs.pol.ac.uk/mod

Figure 2.14 Vertical and horizontal temperature variation in the Irish Sea

2.3.4.2 Significance of Temperature

Water temperature regulates ecosystem functioning both directly through physiological effects on organisms, and indirectly, as a consequence of habitat loss. Photosynthesis and aerobic respiration, growth, reproduction, metabolism and the mobility of organisms are all affected by changes in water temperature. Indeed, the rates of biochemical reactions usually double when temperature is increased by $10^{o}C$ within the given tolerance range of an organism (ANZECC/ARMCANZ 2000). This is called the Q_{10} *rule*, and it also applies to microbial processes such as nitrogen fixation, nitrification and denitrification. If temperature goes too far above or below the tolerance range for a given organism (*e.g.* fish, insects, zooplankton, phytoplankton, microbes), its ability to survive may be compromised. For example, coral species live within a relatively narrow temperature range, and positive or negative temperature anomalies of only a few degrees can induce bleaching or paling (Hoegh-Guldberg, 1999).

Unnatural changes in water temperature can lead to the loss of supporting habitat such as coral reefs, by changing the solubility of oxygen and calcium carbonate in water, or by influencing the extent to which metal contaminants and other toxicants are assimilated by physiological processes. Temperature is also probably the most important factor influencing viral persistence in estuarine environments. Generally water temperature influences the density, conductivity, pH and the saturation states of minerals of seawater.

2.3.5 Sediment Transport

Sediment transport is the movement of seabed material from one location to another. It occurs by the action of seabed currents. These seabed currents are mainly caused by the ebb and flood of the tides (over periods of hours) and by surface-waves passing overhead in shallow water (over periods of seconds). The waves break up the bed structure, lifting sediment into the water column. That is, the sediments ranging in size from small rocks and coarse gravel to silt and clay particles as fine as talcum powder enter the water where the currents carry them downstream. The faster the current, the greater the size of sediment particles a stream can move.

Since the sand and mud take a finite time to fall back to the bed, the tidal currents sweep them away from their starting point to towards areas of quieter conditions, where they accumulate, (e.g., into a harbour, where they must be removed by dredging). Alternatively, sediments can be concentrated into areas where they are constantly moving about a fixed point. This occurs in the sandbanks off the Norfolk coast, which are fixed in location, but where sand is continually moving as bed load up one side of the bank and then down the other side and then round again.

The marine environment, especially those areas with high tidal currents have complex sediment transport dynamics (Pandoe and Edge 2004). Deposition outside the natural variability of an area will cause changes to the local seabed and sediment dynamics of the area. If severe enough, changes in the coastal dynamics and intertidal areas, as well as already defined navigation channels may occur. All consequence pathways could cause potential impacts with regard to marine ecology, whether positively or detrimentally. For example early deposition may create new habitat areas and may result in the colonisation by benthic communities.

2.3.6 Turbidity

Turbidity is a measure of the ability of light to transmit down through the water column. As suspended solids increase in the water, the amount of light travelling through the water column is reduced. Turbidity therefore gives an indication of water clarity or murkiness. This can influence the populations of organisms that are directly dependent upon light (phytoplankton and aquatic plants) and those that in turn depend on them for food. The suspended solids include particles of organism (e.g. algae), clay and silt (e.g. suspended sediment), detritus or solid waste. Since sunlight is the basic energy source for most life forms, the degree of turbidity of the water has an important effect and hence is used as an indicator of the state of the aquatic environment.

2.3.6.1 Significance of Turbidity

Water clarity is a major determinant of the condition and productivity of an aquatic system, increased turbidity can therefore change an ecosystem significantly. The most obvious effects are:

- A reduction in light available for photosynthesis. According to Duate (1995) phytoplankton and free-floating macroalgae are better competitors for light than seabed plants including seagrasses, and will tend to outcompete them as light becomes limiting.

- Smothering of organisms and habitats. Suspended particles can cause mechanical and abrasive impairment of gills of fish and crustaceans and also clog the feeding apparatus of bottom dwelling animals.

- Promotion of the growth of pathogens and waterborne diseases. This because suspended sediments transport contaminants (particulate nutrients, metals and other potential toxicants) and also makes marine pests difficult to detect.

- Obscuring of the vision of fish as they hunt for food

Overall, unnaturally high turbidity levels can lead to a reduction in the production and diversity of species.

It is apparent from the review above that the environmental impacts of marine current development are site specific. The production, distribution and diversity of species will depend on the level and variation of these physical characteristics. The extent of this impact will depend on the extent of exploitation of the resource. This is because a high level of exploitation may result in significant reduction of current speeds and its attended effects on adjacent aquatic environment. This decrease in current speed may also attract fishes. In conclusion marine current developments are likely to have positive and negative impacts on the environment. The levels however need quantification to make informed judgments.

2.4 Overview of Computational Fluid Dynamics (CFD)

With the rise in complexity of engineering problems and the need to minimise costs while increasing productivity, the use of computer-aided simulation has become widespread. Experiments both on site and in the laboratory, although of great importance, cannot give complete information on their own, not to mention the high

costs involved. Numerical simulation combined with measurements is therefore most likely to constitute the basis for the analysis and design of marine current devices and farms. This section overviews one technique which will be of great use in this regard: Computational Fluid Dynamics (CFD). Versteeg & Malalasekera (1995) was used extensively for this write-up because of its precise and concise treatment of the subject.

2.4.1 What is Computational Fluid Dynamics?

Computational Fluid Dynamics (CFD) is the analysis of systems involving fluid flow, heat transfer and associated phenomena such as chemical reactions by means of computer-based simulation (Versteeg & Malalasekera 1995). It is computationally-based and enables the creation of a 'virtual prototype' of a system or device that is to be analysed and then applying physics and chemistry to the model, predictions are made as to how the system will perform. Some examples are:

- Aerodynamics of wind turbine blades: lift and drag
- Heating and ventilation in buildings
- Flow in the ocean and rivers
- Weather prediction
- Cooling of equipment in electric circuits
- Blood flow through arteries and veins

From the 1960s onwards the aerospace industry integrated CFD techniques into the design, R&D and manufacture of aircraft and jet engines. More recently the methods have been applied to the design of internal combustion engines, combustion chambers of gas turbines and furnaces (Versteeg and Malalasekera 1995). Increasingly CFD is becoming a vital component in the design of products and processes.

The costs involved in investing in CFD, though not cheap, are lower compared with high quality experimental facilities. For instance the costs involved in designing, building and commissioning of a purpose built wave tank for wave energy device

testing far outweigh that involved in the CFD analysis of the problem. Other advantages include:

- Ability to study the problem at a larger scale than the tank can handle
- Substantial reduction of time and effort
- Higher level of detail of the interaction between the device and the wave resource can be examined
- Ability to test the device under hazardous conditions at and beyond their normal performance limits (e.g. safety studies and accident scenarios)

2.4.2 How does a CFD code work?

The basic principle of CFD is to split the domain that is to be analysed into small elements. For each of these elements, a set of partial differential equations are solved, which approximates a solution for the flow in order to achieve the conditions of conservation of mass, momentum and energy. The three basic equations are solved simultaneously with any additional equations implemented in a particular model to obtain the flow velocities, pressure and, therefore, any derived quantities.

For easy access to their solving power all commercial CFD packages contain three main elements:

(i) A Pre-processor
(ii) A Solver
(iii) A Post-processor

A brief description of their respective functions is as follows:

2.4.2.1 Pre- processor

The pre-processor serves as a source of input of the flow problem to the CFD program by means of an operator interface. This is then transformed into a form suitable for the solver. The user activities at the pre-processing stage involve:

- Definition of the geometry of the region of interest
- Mesh or Grid generation: the sub-division of the domain into a number of smaller, non-overlapping sub-domains

- Selection of the physical and chemical phenomena that is to be modelled
- Definition of fluid properties
- Specification of the appropriate boundary conditions

The solution to the flow problem (velocity, pressure, temperature etc.) is defined at nodes inside each cell. Generally, the larger the number of cells in the domain the better the solution accuracy. Both the accuracy of the solution and its costs in terms of necessary computer hardware and calculation time are dependent on the fineness of the grid. It is good practice to have non-uniform meshes: finer in areas where large variations occur from point to point and coarser in regions with relatively little change.

Over 50 % of the time spent in industry on a CFD project is devoted to the definition of the domain geometry and grid generation ((Versteeg & Malalasekera 1995)). Currently almost all major codes now include their own CAD-style interface facilities to import data from surface modellers and mesh generators such as PATRAN, GAMBIT and I-DEAS. This helps to maximise productivity. Up-to-date pre-processors also give the user access to libraries of material properties for common fluids and a facility to invoke special physical and chemical process models (e.g. turbulence models, radiative heat transfer, combustion models) alongside the main fluid flow equations.

2.4.2.2 Solver

Numerical methods form the basis of the solver. They perform the following steps:

- Approximation of the unknown flow variables by means of simple functions
- Discretisation by substitution of the approximation into the governing flow equations and subsequent mathematical manipulations
- Solution of the algebraic equations

There are three distinct streams of numerical solution techniques:

(i) finite difference
(ii) finite element and
(iii) spectral methods

The main difference between these methods is the way in which the flow variables are approximated and with the discretisation process.

Finite Difference Method: This method was introduced by Euler in the 18th century (Douglas et al). It is much like a differential quotient, except that it uses finite quantities instead of infinitesimal ones. The unknowns of the flow problem are described by point samples at the node points of the grid. This means each node has one unknown and one algebraic equation which is a relation between the variable values at that node and those at some of the neihbouring nodes.

Finite Element Method: This theory was at first developed for stress analysis of structures. Simple piecewise functions (e.g. linear or quadratic), valid on elements, are used to describe the local variations of the unknown flow variables. The governing equation is satisfied by exact solution of the unknown variable. A residual is defined to measure the errors if the piecewise approximating functions for the unknown variable are substituted into the equation. Next the residuals (and hence the errors) are then minimised by multiplying them by a set of weighting functions and integrating. As a result a set of algebraic equations for the unknown coefficients of the approximating functions are obtained.

Spectral Methods: This method was originally developed for global weather modelling. It involves the approximation of the unknowns by truncated Fourier series or series of Chebyshev polynomials. In this case the approximations are valid throughout the entire computational domain. The constraint that leads to the algebraic equations for the coefficients of the Fourier or Chebyshev series is provided by a weighted residual concept similar to the finite element method or by making the approximate function coincide with the exact solution at a number of grid points.

2.4.2.2.1 The Finite Volume Method

The finite volume method was at first developed as a special finite difference formulation. It is a well-established and thoroughly validated general purpose CFD technique and it is central to most of the commercially available CFD codes:

FLUENT, PHOENICS, FLOW3D and STAR-CD (Versteeg & Malalasekera 1995). The numerical algorithm consists of the following steps:

- Formal integration of the governing equations of fluid flow over all the control volumes of the solution domain.
- Discretisation involves the substitution of a variety of finite-difference-type approximations for the terms in the integrated equation representing flow process such as convection, diffusion and sources. This converts the equations into a system of algebraic equations.
- Solution of the algebraic equations by iteration.

The control volume integration, distinguishes the finite volume method from all other CFD techniques. The resulting statements express the conservation of relevant properties for each finite size cell. This clear relationship between the numerical algorithm and the underlying physical conservation principle forms one of the main attractions of the finite volume method and makes its concepts much simpler to understand by engineers than the finite element and spectral methods (Versteeg & Malalasekera 1995). The conservation of a general flow variable e.g. a velocity component, within a finite control volume can be expressed as a balance between the various processes tending to increase or decrease it.

CFD Codes contain discretisation techniques suitable for the treatment of the key transport phenomena, convection (transport due to fluid flow) and diffusion (transport due to variations of the variable from point to point) as well as for the source terms and the rate of change with respect to time. The underlying physical phenomena are complex and non-linear so an iterative solution approach is required. The most popular solution procedures are the TDMA line-by-line solver of the algebraic equations and the SIMPLE algorithm to ensure correct linkage between pressure and velocity (Versteeg & Malalasekera 1995).

2.4.2.3 Post-processor

As in pre-processing a huge resource has been devoted to the development post-processing techniques and display. Owing to the increased popularity of engineering workstations, many of which have outstanding graphics capabilities, the leading CFD packages are now equipped with versatile data visualisation tools. These include:

- Domain geometry and grid display
- Vector plots
- Line and shaded contour plots
- 2D and 3D surface plots
- Particle tracking
- View manipulation (translation, rotation, scaling etc)
- Colour postscript output

Currently animation facilities for dynamic result display have been included in many CFD packages. In addition to graphics all codes produce trusty alphanumeric output and have data export facilities. As in many other branches of CAE the graphics output capabilities of CFD codes have revolutionised the communication of ideas to the non-specialist and specialist alike.

2.4.3 Problem Solving With CFD

The results generated by a CFD code are at best as good as the physics (and chemistry) embedded in it and at worst as good as its operator. Prior to setting up and running a CFD simulation there is a stage of identification and formulation of the flow problem in terms of the physical and chemical phenomena that need to be considered as discussed earlier. Typical decisions that might be needed are whether to model a problem in two or three dimensions, to exclude the effects of ambient temperature or pressure variations on the density of an air flow, to choose to solve the turbulent flow equations or to neglect the effects of small air bubbles dissolved in tap water. To make the right choices requires good modelling skills, because in all but the simplest problems assumptions need to be made to reduce the complexity to a manageable level whilst preserving the salient features of the problem in hand (Versteeg & Malalasekera 1995). It is appropriate that the simplifications introduced

partly govern the quality of the information generated by CFD, so the user must continually stay aware of all the assumptions which have been made.

2.5 Wind Analogy

Most of the technologies under development, as found in the previous section, have a more than passing resemblance to technologies already being utilised to harness wind energy resources. It is therefore imperative that the development of marine current energy will draw much experience from the wind energy industry. This section reviews some of the CFD studies in wind energy related to the interaction of the turbines to each other and the environment. Particular reference is given to wake development downstream of the units.

2.5.1 CFD Modelling in Wind Energy Industry

The aerodynamic research on wind turbines has contributed significantly to the success of the wind energy industry. Physical understanding and modelling using a fundamental approach have played an important role in this regard (Vermeer et al 2003). Current wind turbine technologies are therefore fairly mature and their efficiency can be tied to a number of factors, one of which is the positioning of the wind turbines near other wind turbines or structures. Decreased distances give rise to wake effects for the downstream units, which can lead to changeable wind loads, reduced energy yield and vibration induced fatigue on the rotors and potentially on nearby power lines. Wake modelling made up of near and far wake have helped to better design wind turbine blade profiles as well as optimise farm layout. The near wake is taken as the area just behind the rotor, where the properties of the rotor can be discriminated, approximately up to one rotor diameter downstream. Here, the presence of the rotor is apparent by the number of blades, blade aerodynamics, including stall flow, 3-D effects and tip vortices. The far wake is the region beyond the near wake, where the focus is put on the influence of wind turbines in farm situations, so modelling actual rotor is less important. Here the main attention is put on wake models, wake interference, turbulence models, and topographical effects. The near wake research is focussed on performance and the physical process of

power extraction, while the far wake research is more focused on the mutual influence when the wind turbines are placed in clusters, like wind farms.

Early studies approximated the rotor area as a semi-permeable disk. This helped to simulate the pressure drop across the rotor and an indication of the far wake development and its effects. Recent advances in CFD codes with the incorporation of CAD facilities have helped to model the blades once the dimensions are known, just as in reality. As a result better blade profiles have been developed and wind farm layout improved. A typical example is discussed as follows.

2.5.2 Sample Studies

TUV Nord e.V., a technical inspection agency in Germany, examined the wake behind pitch-regulated wind turbines on the basis of their geometry and operating characteristics using FLUENT. In a typical simulation, approximately 650 data points were used to create the geometry of a single rotor blade. A fine grid on the whole rotor surface was used to create a volume mesh of about 750,000 cells that coarsens as the distance from the blades increases. Downstream distances of six to ten times the rotor diameter were modelled. The multiple reference frames (MRF) model was used to account for the rotation of the blades. Blade pitch, wind speed and direction, turbulence intensity and length scale, and rotor speed were input for each simulation.

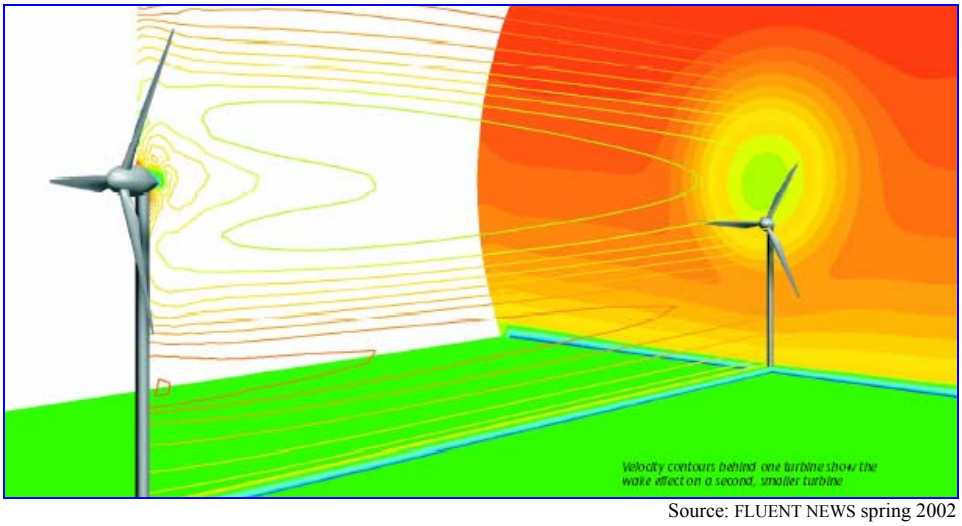

Source: FLUENT NEWS spring 2002

Figure 2.15 Wake effect of a larger wind turbine on a small one

The model was then validated using wake measurements behind a 55 kW pitch-regulated turbine and then several investigations undertaken. *Figure 2.13* shows one wind turbine operating in the wake of a second, large one. A wind velocity of 12.5 m/s with a turbulence intensity of 13 % was imposed upstream of the front turbine.

Filled contour of constant mean velocity in the plane of the smaller turbine, four diameters behind the front turbine, show that the velocity field is not uniform and not centred on the hub. Line contours in the plane containing the two turbines illustrate the decay in the wake as a function of distance behind the turbine. (Source: FLUENT NEWS spring 2002).

It should be noted that, though there are tempting similarities between the nature of wind and marine current extraction, there are substantial differences between the natures of the underlying resources. Unlike the wind the marine current energy fluxes are constrained between the seabed and the sea surface and may be further constrained in a channel.

CHAPTER THREE - ANALYTICAL FRAMEWORK

3.0 Introduction

Practically every problem in fluid engineering hydraulics involves the prediction of one or more flow characteristics by either analytical or experimental methods. This chapter looks at the theories underlying the velocity distribution in open channel flows with particular reference to tidal current flows. The theory of the energy conversion taking into account the varying tidal flow has also been reviewed. Lastly a review of the theory of turbulence modelling with particular reference to its application in FLUENT has been included. The practical as well as experimental implications of certain assumptions have been highlighted where necessary.

3.1 Natural Open Channels

An open channel is a conduit in which water flows with a free surface. Marine current channels such as straits between islands and, are classified under natural open channels. The hydraulic properties of these natural open channels are generally very irregular. In some cases empirical assumptions reasonably consistent with actual observations and experience may be made such that the conditions of flow in these channels become amenable to the analytical treatment of theoretical hydraulics (Chow, 1959). The cross sections of natural channels are also generally very irregular, usually varying from an approximate parabola to an approximate trapezoid. For streams subject to frequent floods, the channel may consists of a main channel section carrying normal discharges and one or more side channel sections for accommodating overflows.

3.2.1 Velocity Distribution in a Channel Section

Generally the velocities in a channel are not uniformly distributed owing to the presence of the free surface and friction along the channel walls. The velocity distribution in a uniform channel flow will however become stable when the turbulent boundary layer is fully developed. Within the turbulent boundary layer Prandtl demonstrated that the vertical velocity profile is approximately logarithmic. The shearing stress τ, at any point in the turbulent flow moving over a solid surface is therefore given by:

$$\tau = \rho l^2 \left(\frac{du}{dy} \right)^2 \qquad \text{i.e.} \quad du = \sqrt{\frac{\tau}{\rho l^2}} dy \qquad \ldots (1)$$

where

ρ is the mass density

l is a characteristic length known as the mixing length

du/dy is the velocity gradient at a nominal distance y, from the solid surface

Two assumptions are introduced at this stage:

- The mixing length is proportional to y, i.e. $l = ky$, where k is von Karman's turbulence constant; it is perhaps more accurate to term k a coefficient since there is some evidence that it may vary over a range of values as a function of the Reynolds number (Hinze 1964). Notwithstanding k can be approximated as 0.4 (Chow 1957)

- The shearing stress is constant. Since the shearing stress at the channel surface is equal to the unit tractive force then $\tau = \tau_0$

Making use of these assumptions and integrating gives:

$$u(y) = 2.5\sqrt{\frac{\tau_0}{\rho}} \ln \frac{y}{y_0} \; ; \qquad u(y) = 2.5 u_f \ln \frac{y}{y_0} \qquad \ldots (2)$$

where

$u(y)$ is the average turbulent velocity at a distance y above the bottom

u_f is the friction velocity or shear velocity

y_0 is a constant of integration

The constant of integration y_0, is of the same order of magnitude as the viscous sub layer thickness and is a function of whether the boundary is hydraulically smooth or

rough. If the boundary surface is hydraulically smooth, then y_0 depends solely on the kinematic viscosity and shear velocity. For a hydraulically rough boundary surface y_0 depends only on the roughness height. See Chow (1959) for further details.

This equation indicates that the velocity in the turbulent region is a logarithmic function of the distance y. It is commonly known as the *Prandtl-von Karman universal velocity distribution law.* This law has been verified by several experiments (French 1994). The results show a striking similarity between observed and computed distributions and, therefore, offer reasonable justification for use in practical problems.

The velocity distribution in fully developed turbulent open channel flows can also be written in terms of the maximum velocity u_{max} and the channel depth d. This approximate relation known as the Prandtl power law (Equation 3) is more convenient considering the varying tidal current speeds over the spring-neap cycle.

$$u(y) = \left(\frac{y}{d}\right)^{\frac{1}{N}} u_{\max} \qquad \ldots (3)$$

where N is a function of the flow resistance. In uniform flows this velocity distribution exponent is related to the flow resistance as follows:

$$N = k\sqrt{\frac{8}{f}} \qquad \ldots (4)$$

where f is the Darcy friction factor and k von Karman turbulent coefficient

In practical engineering applications, N can range from 4 (for shallow waters in wide rough channels) up to 12 (smooth narrow channel) (Chanson 2004). For tidal flow, $N = 7$ ($1/7^{th}$ power law) can be assumed (Bryden et al, 1998). It takes the form:

$$u(y) = 0.93\left(\frac{y}{0.32d}\right)^{\frac{1}{7}} u_{\max} \qquad \ldots (5)$$

These velocity profiles describe fairly accurately the vertical velocity variation in the channel column, however their accuracy decreases toward the free surface. According to Chow (1959) the maximum velocity in ordinary (e.g. rectangular cross section) channels usually appears to occur below the free surface at a distance of 0.05 to 0.25 of the depth; the closer to the banks, the deeper is the maximum. This is influenced by the flow regime, usual shape of the section, the roughness of the channel, and the presence of bends. In a broad, rapid, and shallow stream or in a very smooth channel, the maximum velocity may often be found at the free surface making equations (2) and (3) more applicable. As the roughness of the channel increases the curvature of the vertical velocity distribution also increases as shown in *(Figure 3.1)* and equations (2) and (3) become less accurate. On a bend the velocity increases greatly at the convex side, owing to the centrifugal action of the flow.

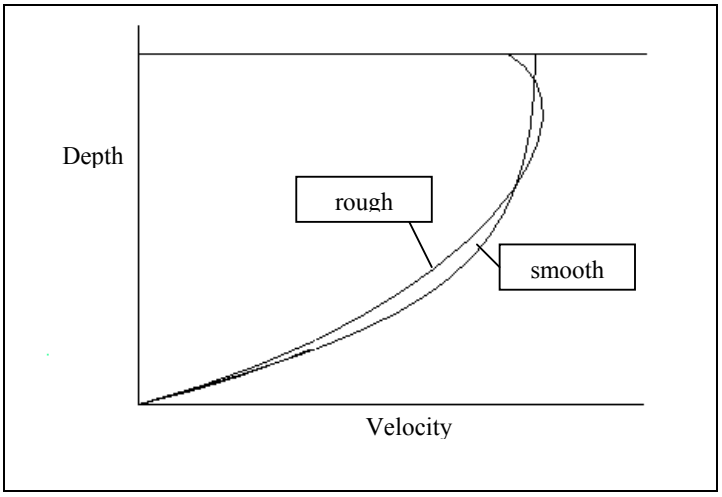

Figure 3.1 Vertical Velocity Distribution in an open channel

Observations in wide open channels like straits between islands have shown that the velocity distribution in the central region of the section is essentially the same as it would be in a rectangular channel of infinite width. Meaning, under this condition, the sides of the channel have practically no influence on the velocity distribution in the central region, hence flow in the central region can be regarded as two-dimensional in hydraulic analyses. Careful experiments indicate, further, that this central region exists in rectangular channels only when the width is greater than 5 to

10 times the depth of flow, depending on the condition of surface roughness (Chow, 1959). Thus, a wide open channel with width greater than 10 times the depth of flow can safely be defined as a rectangular channel.

3.3 Energy Conversion Principles

Moving water has kinetic energy similar to wind. The energy per second intercepted by a device of frontal area A_o (m^2) in water of density ρ, and average actuator disc current velocity $\overline{V}$ (m/s) is therefore given by:

$$P_e(t) = 0.5\rho A_o \overline{V}^3(t) \quad \ldots (6)$$

The power that can be converted to a useable mechanical form is limited for a device in an open water flow to:

$$P_m(t) = 0.5 C_p \rho A_o \overline{V}^3(t) \quad \ldots (7)$$

where C_p is the power coefficient. The value of C_p for a turbine exposed to the flow of an incompressible fluid is limited to a theoretical maximum value of approximately 0.593 according to Betz law. For a device the power coefficient is generally a function of the tip speed ratio (ratio between the turbine blade tip speed and the fluid flow speed), which is dependent on the blade form and the number of the blades.

Assuming a gearbox transmission efficiency of η_1 and generator efficiency of η_2 then the electrical power output is given as:

$$P(t) = \eta_1 \eta_2 0.5 C_p \rho A_o \overline{V}^3(t) \quad \ldots (8)$$

Tidal currents are not constant. As explained earlier they are a combination of quasi-steady marine currents and flows induced by the tides. Estimation of energy capture therefore becomes a fairly complex procedure. However for most sites the flows are purely tidal, making it possible to parameterise the tidal currents as series of simple sinusoids.

$$V(t) = V_{\max} \sin \omega t \quad \text{and} \quad \omega = \frac{2\pi}{T} \quad \ldots (9)$$

where:

V_{max} is the maximum current speed at the surface

ω is the angular velocity of the tide

T is the period of the cycle, typically 12h 25 min or 745 minutes.

Bryden et al (1998) assumed a more elaborate sinusoidal relation based on the semidiurnal and spring-neap cycle. It takes into consideration velocity components as shown below:

$$V_x(t) = A + \left[B + C\cos\left(\frac{2\pi t}{T_1}\right)\right]\cos\left(\frac{2\pi t}{T_0}\right) \quad \ldots (10)$$

$$V_y(t) = F + \left[D + E\cos\left(\frac{2\pi t}{T_1}\right)\right]\sin\left(\frac{2\pi t}{T_0}\right) \quad \ldots (11)$$

where:

$V_x(t)$ represents the East-West current speed and $V_y(t)$ represents the North-South current speed

A and F are related to the residual current speeds

B, C, D and E are amplitude terms

T_0 is the period of the semidiurnal variation and

T_1 is the period of the spring-neap cycle

For a turbine with a yaw mechanism or a vertical axis turbine the absolute value, $|V(t)|$ of the current velocity is of more importance, where:

$$|V(t)| = \sqrt{V_x^{\,2}(t) + V_y^{\,2}(t)} \quad \ldots (12)$$

In many locations, it may not be possible to parameterise the tidal currents in these simple forms, however alternative parametric descriptions based on the underlying astronomic mechanisms may be available (Bryden et al 1998).

3.4 Turbulence Modelling

Turbulent flow is a highly complex phenomenon. This phenomenon has been studied for many years, however it is not yet possible to characterize turbulence from a purely theoretical standpoint. Notwithstanding many important characteristics of turbulence are well-known, including the following:

- Turbulence is time-dependent, three-dimensional, and highly non-linear.

- Fully-developed turbulent motion is characterized by entangled eddies of various sizes. The largest eddies arise from hydrodynamic instabilities in the mean flow field -- for example, shearing between a flowing stream and a solid boundary.

- The largest eddies break down into smaller eddies which, in turn, break down into even smaller eddies. This process of eddy break-down transfers kinetic energy from the mean flow to progressively smaller scales of motion. At the smallest scales of turbulent motion, the kinetic energy is converted to heat by means of *viscous dissipation*.

- The dynamic and geometrical properties of the largest eddies are closely related to the corresponding properties of the mean flow field. For example, large, unstable vortices that form on the perimeter of a turbulent jet tend to possess well-defined toroidal structures.

- The time and length scales of the smallest turbulent eddies are many orders of magnitude greater than the time scales and free paths of molecular motion. As a result, the processes of viscous dissipation are statistically independent of molecular motion.

- Turbulent motion is not a random phenomenon. As a consequence, turbulent fields possess definite spatial and temporal structures.

3.4.1 General Equations

For steady, incompressible flow the instantaneous continuity, momentum (*Navier-Stokes*) and scalar transport equations may be written in the following Cartesian tensor form:

Continuity

$$\frac{\partial U_i}{\partial x_i} = 0 \qquad \ldots (13)$$

Instantaneous Momentum Transport

$$\frac{\partial(\rho U_i U_j)}{\partial x_j} = -\frac{\partial P}{\partial x_i} + \frac{\partial}{\partial x_j}\left\{\mu_l\left(\frac{\partial U_i}{\partial x_i} + \frac{\partial U_j}{\partial x_i}\right)\right\} \qquad \ldots (14)$$

Instantaneous Scalar Transport

$$\frac{\partial(\rho U_j \phi)}{\partial x_j} = \frac{\partial}{\partial x_j}\left\{\left(\frac{\mu_l}{\sigma_l}\right)_\phi\left(\frac{\partial \phi}{\partial x_j}\right)\right\} \qquad \ldots (15)$$

To create a usable numerical model of a turbulent flow field, it is necessary to describe turbulent motion in terms of *averaged* quantities. Employing normal *Reynolds* decomposition with $U_i = \overline{U_i} + u_i'$ and $\phi_i = \overline{\phi_i} + \varphi_i'$ and time-averaging the Reynolds-averaged mean flow equations may be written in the following Cartesian tensor form:

Continuity

$$\frac{\partial \overline{U_i}}{\partial x_j} = 0 \qquad \ldots (16)$$

Mean Momentum Transport

$$\frac{\partial(\rho \overline{U_i}\,\overline{U_j})}{\partial x_j} = -\frac{\partial \overline{P}}{\partial x_i} + \frac{\partial}{\partial x_j}\left\{\mu_l\left(\frac{\partial \overline{U_i}}{\partial x_j} + \frac{\partial \overline{U_j}}{\partial x_i}\right) - \rho\overline{u_i' u_j'}\right\} \qquad \ldots (17)$$

Mean Scalar Transport

$$\frac{\partial(\rho\overline{U}_j\overline{\phi})}{\partial x_j} = \frac{\partial}{\partial x_j}\left\{\left(\frac{\mu_l}{\sigma_l}\right)_\phi\left(\frac{\partial\overline{\phi}}{\partial x_j}\right) - \rho\overline{u_i'\phi'}\right\} \quad \ldots (18)$$

Due to the random nature of the production and dissipation of turbulence (broad spectra of turbulent length and times scales) it is not possible to solve equations (16), (17) and (18), although research work on such *Direct Numerical Simulations* is currently active using large scale parallel or supercomputers. A good source for a step by step derivation of these equations is (Mathieu and Scott 2000). The FLUENT manual is also a good reference.

3.4.3 Turbulence Models

For all realistic engineering problems which are solved by CFD the effects of turbulence (via the *Reynolds stresses* - $\rho\overline{u_i'u_j'}$) must be modelled and whole areas of research are devoted to finding appropriate turbulence models. From a numerical point of view turbulence models fall into two broad categories:

- Second-Moment Stress Models
- Isotropic Eddy-Viscosity Models

The division is determined by how the relationship between the *Reynolds stresses* and the mean flow-field (strain rates), frequently referred to as the *stress-strain* relationship, is represented.

Second-Moment Stress Models relate the Reynolds stresses in equation (17) to the mean velocity field using approximations for Reynolds stresses which can either be *algebraic* or *differential* with the latter requiring six additional transport equations for the six independent Reynolds stresses. These are more elaborate and complicated (and more realistic) models in comparison with *Eddy-Viscosity Models*. However, the augmentation of the number of transport equations in the *Second-Moment Stress Models* presents computer hardware restrictions and coupled with numerical stability problems this has restricted their general use in the CFD community.

Eddy-Viscosity Models approximate the Reynolds stresses through the *Boussinesq* relations where, in analogy with molecular (laminar) stresses, it takes the form:

$$\rho\overline{u_i' u_j'} = -\mu_t\left(\frac{\partial\overline{U_i}}{\partial x_j} + \frac{\partial\overline{U_j}}{\partial x_i}\right) \quad \ldots (19)$$

The purpose of any eddy-viscosity model is to describe the relationship between the eddy viscosity, μ_t, and physically tangible flow quantities.

3.4.4 Turbulence Models in FLUENT

FLUENT has many different turbulence models of which the majority are based on the *Eddy-Viscosity Model* concept. Equation (19) represents the *Eddy-Viscosity Model* treatment of the Reynolds stresses. It is at this stage an expression to represent the turbulent viscosity μ_t must be formulated. Considering the dimensions of ν_t it is observed that it can be constructed from the product of a turbulent velocity scale multiplied by a turbulent length scale (m*m/s = m^2/s). In this way the formulations for ν_t are described in terms of the number of transport equations used to solve for the velocity and length scales.

3.4.4.1 The Zero-Equation Model

Although there are many different forms of the *zero-equation model*, FLUENT employs a model known as the *Prandtl mixing length* model. In this model, ν_t is given by:

$$\nu_t = l_m^2(y)\left|\frac{\partial\overline{U}}{\partial y}\right| \quad \ldots (20)$$

where the only unknown l_m, is the mixing length, the modulus of the velocity gradient (strain rate) is taken to avoid negative ν_t.

The mixing-length hypothesis works well for relatively simple flows such as thin shear-layer flows, wall boundary-layer flows, jets and wake flows, because l_m can be specified by simple empirical formulas in such situations. However, the model does not account for the transport and history effects of turbulence. In particular, the model is not suitable when processes of convective or diffusive transport of turbulence are important, such as in rapidly developing flows, heat transfer across planes with zero velocity gradient and recirculation flows. More generally, the model is often difficult to apply in complex flows because of the difficulties in specifying l_m.

3.4.4.1 The One- Equation Model

The *one-equation model* solves a transport equation for the fluid turbulent kinetic energy k (defined as $\frac{1}{2}\overline{u_i' u_j'}$) where $\sqrt{k}$ represents the velocity scale of the turbulence. The value of u_t is calculated from *the Prandtl-Kolmogorov* formula:

$$\nu_t = C_\mu l_m k^{1/2} \qquad \ldots (21)$$

where C_μ is an empirical constant and k is the turbulent kinetic energy per unit mass. The *one-equation model* can take into account the influences of convection and diffusion of the turbulent velocity scale but the mixing length l_m must still be specified via a known empirical relationship.

3.4.4.1 The Two-Equation Model

Two equation models take into account the convective and diffusive transport of the turbulence itself. The most commonly used *two-equation model* in turbulent flow simulations is the $k - e$ model. In common with all other *eddy-viscosity models*, the Reynolds stresses are obtained from:

$$-\overline{u_i' u_j'} = \nu_t \left(\frac{\partial \overline{U_i}}{\partial x_j} + \frac{\partial \overline{U_j}}{\partial x_i} \right) - \frac{2}{3}\delta_{ij} k \qquad \ldots (22)$$

where the final term on the right hand side of this equation is necessary such that the sum of the normal stresses is not zero by continuity but 2*k*.

The introduction of the *Boussinesq* approximation (equation (22)) into the mean-momentum equation (17) leads to the following simplification:

$$\frac{\partial(\overline{U_i}\overline{U_j})}{\partial x_j} = -\frac{1}{\rho}\frac{\partial \overline{P}}{\partial x_i} + \frac{\partial}{\partial x_j}\left\{\nu_{eff}\left(\frac{\partial \overline{U_i}}{\partial x_j} + \frac{\partial \overline{U_j}}{\partial x_i}\right)\right\} \qquad \ldots (23)$$

where $\nu_{eff} = \nu_l + \nu_t$

It is important to highlight that unlike the molecular kinematic viscosity (ν_l), ν_t is not a fluid property but depends only on the state of the turbulence at any one point. The effects of turbulence are thus modelled through the introduction of an effective viscosity ν_{eff}. The turbulent kinematic viscosity once more takes the *Prandtl-Kolmogorov* form of equation (21) and the length of the turbulence is calculated from:

$$l_m = C_d k^{3/2} \qquad \ldots (24)$$

substituting this into equation (21) gives:

$$\nu_t = \frac{C_D k^2}{\varepsilon} \qquad \ldots (25)$$

where the empirical constant $C_D = C_\mu . C_d$

Two equation models involve the solution of transport equations for the turbulent kinetic energy *k* and its dissipation rate *e*, given by:

k-transport equation

$$\frac{\partial(\overline{U_j}k)}{\partial x_j} = \frac{\partial}{\partial x_j}\left\{\left(\frac{\nu_l}{\sigma_l} + \frac{\nu_t}{\sigma_k}\right)\left(\frac{\partial k}{\partial x_j}\right)\right\} + P_k - \varepsilon \qquad \ldots (26)$$

e-transport equation

$$\frac{\partial(\overline{U_j}\varepsilon)}{\partial x_j} = \frac{\partial}{\partial x_j}\left\{\left(\frac{\nu_l}{\sigma_l} + \frac{\nu_t}{\sigma_\varepsilon}\right)\left(\frac{\partial \varepsilon}{\partial x_j}\right)\right\} + C_{\varepsilon 1}\frac{\varepsilon}{k}P_k - C_{\varepsilon 2}\frac{\varepsilon^2}{k} \qquad \ldots (27)$$

where $P_k = \nu_t \frac{\partial U_i}{\partial x_j}\left(\frac{\partial \overline{U}_i}{\partial x_j} + \frac{\partial \overline{U_j}}{\partial x_i}\right)$ is the production rate of turbulent kinetic energy.

The *k-e* model has been used extensively over the years by CFD engineers as it possesses a large width of applicability. In general it is also numerically stable. The basic assumption made in the *k-e* model is that the turbulence is *isotropic* (independent of coordinate direction). For certain flows this will be a reasonable assumption, however, in flows where *anisotropy* effects are important (e.g. flows involving buoyancy, secondary flows, flows with strong streamline curvature) the *k-e* model performs poorly as ν_t will be coordinate dependent. More realistic models such as the algebraic or differential stress models will provide better estimates of the stress-strain relationship.

CHAPTER FOUR: METHODOLOGY

4.0 Introduction

The results generated by a CFD code are at best as good as the physics embedded in it and at worst as good as its operator. Identification and formulation of the flow problem in terms of the computational domain, the physical as well as the chemical phenomena that need to be considered is therefore crucial. To make the right choices requires good modelling skills, because in all but simple problems assumptions need to be made to reduce the complexity to a manageable level whilst preserving the salient features of the problem. This section describes the basic procedure employed in the modelling and simulation of the problem at hand, from pre-processing, to solution and to post-processing. The inputs as well as the assumptions made have also been included. A simple analytical method used to validate the model concludes the chapter. A summary report generated by FLUENT has been included in the appendix.

4.1 Modelling and Simulation Procedure

This section gives a descriptive account o the modelling and simulation procedure employed; from pre-processing, to solving and to post-processing.

4.1.1 Pre-processing

This is one of the most important steps in the study. It is involves the creation of the model (geometry and mesh) in GAMBIT followed by further processing of the model (selection of appropriate physical phenomena, fluid properties and necessary boundary conditions) in FLUENT prior to the simulation.

4.1.1.1 Creation of the Simulation Model

The procedure involved in creating the simulation model in GAMBIT is as follows:

(i) **Definition of the Geometry of the Region of Interest:** The geometry of the region of interest was created in two main stages. The first was the modelling of the resource which was represented by a uniform channel with a rectangular cross-section. The bottom surface of the cuboid represented the seabed while the top represented the free surface. The second was the

modelling of the turbine made up of the rotor blades, hub, pod and monopile. The "Seaflow" turbine discussed earlier on in *Chapter Two* served as the basis for this model. Simple geometrical shapes were used to represent these features. Of particular interest was the twin turbine blade which was represented by an oval cross sectioned cylinder which tapers at the end. The blades were tilted to and angle of attack of 20 degrees. The monopile as well as the pod were represented by 2 m diameter cylinders whiles the hub was represented by a 2 m diameter semi-sphere.

(ii) Creation of Boundary Layer and Mesh: Once the region of interests was defined it was divided into a number of cells. The first step was to impose a boundary layer on all wall surfaces; rotor blades, hub, pod, monopile and seabed. This was necessary to increase the accuracy of the results close these surfaces. An unstructured triangular (Tri, Pave) face mesh was then generated on all surfaces after imposing reasonable mesh spacing on all edges. The mesh was then examined and refined making it finer especially on the rotor blade surface and areas close to it. The L-W facility in GAMBIT was used to smoothen the mesh on the free surface and sea bed. A volume mesh primarily composed of tetrahedral mesh elements was then generated for the computational domain. This was further examined and refined where necessary.

(iii)Definition of Boundary Conditions: This was the final step carried out in GAMBIT to create the model. Here the solver, boundary type and fluid domain were specified. FLUENT 5 was selected as the solver. Boundary types (wall, symmetry, velocity inlet etc) were then specified for each surface (rotor blades, free surface, inlet etc) while domain fluid was set to liquid. Finally the model was exported to the Fluent solver for further processing and simulation.

4.1.1.2. Processing of Simulation Model for Simulation

At this stage the 3D model was read into FLUENT and the grid examined to ensure that it has been imported successful. The physical phenomena to be simulated

together with the fluid properties and boundary conditions were then specified as described below:

(i) **Selection of Physical Phenomena:** In this case a segregated solver and an implicit formulation were selected for the 3D model. Steady conditions were applied and the velocity formulation was absolute. Further more the *k-epsilon (2 equation)* viscous model, with standard wall functions, was selected to account for the turbulent flow.

(ii) **Definition of fluid Properties:** The property database for liquid water was loaded and necessary changes (density, viscosity etc) were made to suit seawater. These properties were assumed constant over the computational domain.

(iii) **Specification of Boundary Conditions:** With reference to the boundary types specified earlier on appropriate boundary conditions were applied to the various surfaces. The velocity at inlet was assumed to be in the x-direction only. A vertical velocity profile in the x-direction created in notepad was therefore applied. The turbulence intensity as well as the hydraulic diameter was also specified for the inlet. A condition of velocity continuity was assumed at the outlet in which case there was no backflow. The Multiple Reference Frame (MRF) model was used to account for the rotation of the rotor blades. Appropriate roughness heights were also applied to all wall surfaces.

4.1.3 Initialisation and Solving the Model

At this stage the solution scheme was specified as flow and turbulence, and relaxation factors set. The solution was then initialised with the inlet as the reference. Also the grid was adapted using the Y^+ facility. The convergence criteria were also set followed by the force monitors (drag and lift). The simulation process was then invoked after setting the number of iterations. The simulation was interrupted at regular intervals and saved. This was necessary to prevent loss of data due to a

change in say, the relaxation settings which may result in a divergence of the solution.

4.1.4 Post-processing

Once the solution converged different aspects of the solved flow regime was examined in detail. By defining planes parallel to existing ones but close to the blades the change in the flow pattern was examined in different directions (front, plan and end views)

4.1.5 Validation of CFD Solution

In the absence of measurements from actual devices a simplified analytical method was used to validate the model.

4.1.6 Further Investigation

Once the model was validated, it was used for further investigations. The surface current speed was varied to create two other velocity profiles representing neap and spring tides. The subsequent change in the flow pattern (wake development, upwelling,) were then examined.

4.2 Inputs and Assumptions

The input values used in creating the model as well as that for simulation process has been presented as follows in this section. The assumptions employed have also been included.

4.2.1 Channel Dimension

The *Tables 4.1* below shows the dimensions of the rectangular channel.

Table 4.1 Dimensions of Channel

Description	**Dimension (m)**
Length	1000
Width	500
Depth	40

4.2.2 Turbine Configuration

The "seaflow" turbine discussed in the literature review was chosen for this investigation. Its specifications are displayed in *Table 4.1.* Due to unavailable data a combined gearbox and transmission efficiency of 90 % was assumed to calculate the mechanical power. Moreover detailed turbine dimensions were estimated from photos.

Figure 4.2 Technical specification of "seaflow" turbine

Specification	Value
Rated speed (m/s)	2.7
Rated power (kW)	300
Rated mechanical power (kW)	334
Rotational speed (rpm)	10

Table 4.3 Dimensions of Turbine

Description	Dimension (m)
Diameter of rotor blades	11
Major diameter at blade root	0.5
Minor diameter at blade root	0.1
Major diameter at blade tip	0.3
Minor diameter at blade tip	0.1
Diameter of pod	2
Diameter of hub	2
Diameter of monopile	2

Two configurations of this turbine were modelled.

- ***Turbine 1:*** This turbine has its rotor blades 5 m below the sea surface to account for different tidal heights. That is 1 m for the lowest astronomic tide (LAT), 1.5 m for the lowest negative storm surge and a further 2.5 m for the trough of a 5 m wave. (Bryden et al, 1998)

- ***Turbine 2.*** In this case the rotor blades are 10 m (additional 5 m) below the free surface to allow for shipping purposes.

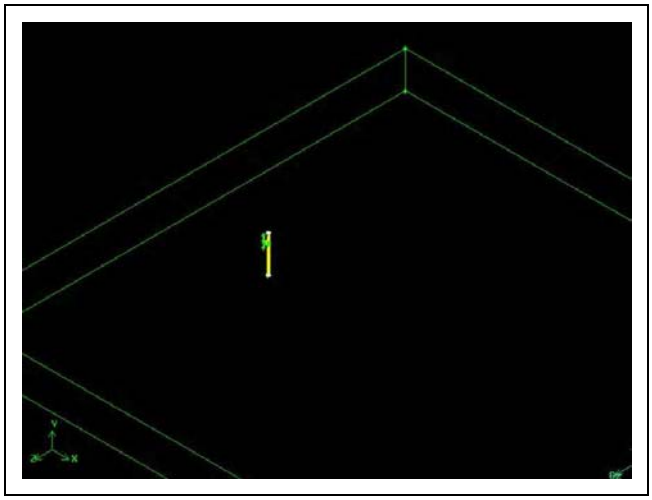

Figure 4.1 Model of channel and turbine in position

4.2.3 Meshed Model

Table 4.3 below gives a summary of the number of cells on each surface as well as the total number of cells in the volume. Figures of sample face mesh of the model are also shown following.

Table 4.2 Number of cells on each surface

Surface	**Number of Cells**
Rotor blades	6 818
Hub	1 473
Pod	7 741
Monopile	37 177
Inlet	1 311
Outlet	1 309
Free surface	96 970
Upper edge	2 493
Lower edge	2 493
Seabed	35 843
Interior	2 394 521
Volume	1 218 980

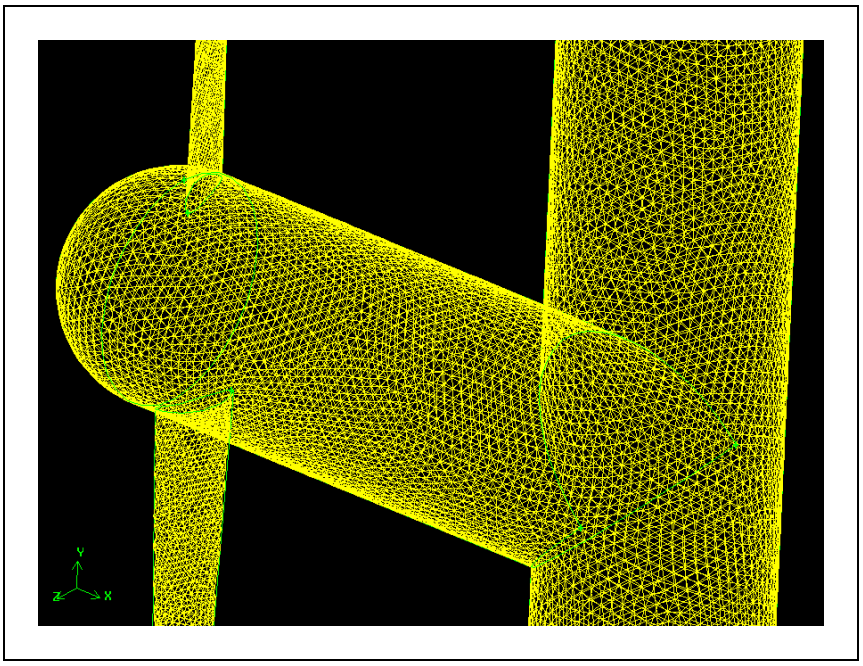

Figure 4.2 Typical surface mesh of the turbine

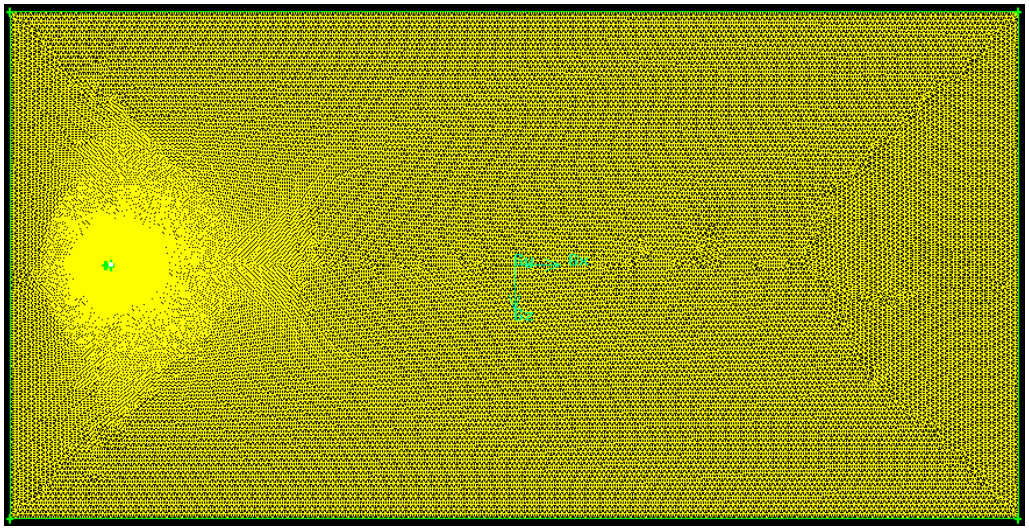

Figure 4.3 Typical surface mesh of the free surface showing a higher cell density closer to the turbine

4.2.4 Fluid Properties

Table 4.3 Properties of seawater

Property	**Value**
Density (m^3/kg)	1030
Dynamic Viscosity (kg/ms)	0.0012051
Kinematic Viscosity (m^2/s)	0.00000117
Temperature (K)	300

Source: www.lmnoeng.com (LMNO Eng Research and Software Ltd)

4.2.5 Boundary Types and Conditions

The boundary type specification of each surface is presented in *Table 4.5* while a summary of the boundary conditions applied to the various surfaces follows.

Table 4.4 Boundary type specification of surfaces

Surface	Boundary Type
Inlet	velocity inlet
Outlet	pressure outlet
Free surface, upper edge, lower edge	symmetry
Rotor blades, hub, pod, monopile, seabed	wall

Velocity Inlet: Owing to the presence of the free surface of the sea and the sea bed the velocity along the column is not constant. The vertical velocity profile for a study (Small 2003) conducted on the Gulf of Corryvereckan was therefore used. This non-dimensional profile is based on a combination of the theory of open channel flow outlined by Chow (1959) and physical measurement and observation in the west coast of Scotland. It is as shown in the *Figure 4.4*.

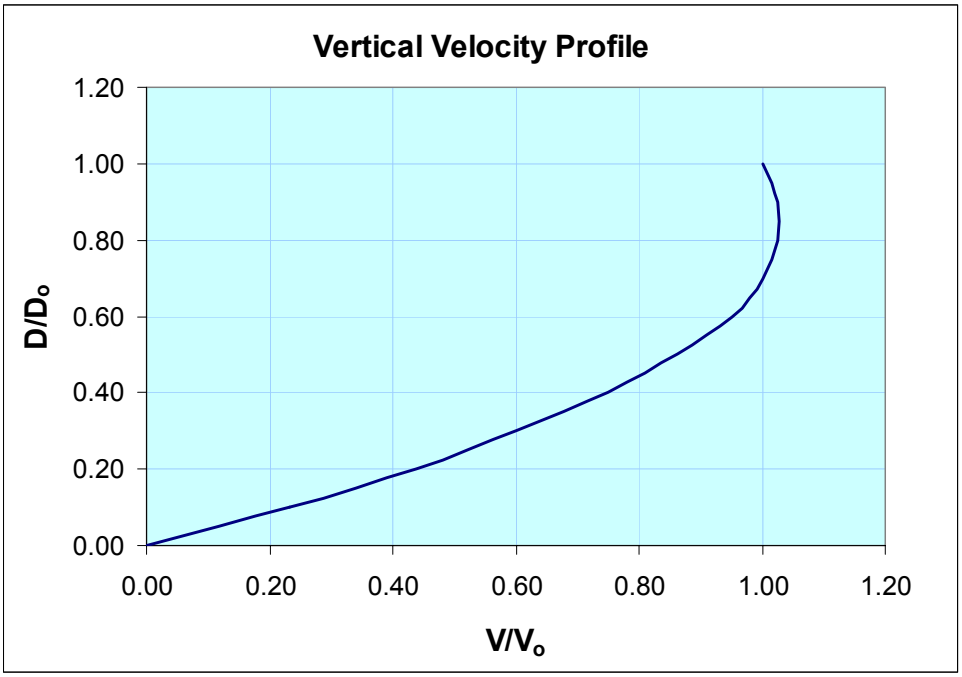

Figure 4.4 Non-dimensional vertical velocity profile typical in the west coast of Scotland

Three regimes of this profile were used. One with a surface current speed of 3 m/s, another with a surface current speed of 4 m/s and yet another with a current speed of

1 m/s as shown in *Figures 4.5*. These values were chosen to investigate the effects of changing tidal speeds from spring tides to neap tides.

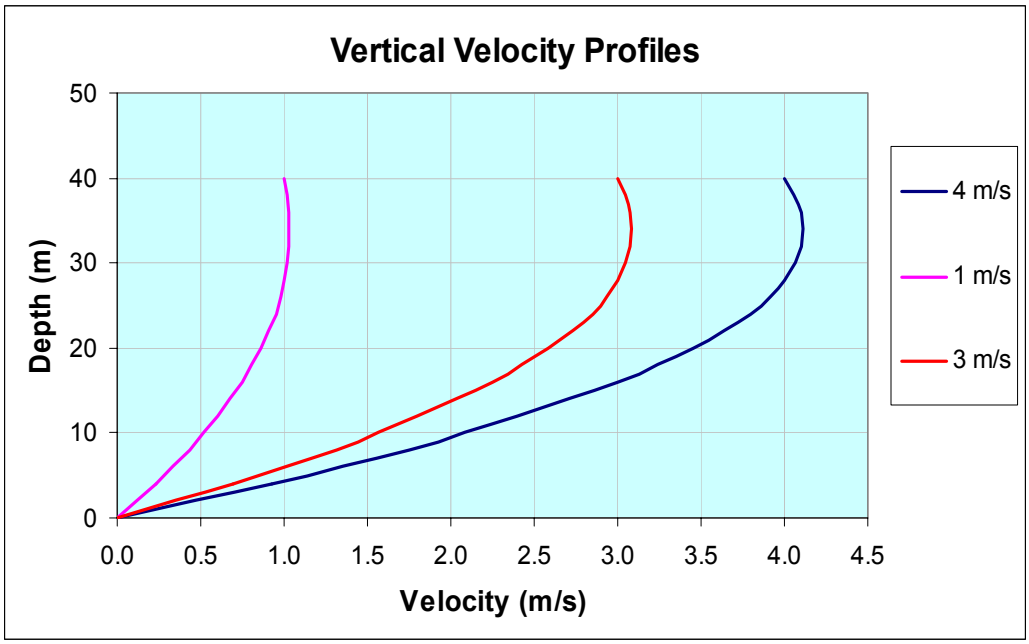

Figure 4.5 Vertical velocity profile of a water depth of 40 m and surface speeds of 4, 3, and 1 m/s

Pressure Outlet: A condition of velocity continuity and no backflow was assumed at the outlet. In this case the "jet" output from the channel does not mix with the ambient waters. Mixing will occur eventually but this will manifest itself outside the channel boundary and therefore was not considered. Atmospheric pressure was therefore specified for the outlet.

Rotor Blades: The turbine blades were assumed to be hydrodynamically smooth. Its rotation was accounted for using the Multiple Reference Frame (MRF) where its rotational speed was set to 10 rpm (1 rad/s).

Hub, Pod, Monopile: These wall surfaces were assumed to be hydrodynamically smooth (negligible roughness effects) with roughness height of 0.2 m.

Seabed: The roughness of the seabed was assumed to be in the transitional regime where the roughness effects become increasingly important.

Free surface, Upper edge, Lower edge: These were specified as symmetry.

4.3 Model Validation

It is a good practice to compare CFD results to experimental data in order to validate the CFD model. However in the absence of experimental data, simplified analytical solutions may be of use. This is what this section seeks to do, compare the CFD results to an analytical treatment of a simple channel. It involves the theory of flow in a channel with energy extraction, a determination of the average velocity along the channel and comparison with that generated by the CFD model.

4.3.1 Flow Equations of a Simple Channel

For a simple channel, with a horizontal bed, linking two infinite oceans, if the dynamic effects resulting from the time variation of the water elevation are neglected, a simple static open water flow model, as in Bryden (2004), can be used to investigate the result of energy extraction.

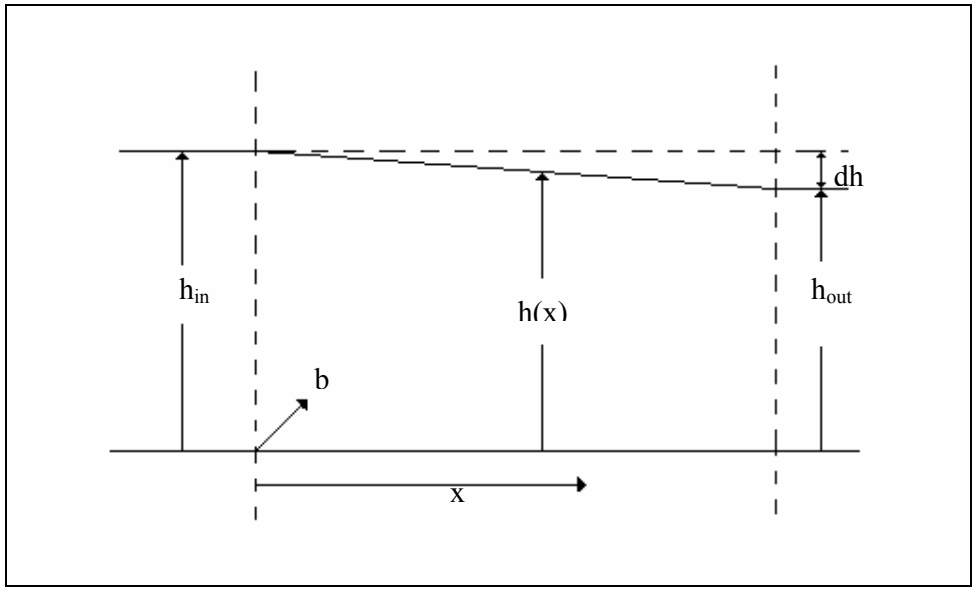

Figure 4.6 Figure Schematic diagram of a simple channel

If the flow is driven by the static head difference, *dh*, between each end of the channel and assuming a constant speed over the cross section, the behaviour of water in the channel can be determined by equation (28).

$$\left(1-\frac{Q^2}{h^3b^2g}\right)\frac{\partial h}{\partial x}=\frac{\partial b}{\partial x}\frac{Q^3}{gh^2b^3}-\frac{1}{\rho gbh}P_{er}\tau_0 \qquad \ldots (28)$$

where

Q is the discharge (m^3/s)

g is the acceleration due to gravity (m^2/s)

P_{er} is the wetted perimeter (m)

τ_0 is the bed shear stress ($kg/m/s^2$)

The shear stress term τ_0 can be expressed in terms of the Chezy friction coefficient C as shown below;

$$\tau_0=\rho\frac{g}{C^2}U^2 \qquad \ldots (29)$$

Chezy coefficient C is calculated using a simple empirical formula produced by Manning given by:

$$C=\frac{R^{\frac{1}{6}}}{n} \qquad \ldots (30)$$

where

R is the hydraulic radius which, in this case is the ratio of the cross sectional area of the flow to the wetted perimeter length

n is a term which characterises the surface roughness

The act of power extraction will result in an additional retarding force on the fluid. If the power is extracted at a rate of P_x W/m^3, the retarding force on a slug of water as it passes through the defined cross section would be equivalent to an additional shear stress given by:

$$\tau_e=\frac{P_xR}{U} \qquad \ldots (31)$$

The effective shear stress for calculation purposes would become:

$$\tau_t = \tau_0 + \tau_e \qquad \ldots (32)$$

4.3.2 Boundary Conditions

The transition between static water in the open ocean and the dynamic conditions within the channel can be modelled by considering an initial drop in the elevation head as a result of accelerating the flow. This drop in elevation can be related to the speed of the flow just down stream from the entrance to the channel using the following equation:

$$\Delta h = \frac{U^2}{2g} \qquad \ldots (33)$$

It can be assumed that the "jet" output from the channel does not rapidly mix with the ambient waters and, as such a condition of velocity continuity can be assumed.

Equation (28) can be integrated from a known depth, h_{out}, to determine the upstream depth, h_{in}, as a function of the discharge rate, Q. If h_{in} is known, then the value of Q can be readily determined by iteration. Once the value of Q has been established as a function of h_{in} and h_{out} it is possible to calculate the depth and water speed as a function of position in the channel.

4.3.3 Determination of Average Velocity along Channel Length

The inputs required to determine the average velocity profile along the channel are as shown in *Table 4.5*. Manning's n was taken from Chow (1959) while the average current speed at inlet is calculated form the velocity profile with surface current speed of 3 m/s. Substituting this values into equation (28) and solving gives the velocity distribution and this is compared to that from the CFD model shown in *Figure 4.7*.

Table 4.5 Inputs to solve equation

Description	Symbol	Value
[5]Manning's n	n	0.03
[6]Average current speed (m/s)	U	2
Channel width (m)	b	500
Density of seawater (kg/m^3)	ρ	1030
Rated mechanical power (kW)	P	334
Channel x-sectional area (m^2)	A	20 000
Channel wetted perimeter (m)	P_{er}	580

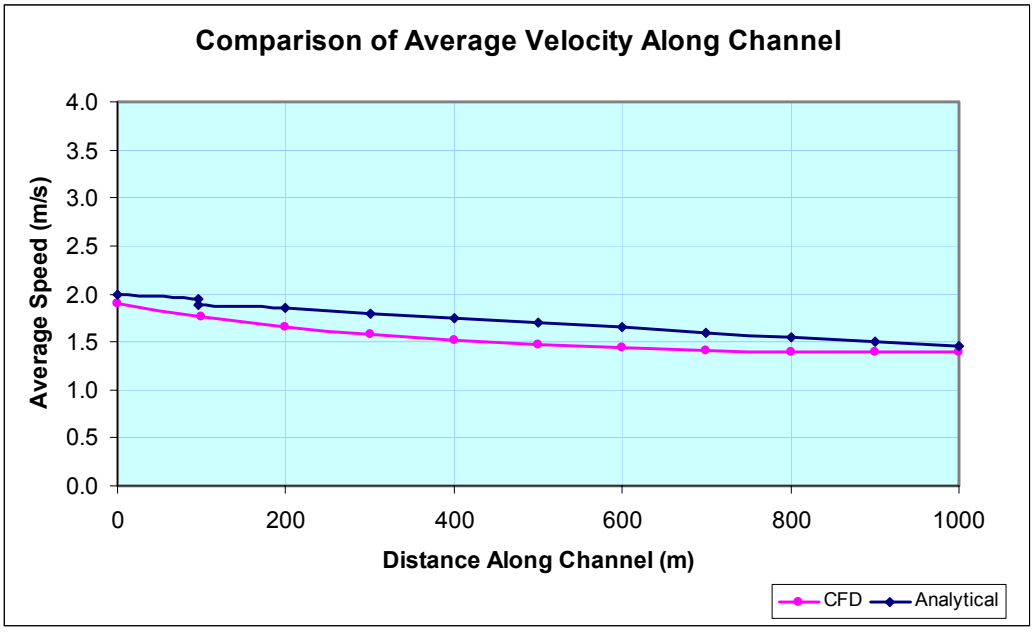

Figure 4.7 Comparison of CFD and analytical average velocity along channel

The results show that there is a close correlation between the results generated by the analytical method and the CFD model. The difference may be due to the fact that the effect of the structure has not been taken into consideration for the analytical method. The result generated by the model is therefore fairly reasonable within the limits of simplifying assumptions.

[5] Taken from Chow (1959)
[6] Calculated from the velocity profile with surface current speed of 3 m/s

CHAPTER FIVE – RESULTS AND DISCUSSION

5.0 Introduction

The graphs generated by CFD programs are almost always pretty, however one need not be deceived by their appeal but rather be mindful of their implications and limitations. This section is in three parts. The first is to compare the results generated for the two depths of deployment of the rotor blades. In this case a surface speed of 3 m/s was used to generate the vertical velocity profile at inlet. Surface speeds of 4 m/s and 1 m/s were then used to generate two other vertical velocity profiles and their effect on the flow past the turbines investigated. For each velocity profile three set of results have been presented; the resource, Turbine 1 and Turbine 2 and each result is examined in three views; plan, front and side views. Flow is from left to right.

5.1 Results for a Surface Current Speed of 3 m/s

5.1.1 Resource

Results of the velocity distribution in the channel without energy extraction are as follows. *Figure 5.1* shows the progress of the solution during the iterative process. It took 239 iterations for the solution to converge.

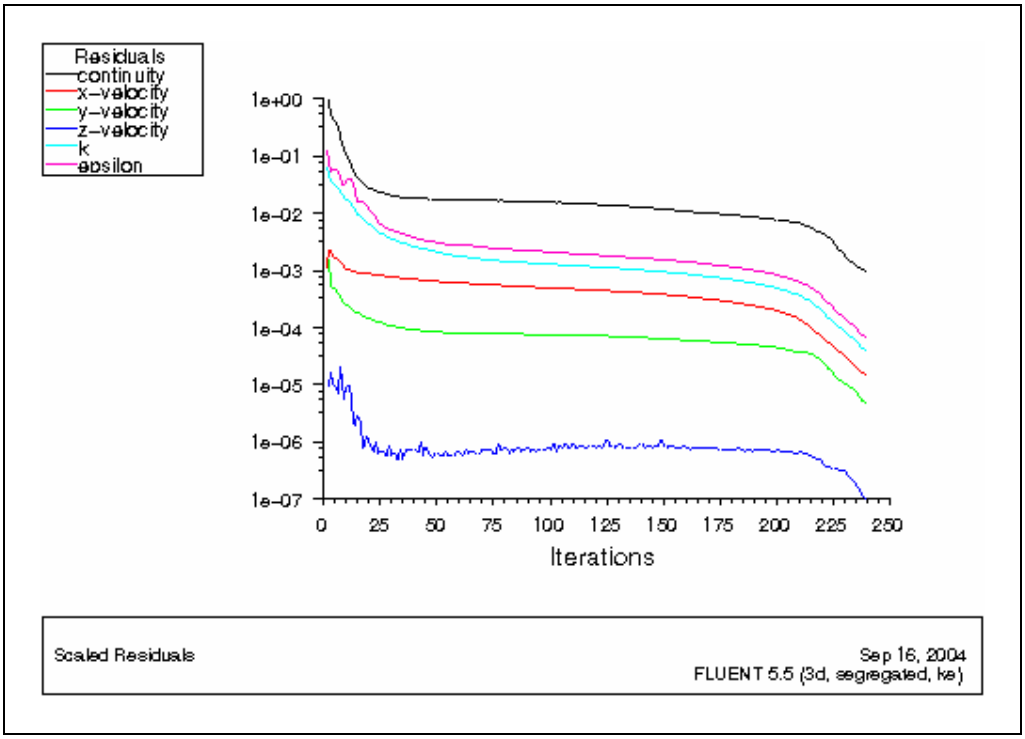

Figure 5.1 A plot of residuals of the resource simulation

Figures 5.2, 5.3 and *5.4* show different views of the velocity distribution in the channel without energy extraction. It is observed that there is little change in the distribution across its length and breath. The slight decrease in the velocity (negligibly small and difficult to see) along the length of the channel is as a result of the resistive frictional force on the seabed.

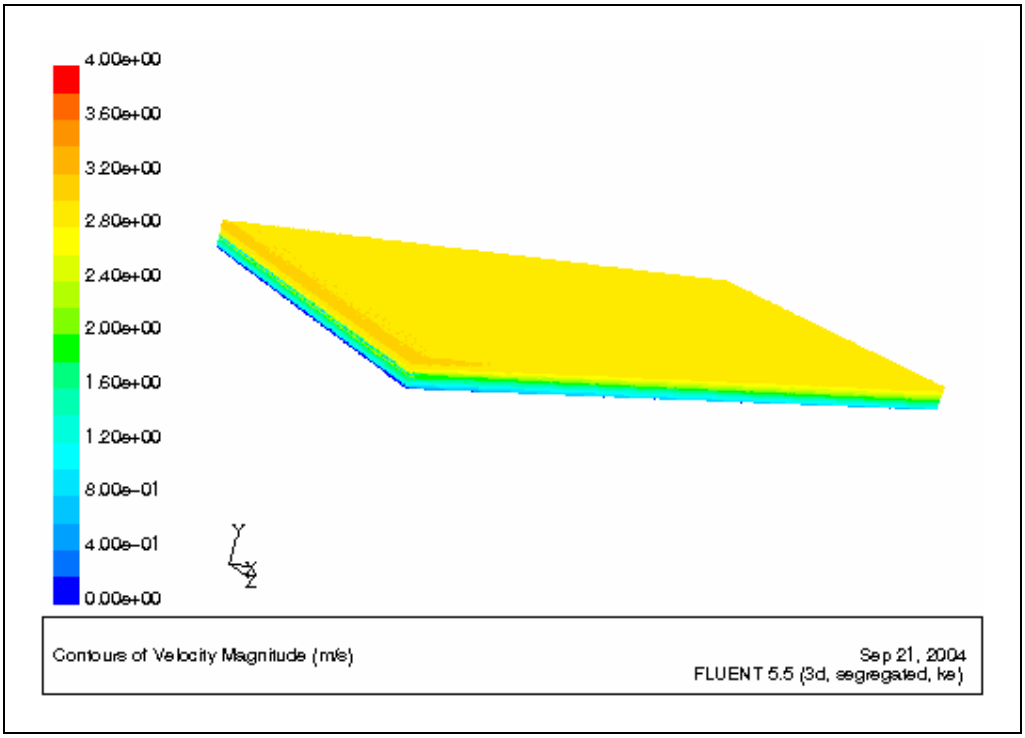

Figure 5.2 3-Dimensional rendering of the velocity distribution in the channel

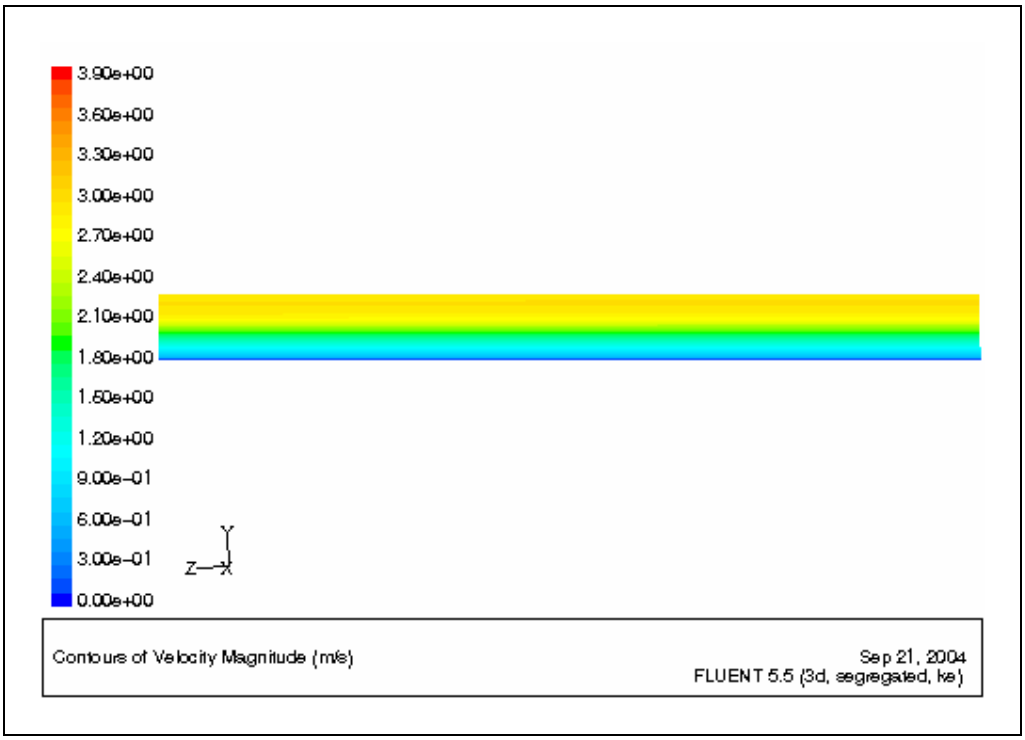

Figure 5.3 Front view of the vertical velocity distribution in the channel

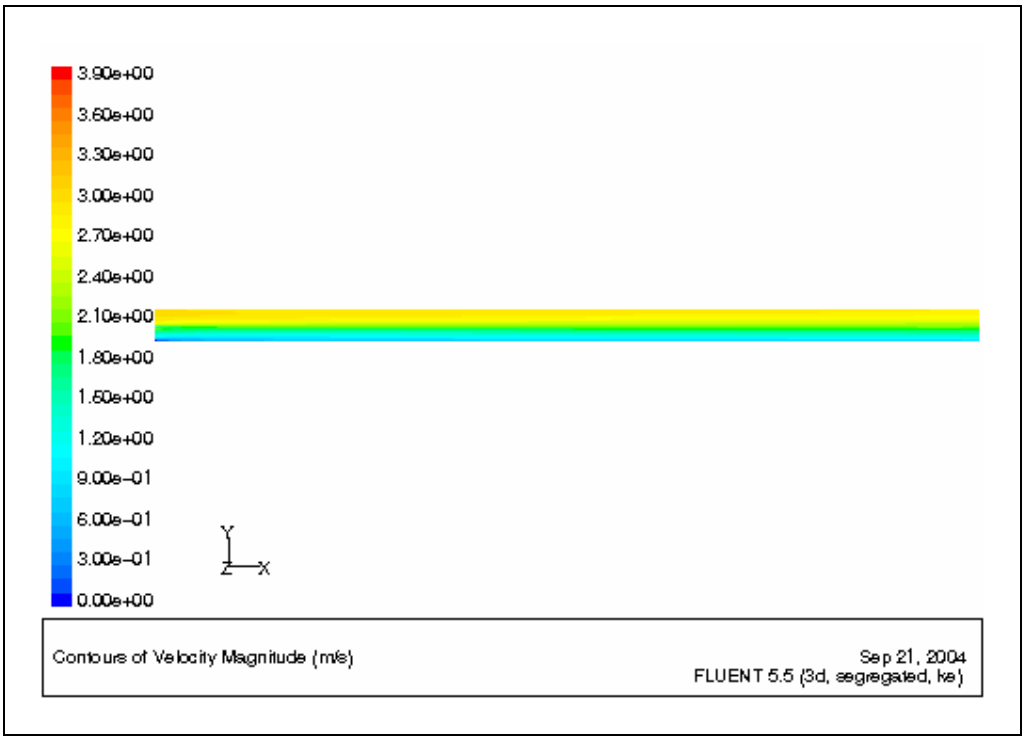

Figure 5.4 Side view of the vertical velocity distribution in the channel from inlet to outlet

5.1.2 Turbine 1

For this turbine the turbine blades are deployed 5 m below the water free surface. The resulting average velocity across the rotor blades is 3 m/s (higher than the rated speed of 2.7 m/s). It took 337 iterations for the solution to converge as shown in *Figure 5.5.*

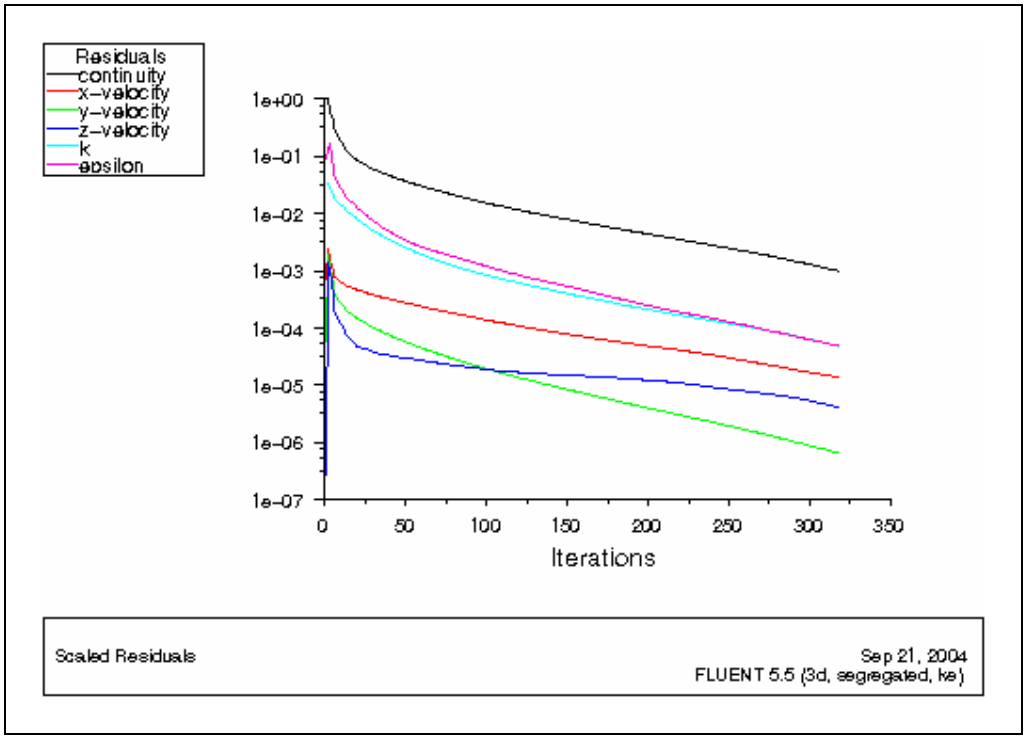

Figure 5.5 Residual plot of the variables for Turbine 1

5.1.2.1 Plan View of Turbine 1 in Channel

The plan view of the turbine 1 in the channel is shown in *Figures 5.6* and *5.7*. The former shows the surface velocity distribution across the turbine. The surface velocity at the inlet is fairly constant across the width. As the flow gets closer to the turbine it deflects, finding the path of least resistance. This is in agreement with Betz Law. This results in a distortion of the profile with the maxim velocity occurring midway between the turbine and the channel edges. Since the monopile serves as an obstacle to the flow the minimum velocity is observed in its wake (0 - 0.3 m/s directly behind it). However this recovers to 2.5 m/s approximately 400 m downstream. *Figure 5.7* gives a close up view of the flow around the turbine.

Vortices generated by the rotation of the rotor blades are observed on either side of the monopile. These vortices contribute to the broadening of wake development downstream. Generally there is approximately 23 % (3 to 2.3 m/s) reduction in the surface velocity with respect to the 1000 m long channel but a 7 % (2 to 1.86 m/s) decrease I the average velocity across the vertical column of the channel.

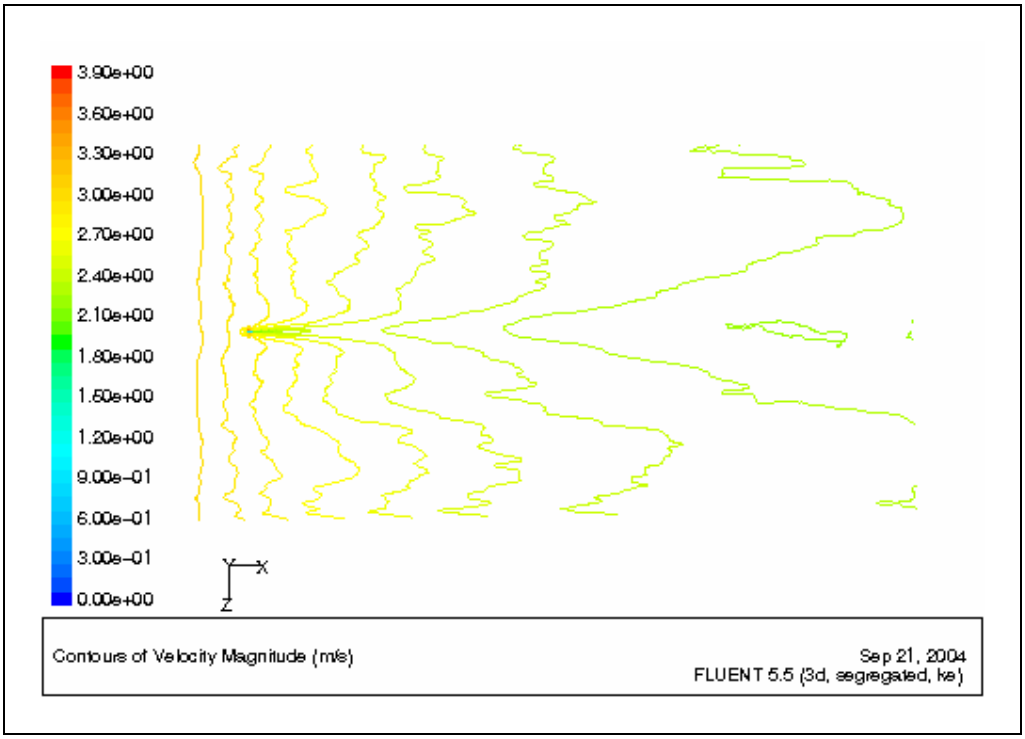

Figure 5.6 Plan view of Turbine 1 in channel showing the deformation of the surface velocity

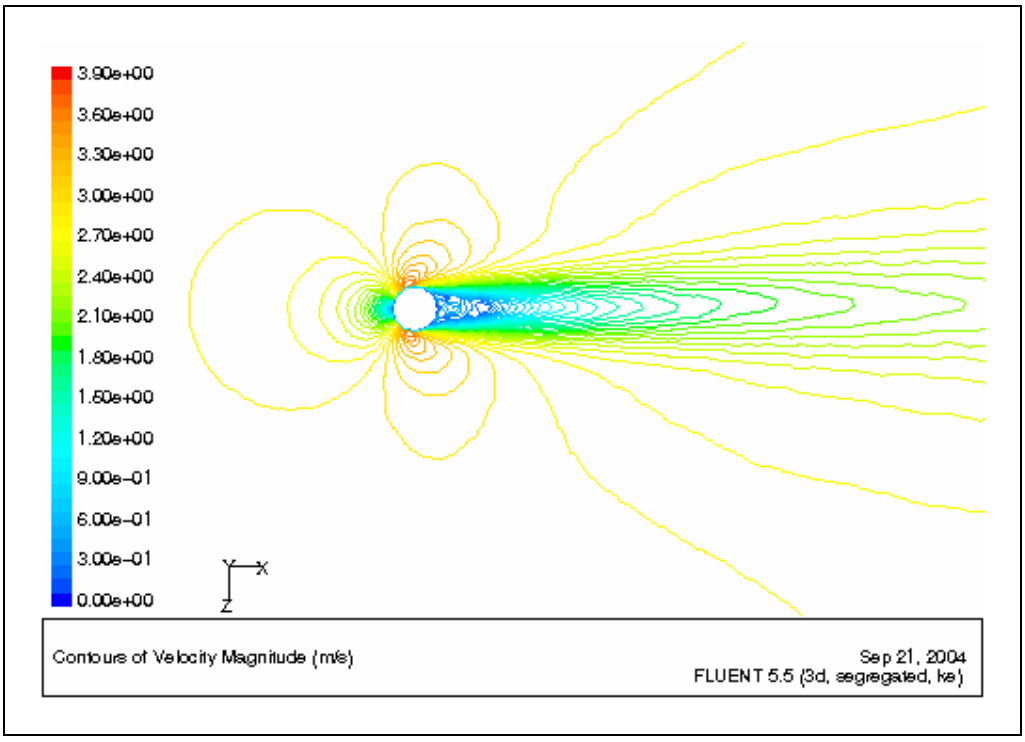

Figure 5.7 Close up plan view of Turbine 1 showing formation of vortices and wake

5.1.2.2 Front View of Turbine 1 in Channel

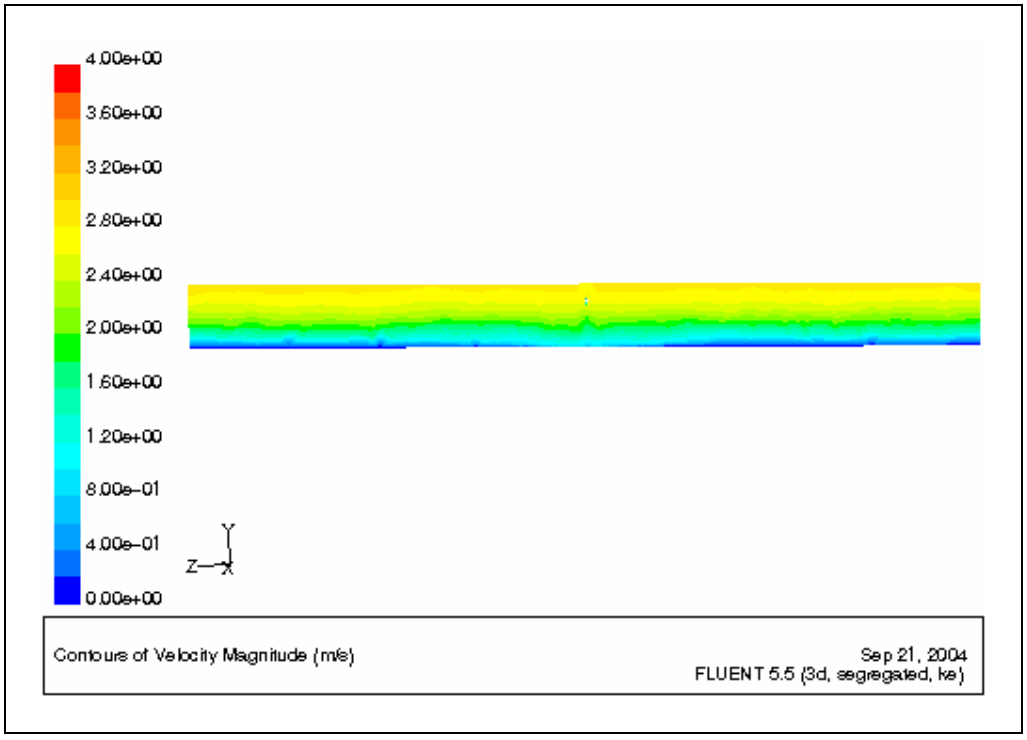

Figure 5.8 Front view of Turbine 1 in channel showing wavy velocity beneath rotor blades

The front view of the turbine is shown in *Figure 5.8 and 5.9.* Comparing *Figure5.8* to *Figure 5.2* it is observed that there is a distortion in the velocity distribution in the former. The energy transfer from the flow to the rotor blades as well as the rotation of the blades causes a scoping effect. A wave pattern is therefore observed across the channel which is stronger beneath the blades. This leads to upwelling of the flow close to the seabed in that region. This is clearer in the close up view shown in *Figure 5.9*.

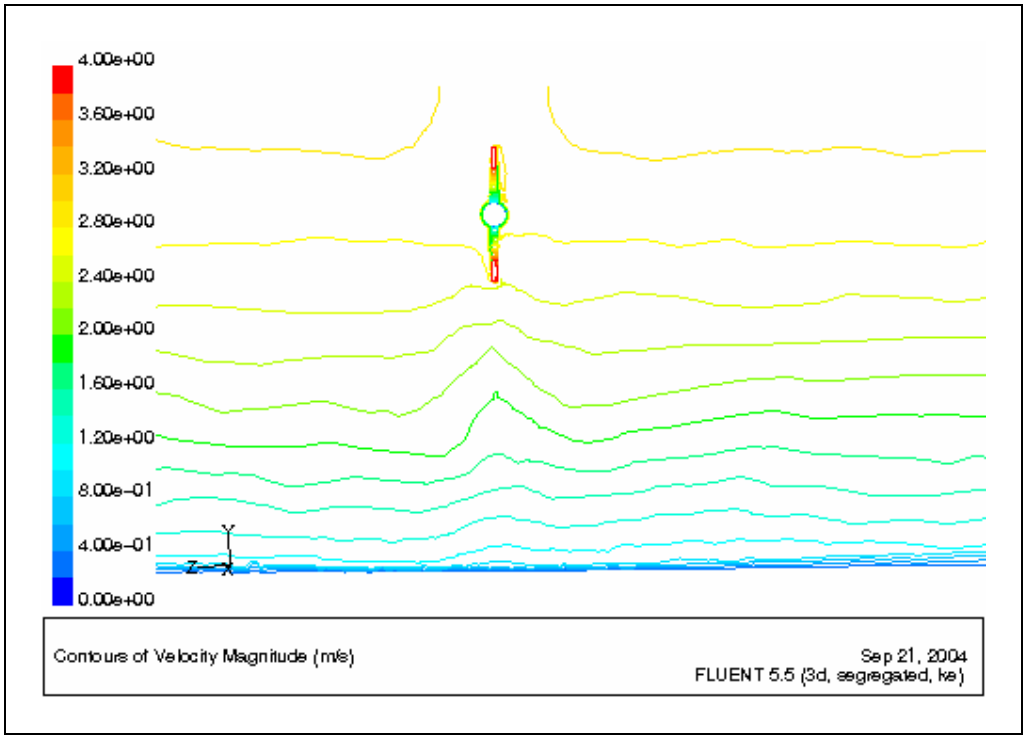

Figure 5.9 Close up front view of Turbine 1 showing upwelling beneath rotor blades

5.1.2.3 Side View of Turbine 1 in Channel

Figure 5.10 and 5.11 shows the side view of the turbine in the channel. It is observed that there is a distortion of the vertical velocity profile. There is mixing and retardation of the flow leading to less varying velocity profile along the length of the channel, approximately constant at the outlet over 80 % of the height from the free surface. The greatest reduction in the speed occurs across the turbine and structure. This is as a result of the energy extraction by the rotor blades and obstruction of the flow by the structure. *Figure 5.11* shows high level of turbulence around the structure.

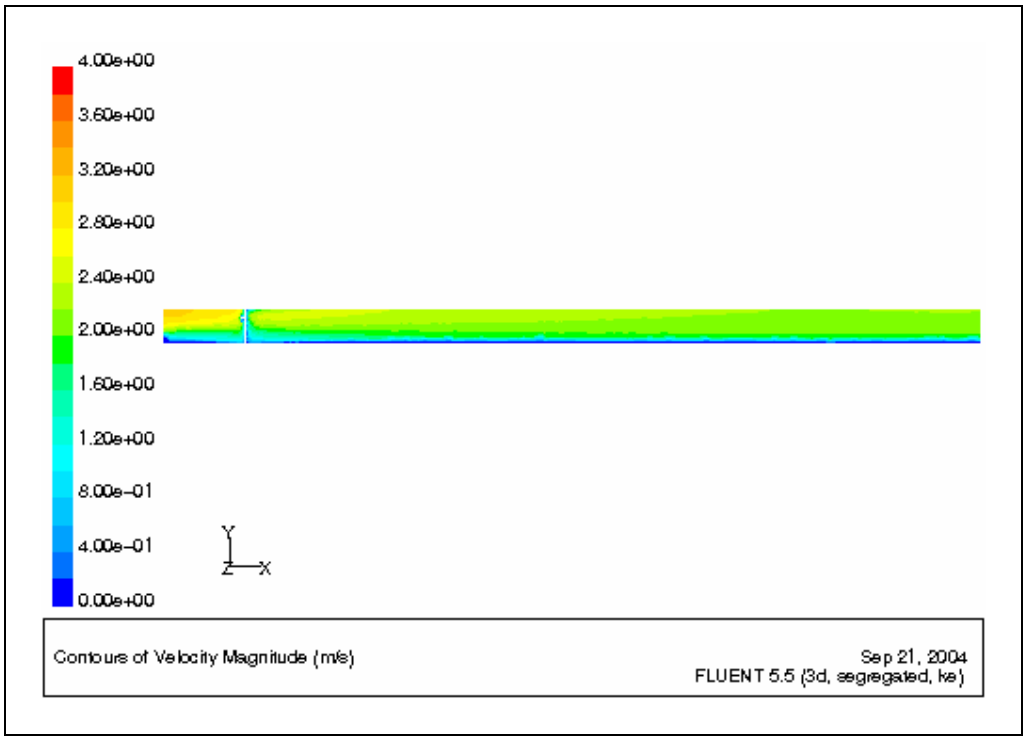

Figure 5.10 Side view of Turbine 1 showing the velocity distribution across the length of the channel

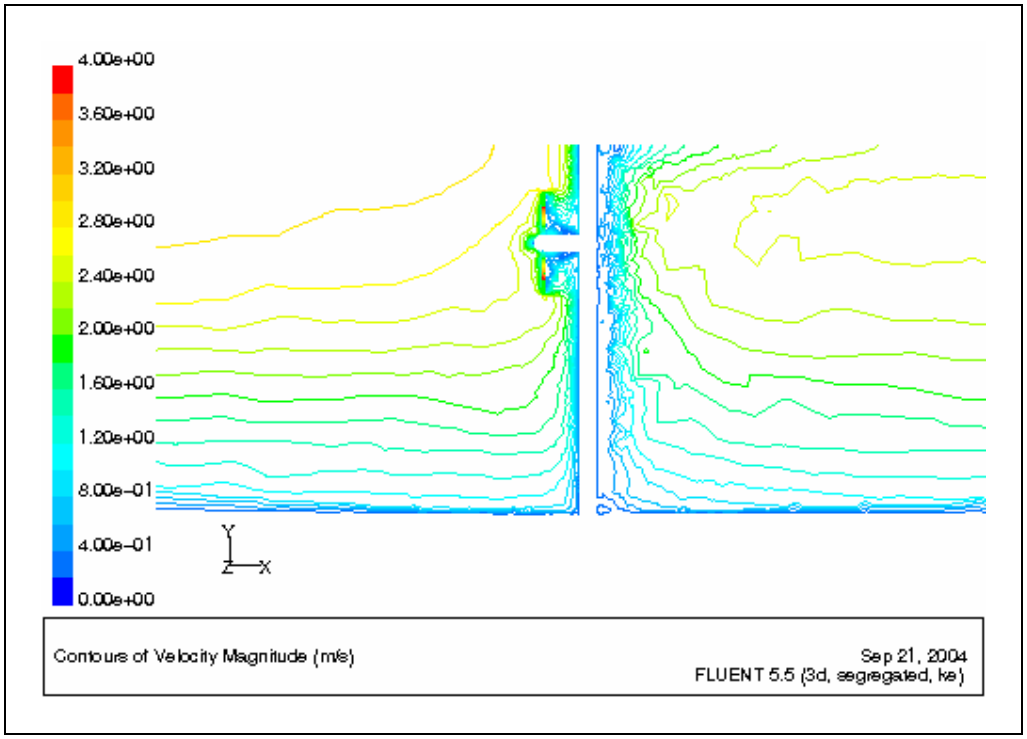

Figure 5.11 Close up view of Turbine 1 showing increased turbulence around the structure

5.1.3 Turbine 2

The turbine blades in this case have been deployed 10 m below the free surface of the channel. The average current speed across the rotor blades is therefore 2.8 m/s. The iterative process went through 361 iterations before convergence as shown in *Figure 5.12.*

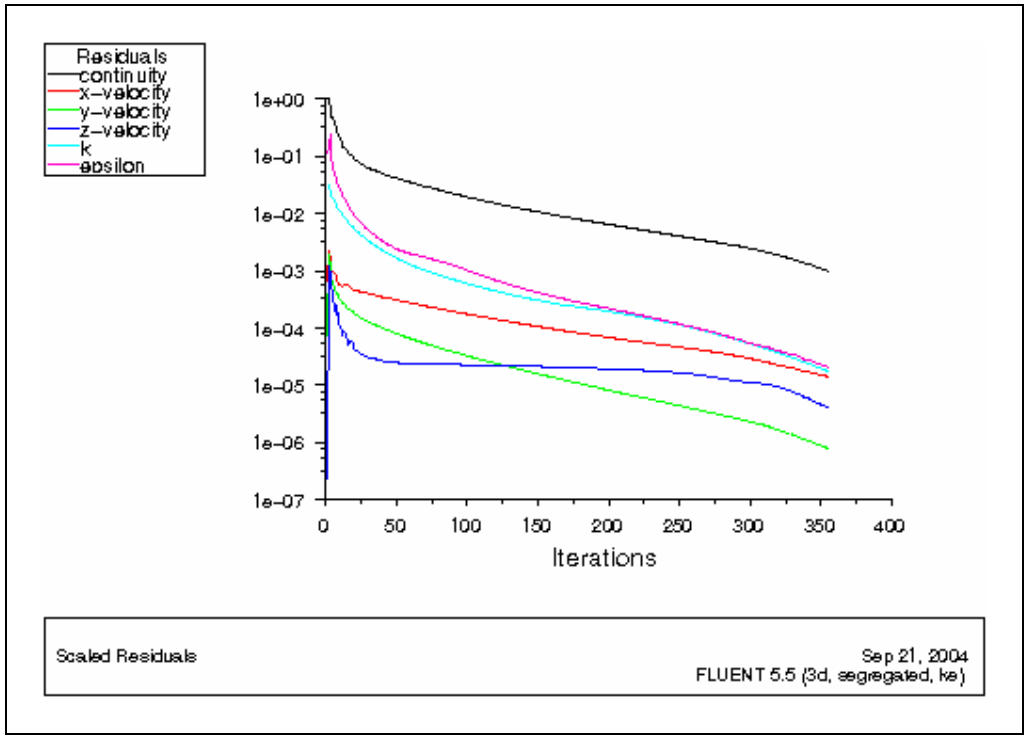

Figure 5.12 Residual plot of the variables for Turbine 2

5.1.3.1 Plan View of Turbine 2 in Channel

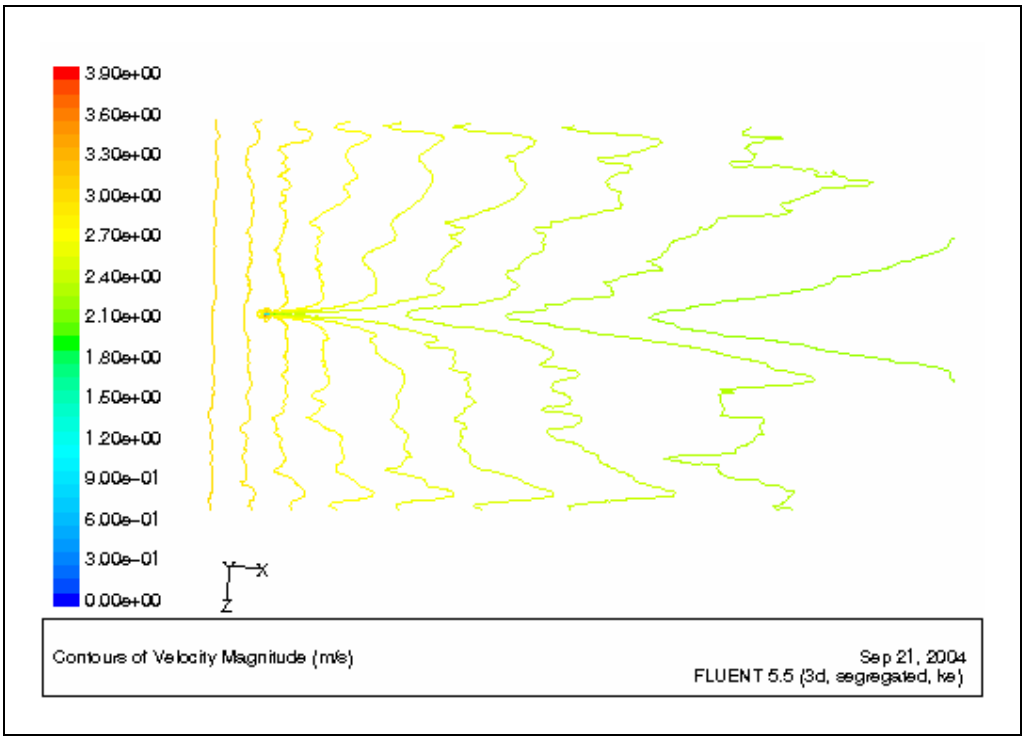

Figure 5.13 Plan view of Turbine 2 in channel showing deformation of the surface velocity

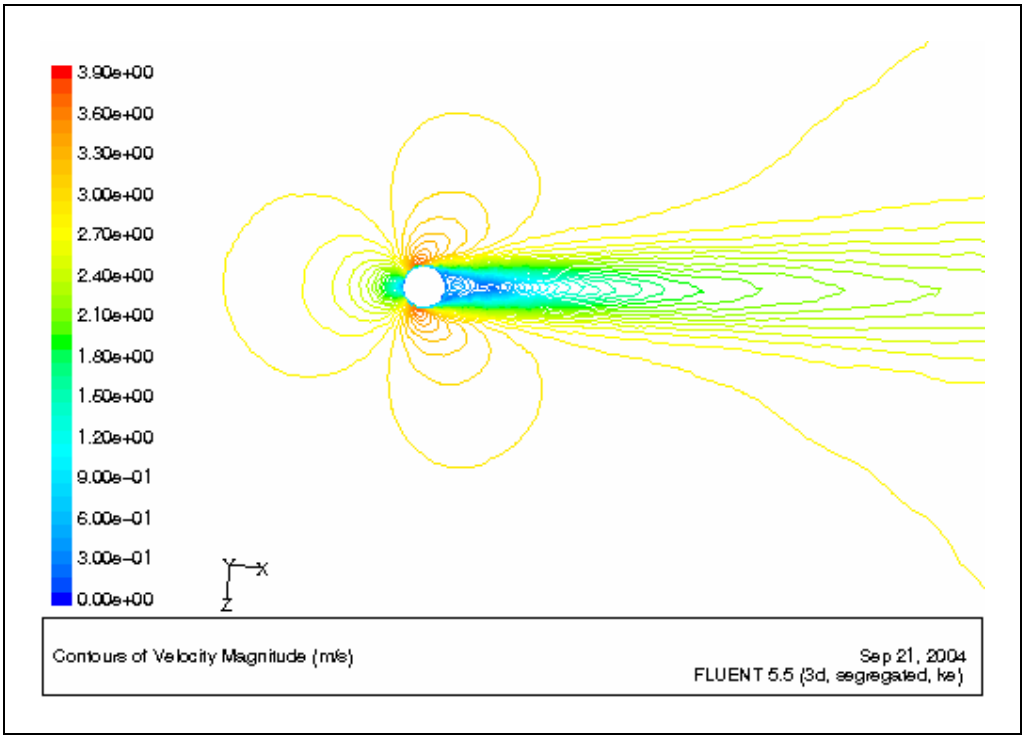

Figure 5.14 Close up plan view of Turbine 2 showing formation of vortices and wake

5.1.3.2 Front View of Turbine 2 in Channel

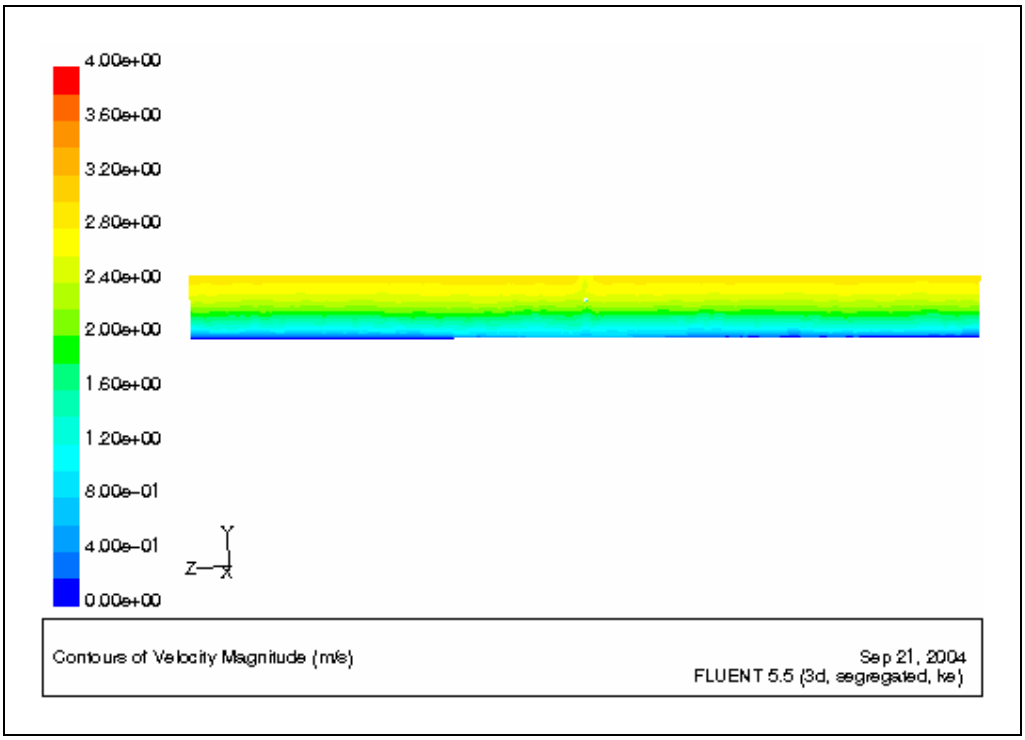

Figure 5.15 Front view of Turbine 2 in channel showing wavy velocity beneath rotor blades

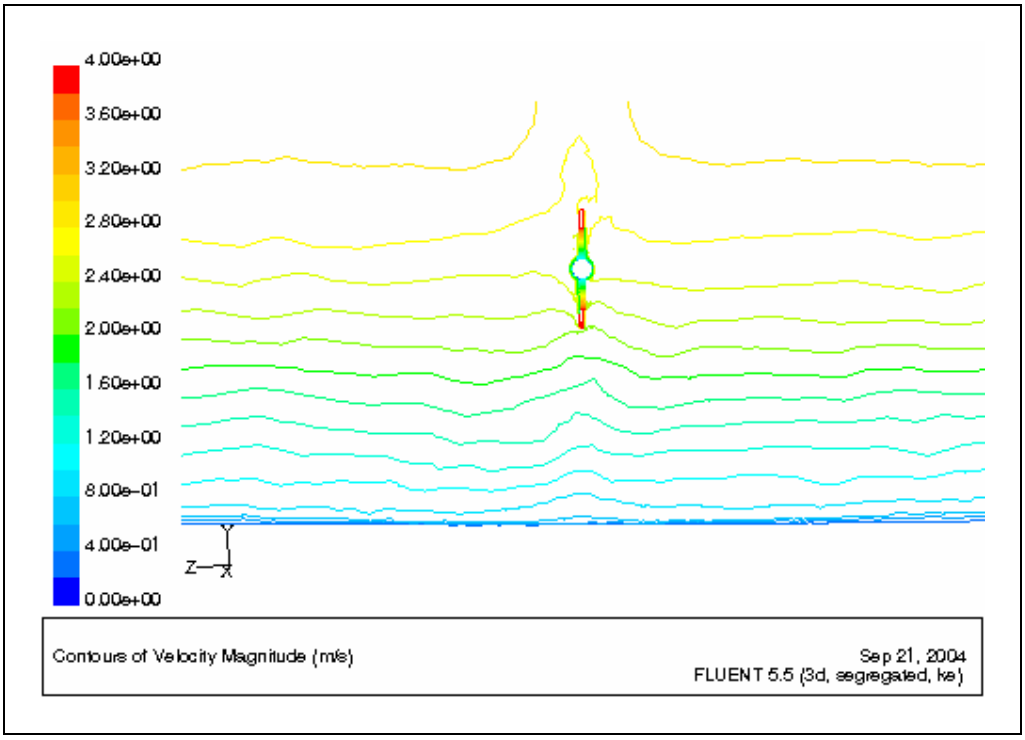

Figure 5.16 Close up front view of Turbine 2 showing upwelling beneath rotor blades

5.1.3.3 Side View of Turbine 2 in Channel

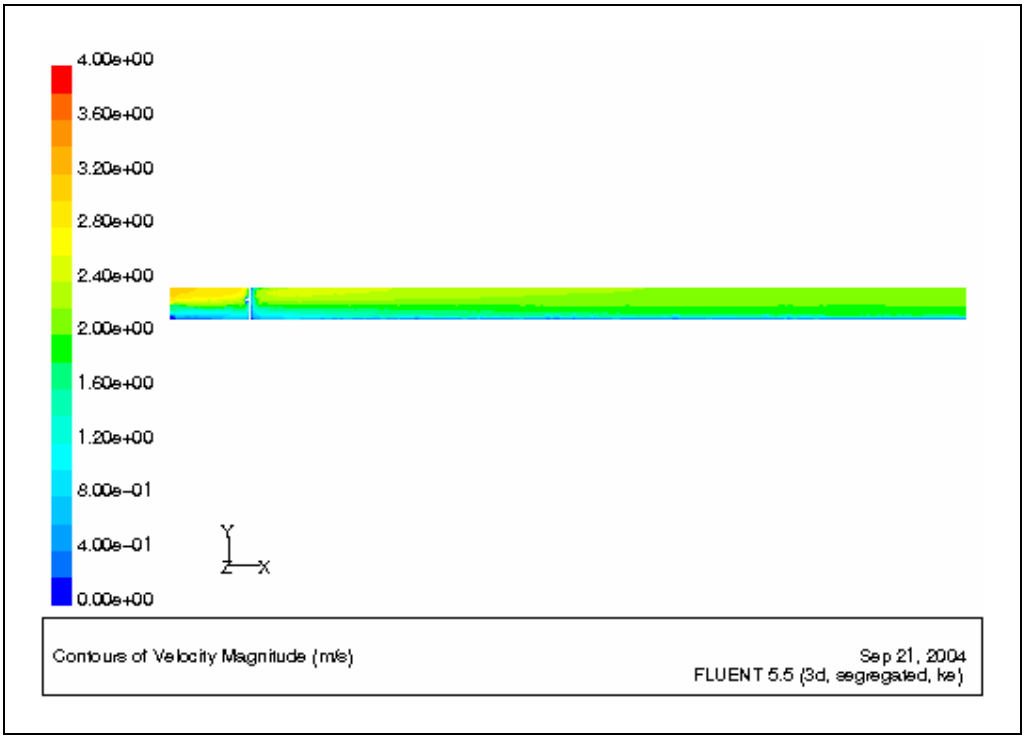

Figure 5.17 Side view of Turbine 2 showing the velocity distribution across the length of the channel

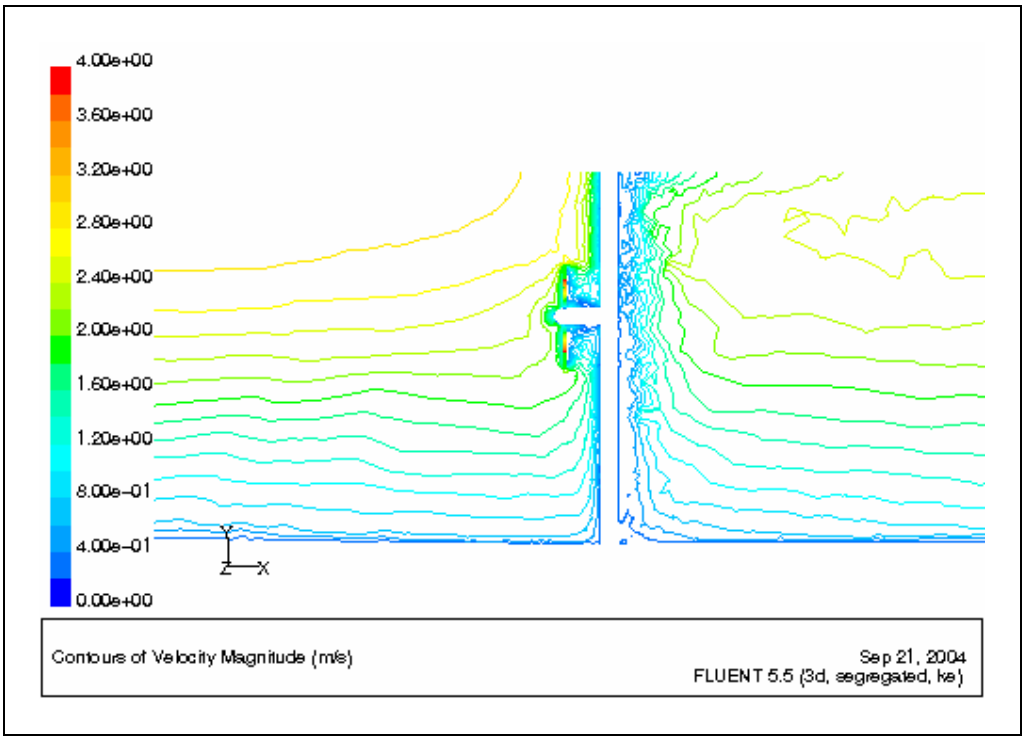

Figure 5.18 Close up view of Turbine 2 showing increased turbulence around the structure

5.1.4 Comparison of Results for Turbine 1 and Turbine 2

Comparing the results of Turbine 1 and Turbine 2 two main observations are evident. The first is the nature of the wake formed behind the structure. The wake formed behind Turbine 1 is more profound or broader than that formed behind Turbine 2. The reason is that Turbine 1 is under the influence of a less water weight (hence less hydrostatic pressure) considering its proximity to the water surface. It is therefore able to manipulate the flow more easily than Turbine 2 which is under the influence of a larger weight of fluid. Moreover the rotor blades for Turbine 2 are exposed to a smaller average current speed, i.e. lower part of velocity profile. There is therefore a greater recovery of the wake in Turbine 2 than Turbine 1.

Secondly there is slightly greater upwelling of the flow under the rotor blades for Turbine 2 than Turbine 1. Moreover the spread of the upwelling is greater for Turbine 2 than Turbine 1. This is because of its closeness to the seabed. For instance at a depth of 2 m from the seabed, a current speed of 0.8 m/s is observed for Turbine 1 while that for Turbine 2 is approximately 0.85 m/s representing an increase of 6 %.

An examination of the side views of both turbines show that for Turbine 1 the distortion of the profile from inlet to outlet is higher resulting in a less varying velocity at the outlet of the channel, i.e. the velocity is fairly constant (approximately 2.3 m/s) over 80 % of the height reducing to zero towards the seabed. For Turbine 2 the velocity at outlet is also fairly constant (2.4 m/s) over approximately 50 % of the height and then decreasing to zero towards the seabed.

5.2 Results for a Surface Current Speed of 4 m/s

5.2.1 Resource

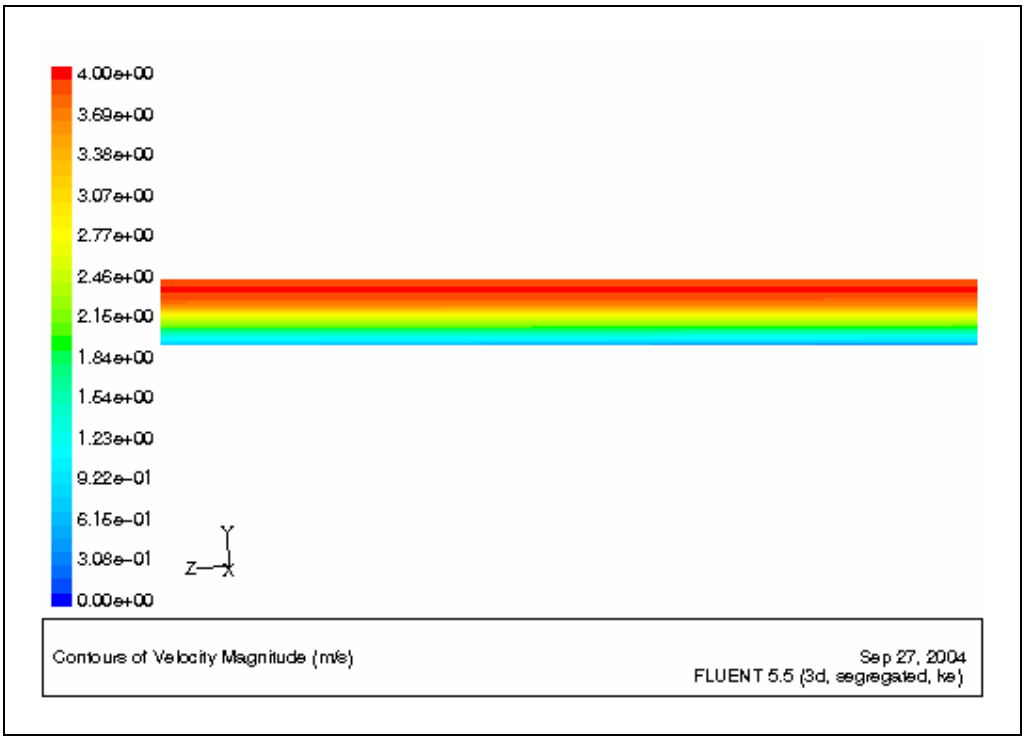

Figure 5.19 Front view of the vertical velocity distribution in the channel

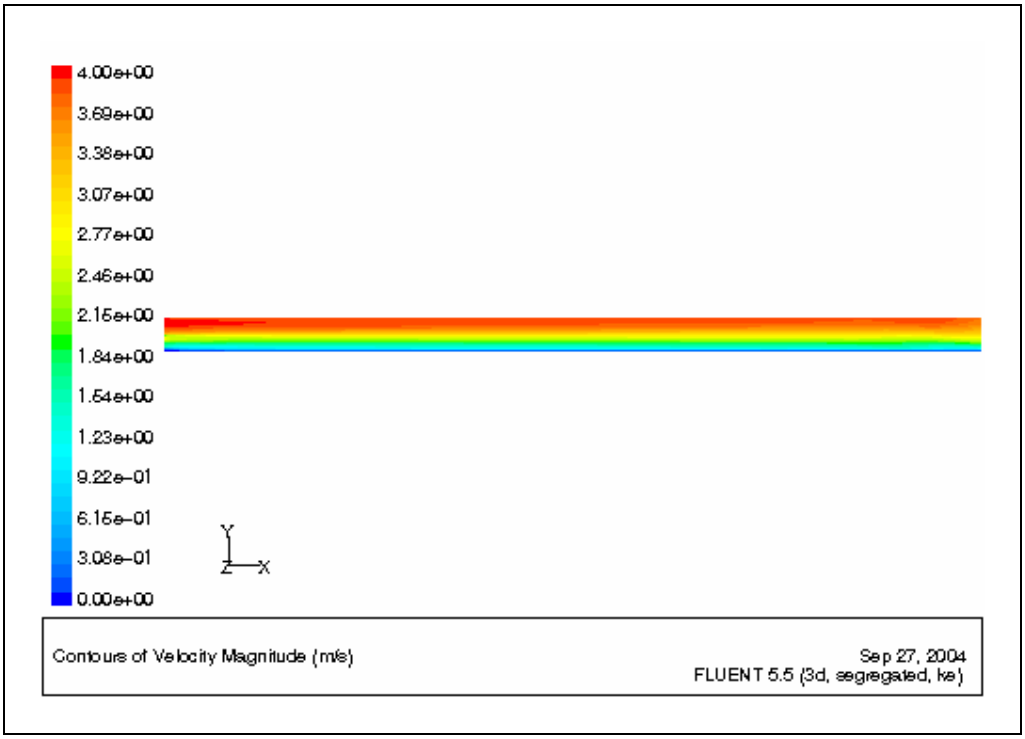

Figure 5.20 Side view of the vertical velocity distribution in the channel from inlet to outlet

5.2.2 Turbine 1

5.2.2.1 Plan View of Turbine 1 in Channel

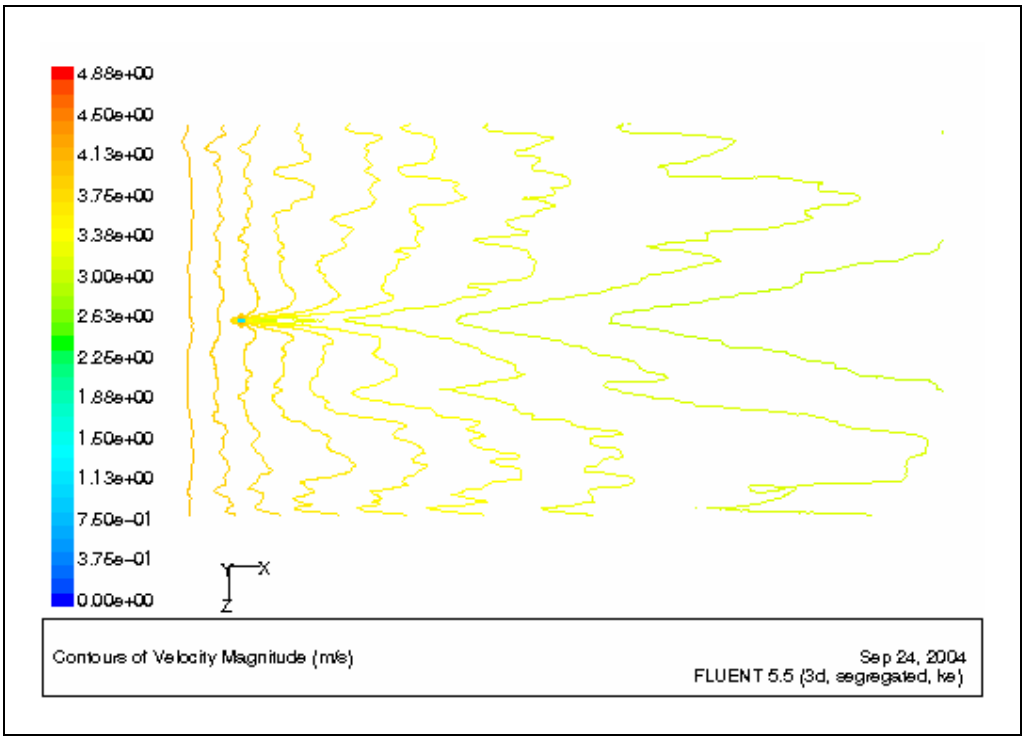

Figure 5.21 Plan view of Turbine 1 in channel showing deformation of the surface velocity

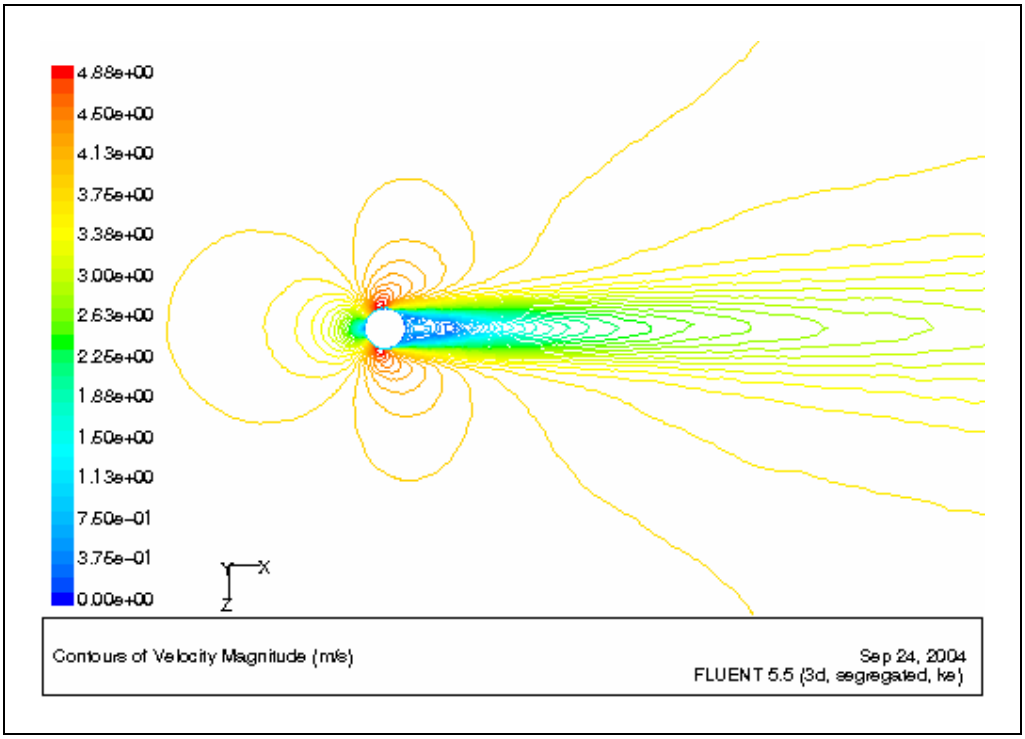

Figure 5.22 Close up plan view of Turbine 1 showing formation of vortices and wake

5.2.2.2 Front View of Turbine 1 in Channel

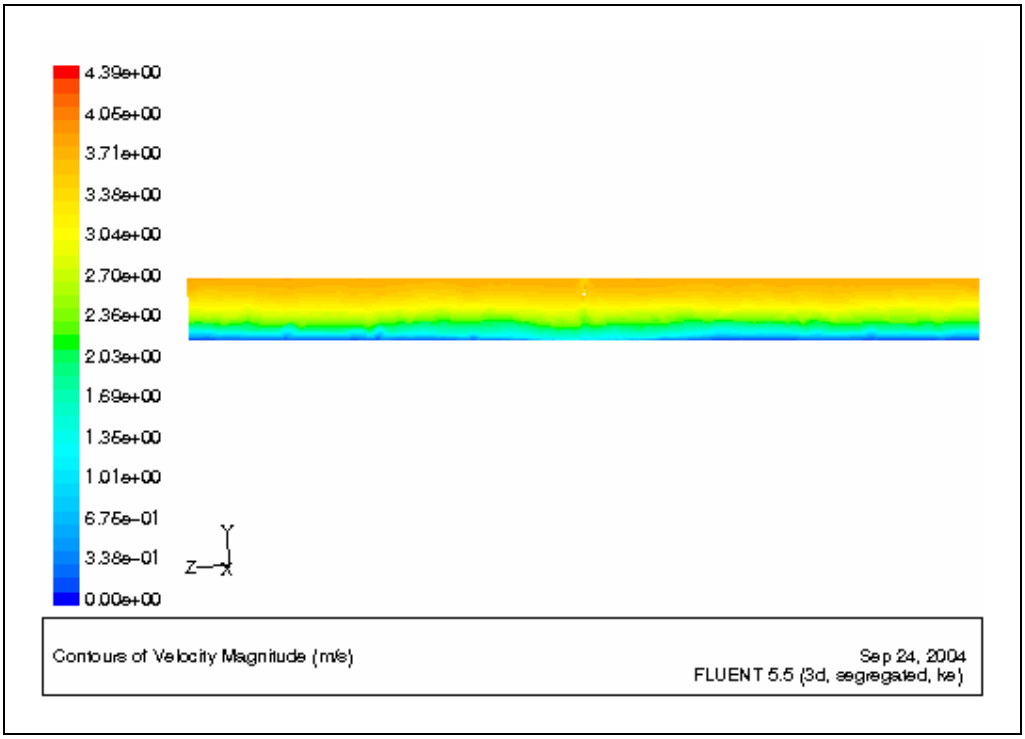

Figure 5.23 Front view of Turbine 1 in channel showing wavy velocity beneath rotor blades

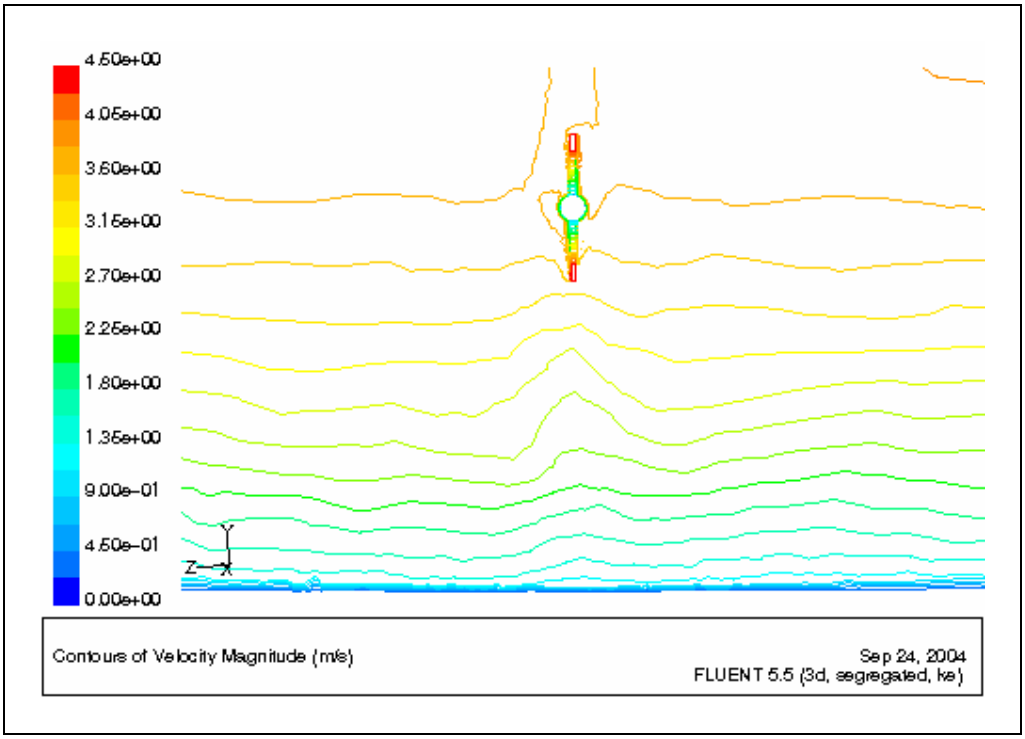

Figure 5.24 Close up front view of Turbine 1 showing upwelling beneath rotor blades

5.2.2.3 Side View of Turbine 1 in Channel

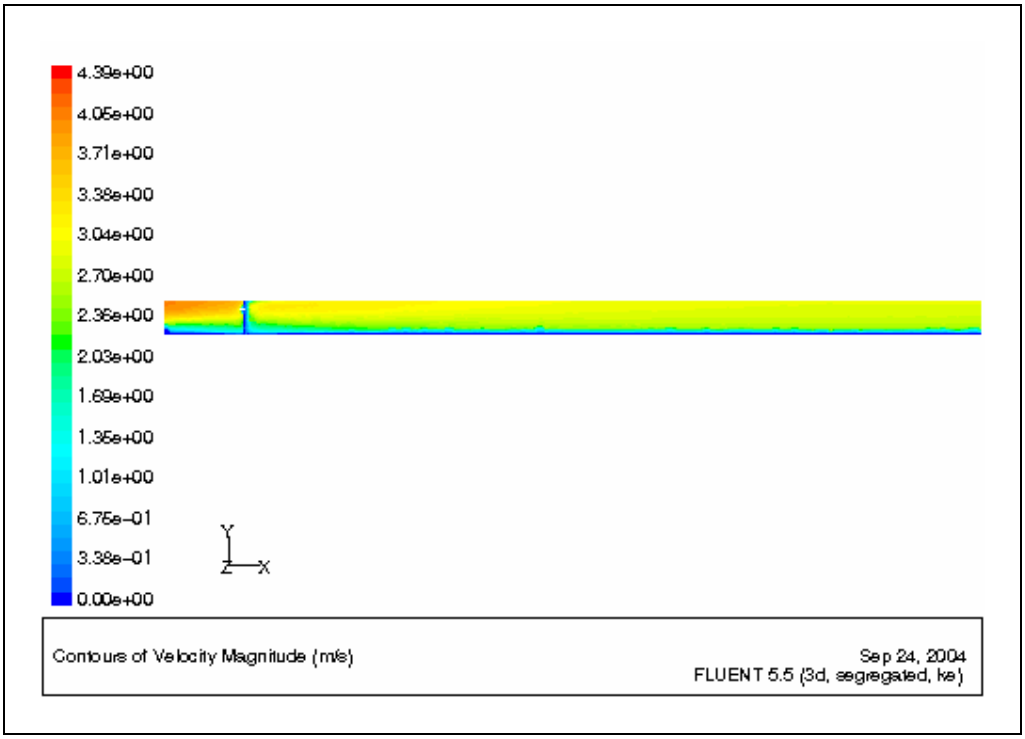

Figure 5.25 Side view of Turbine 1 showing the velocity distribution across the length of the channel

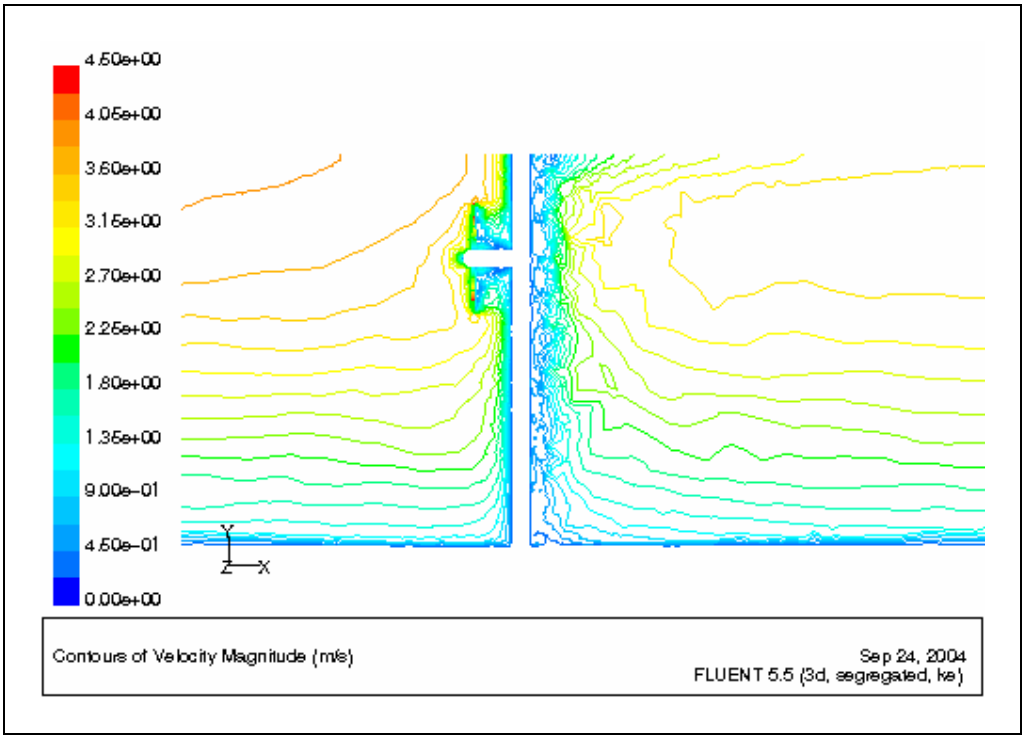

Figure 5.26 Close up view of Turbine 1 showing increased turbulence around the structure

5.2.3 Turbine 2

5.2.3.1 Plan View of Turbine 2 in Channel

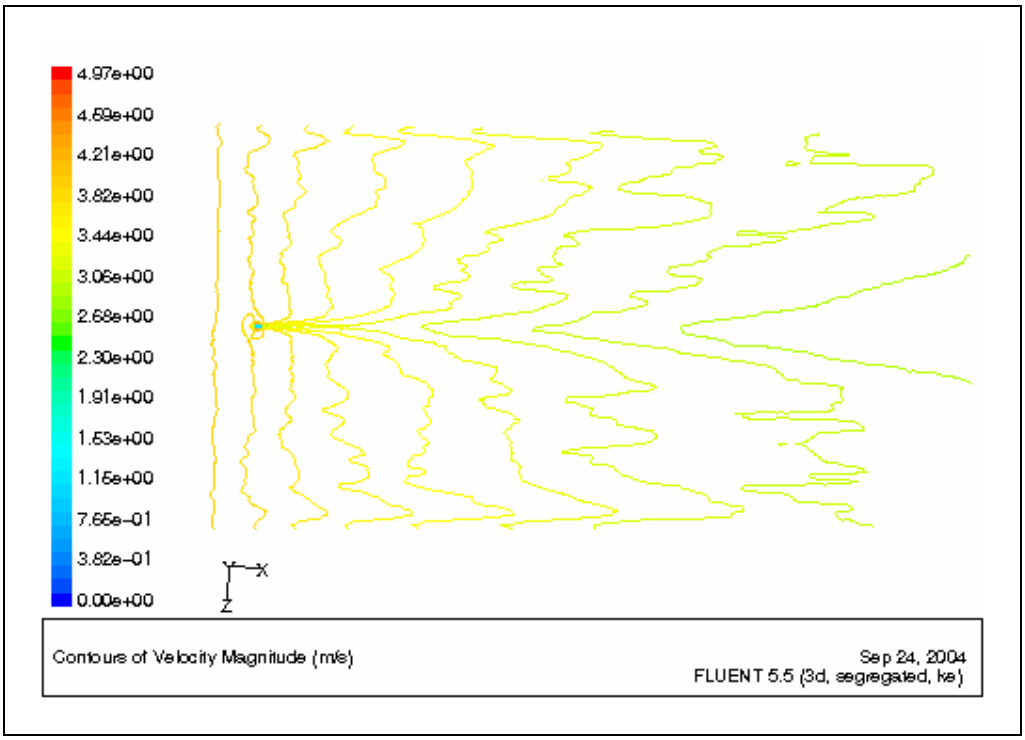

Figure 5.27 Plan view of Turbine 2 in channel showing deformation of the surface velocity

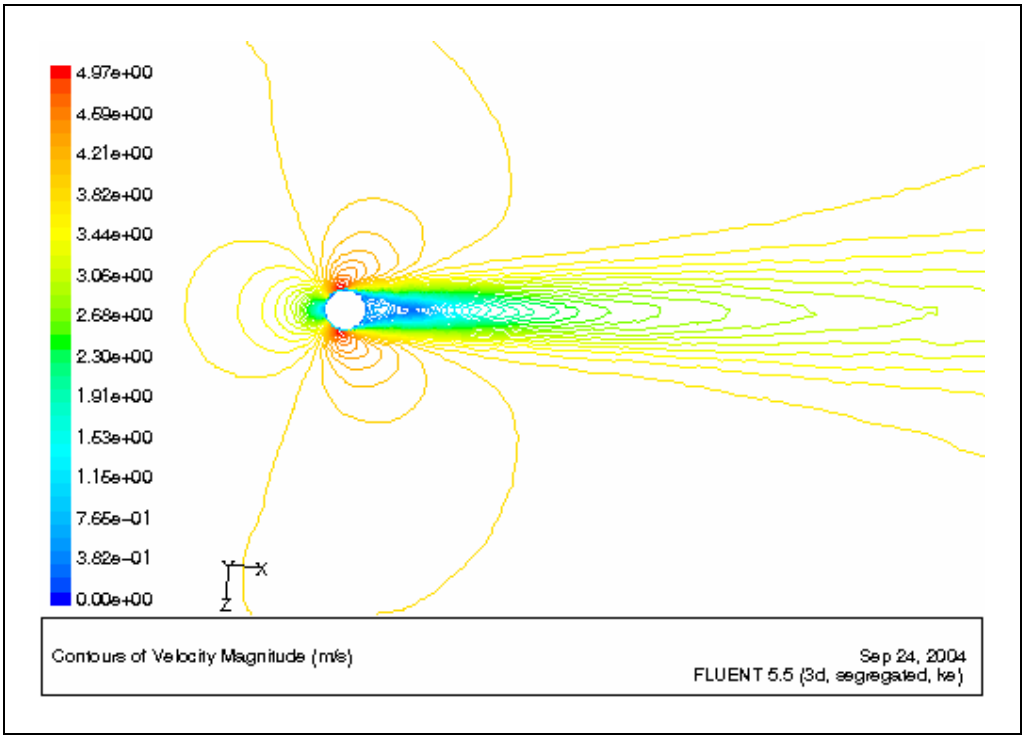

Figure 5.28 Close up plan view of Turbine 2 showing formation of vortices and wake

5.2.3.2 Front View of Turbine 2 in Channel

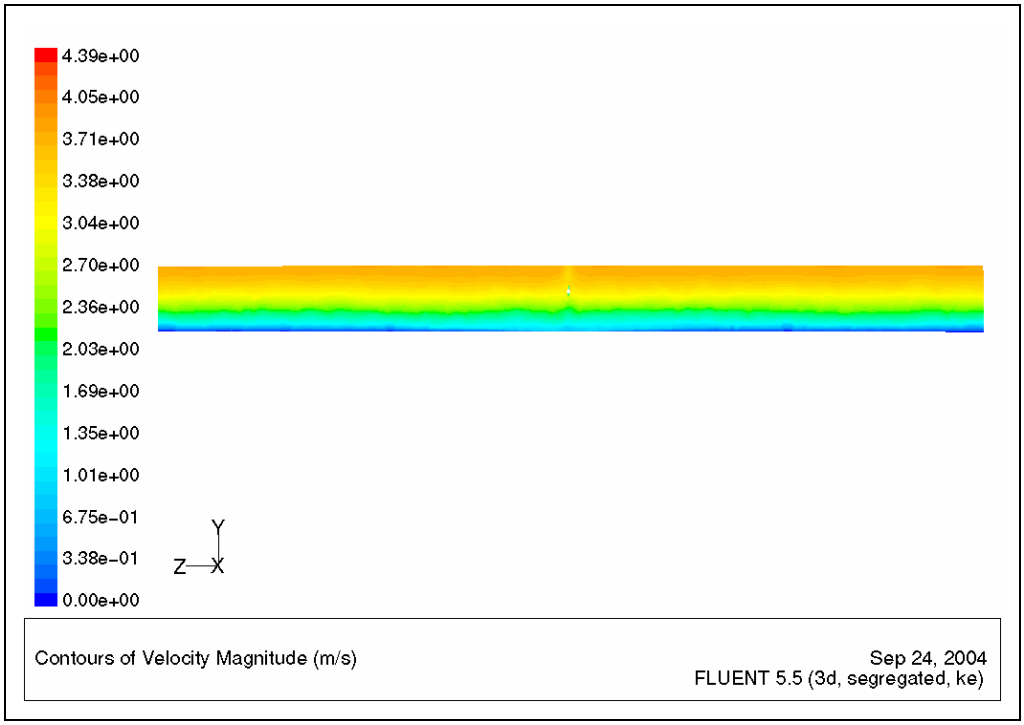

Figure 5.29 Front view of Turbine 2 in channel showing wavy velocity beneath rotor blades

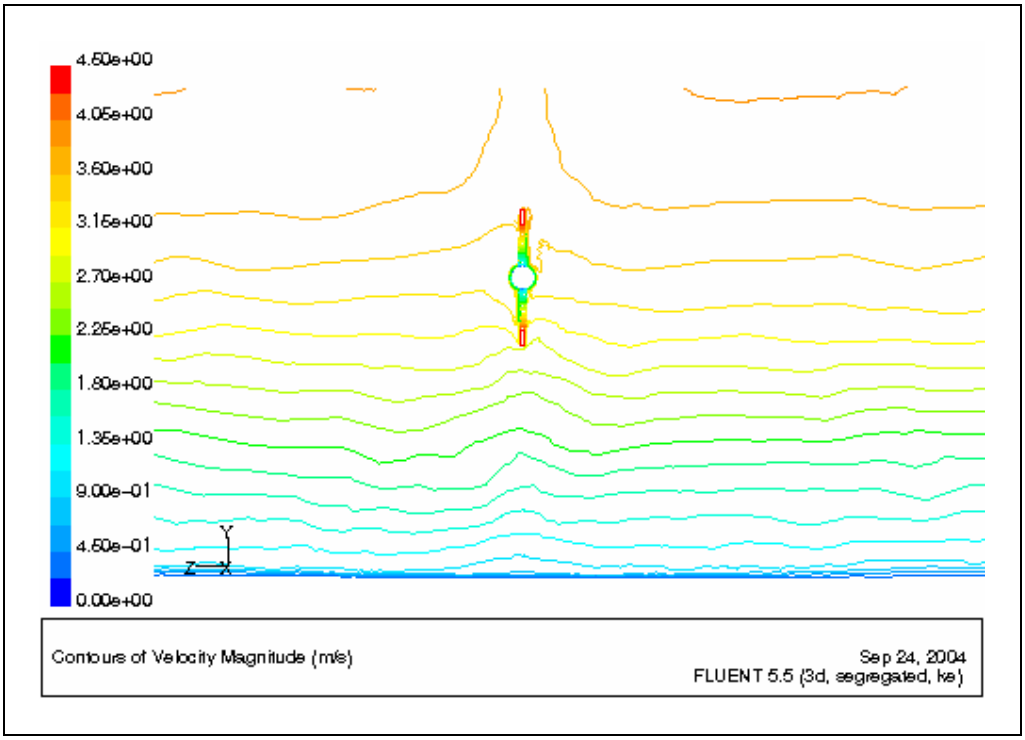

Figure 5. 30 Close up front view of Turbine 2 showing upwelling beneath rotor blades

5.2.3.3 Side View of Turbine 2 in Channel

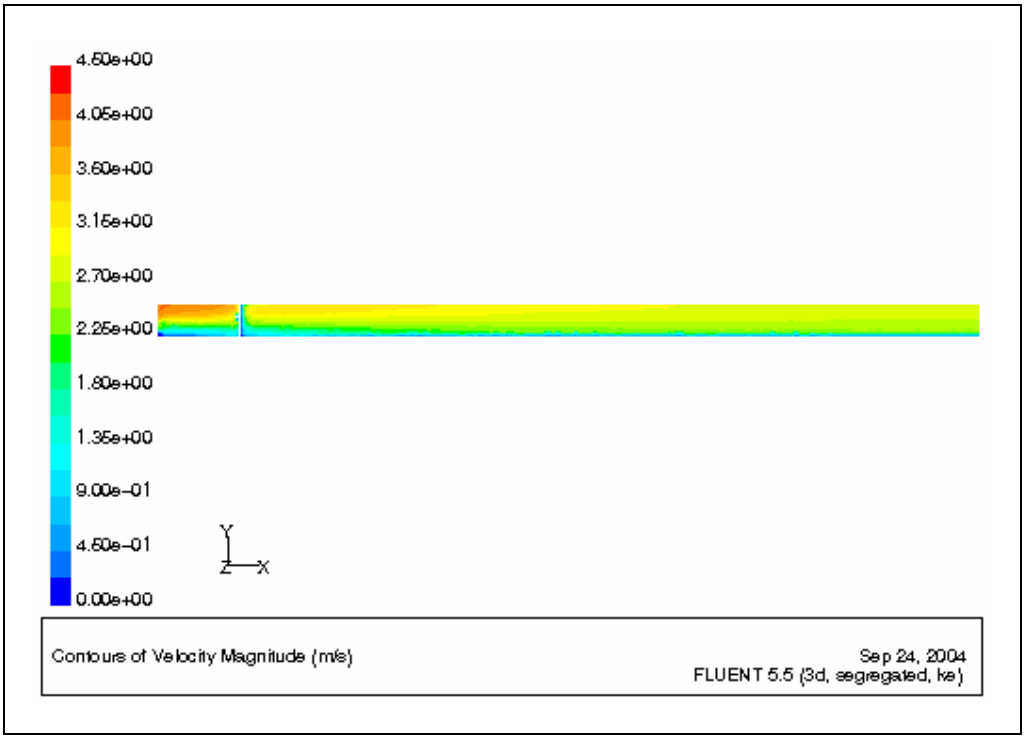

Figure 5. 31 Side view of Turbine 2 showing the velocity distribution across the length of the channel

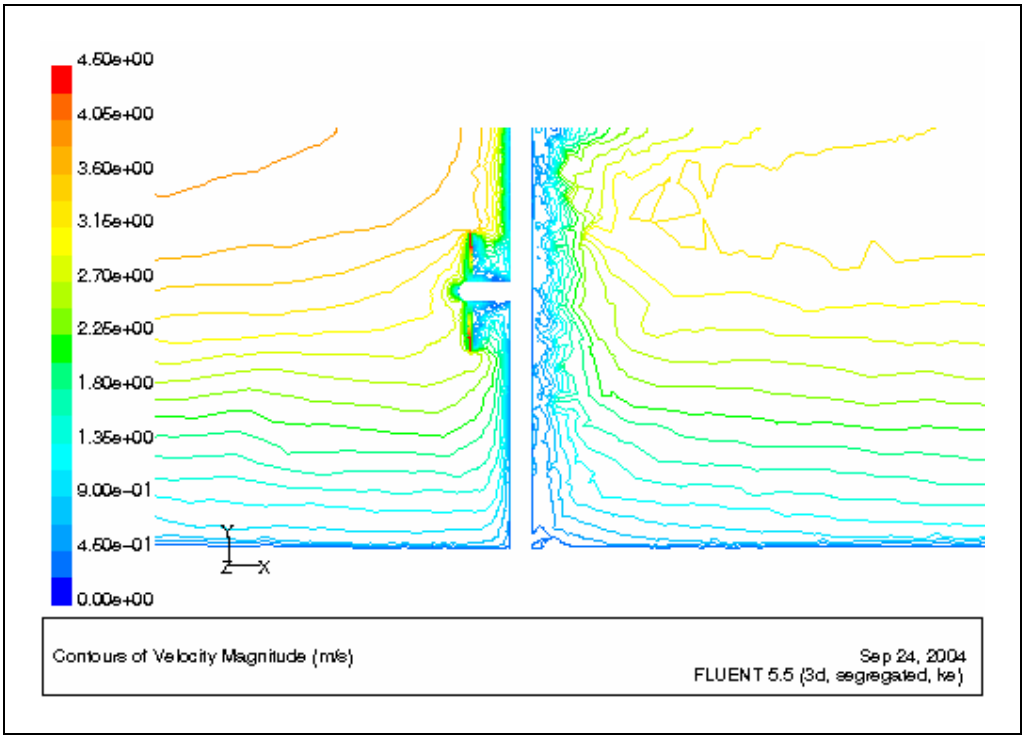

Figure 5.32 Close up view of Turbine 2 showing increased turbulence around the structure

5.2.4 Comparison of Results

The results generated for this velocity profile is not very different for that generated for a surface velocity of 3 m/s. However it is worth noting that the wakes behind both turbines are narrower because of the higher current speed. In addition a higher sea bed current is evident resulting in a broader wavy pattern below the rotor blades. This broader upwelling beneath the rotor blades leads to a less distortion of the velocity profile across the front of the turbine.

5.3 Results for a Surface Current Speed of 1 m/s

5.3.1 Resource

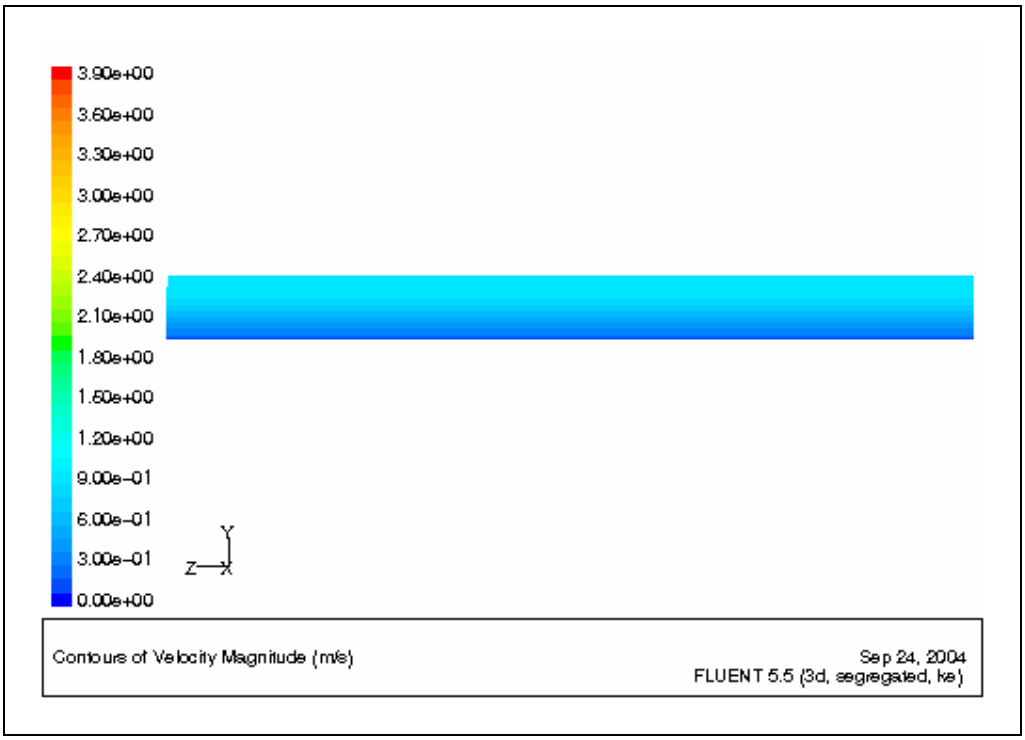

Figure 5.33 Front view of the vertical velocity distribution in the channel

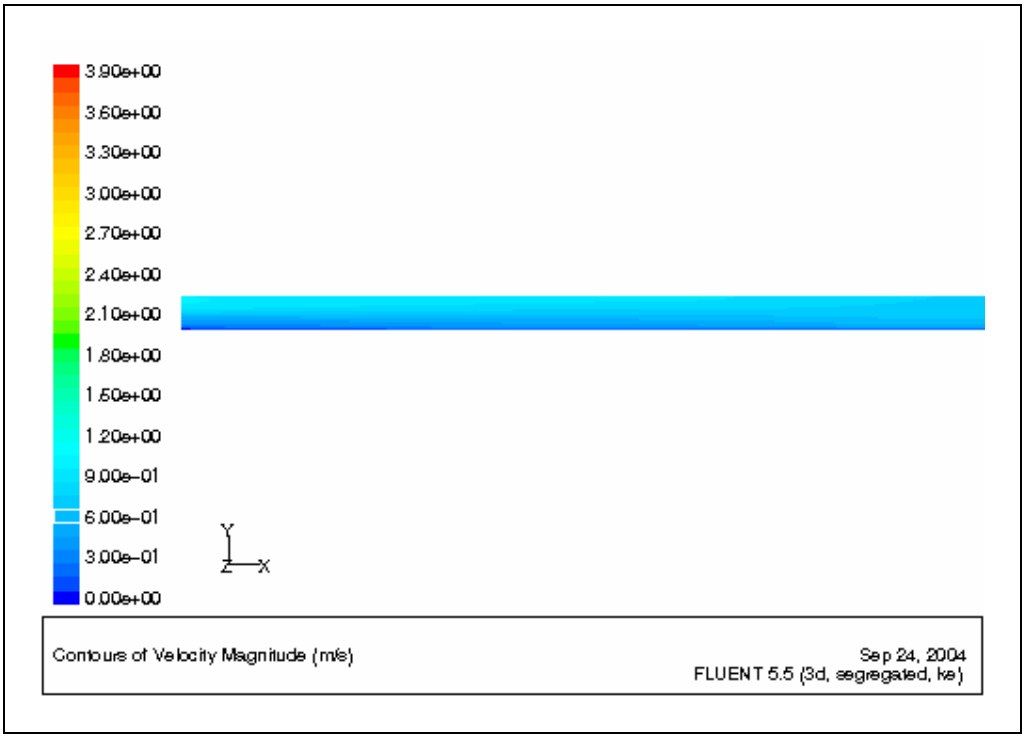

Figure 5.34 Side view of the vertical velocity distribution in the channel from inlet to outlet

5.3.2 Turbine 1

5.3.2.1 Plan View of Turbine 1 in Channel

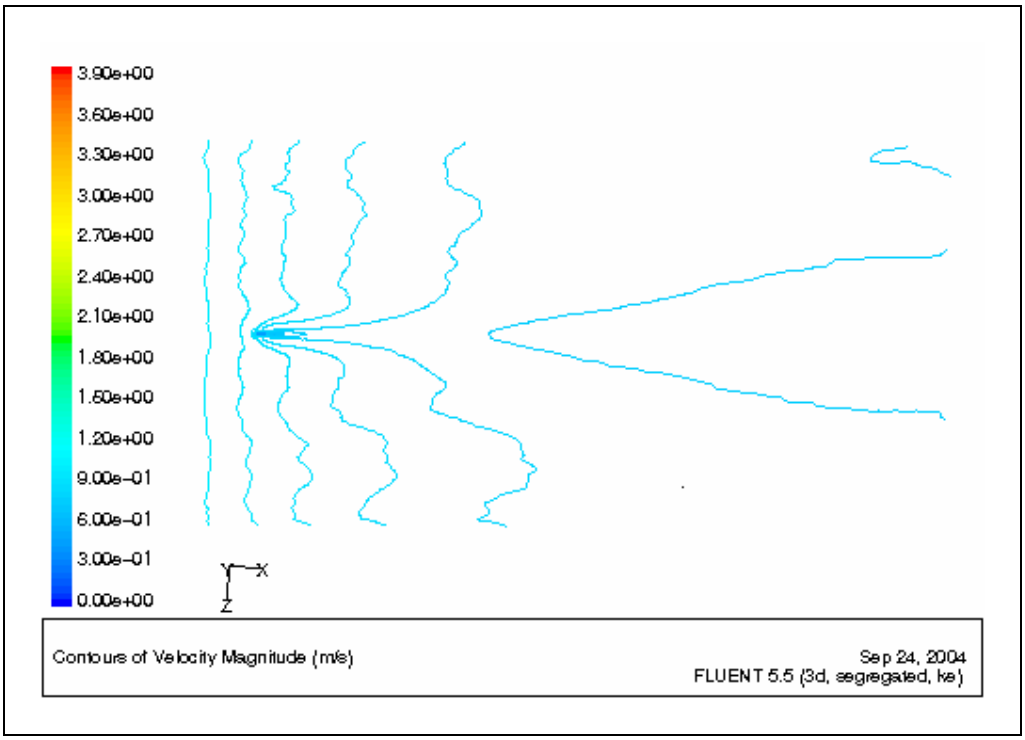

Figure 5.35 Plan view of Turbine 1 in channel showing deformation of the surface velocity

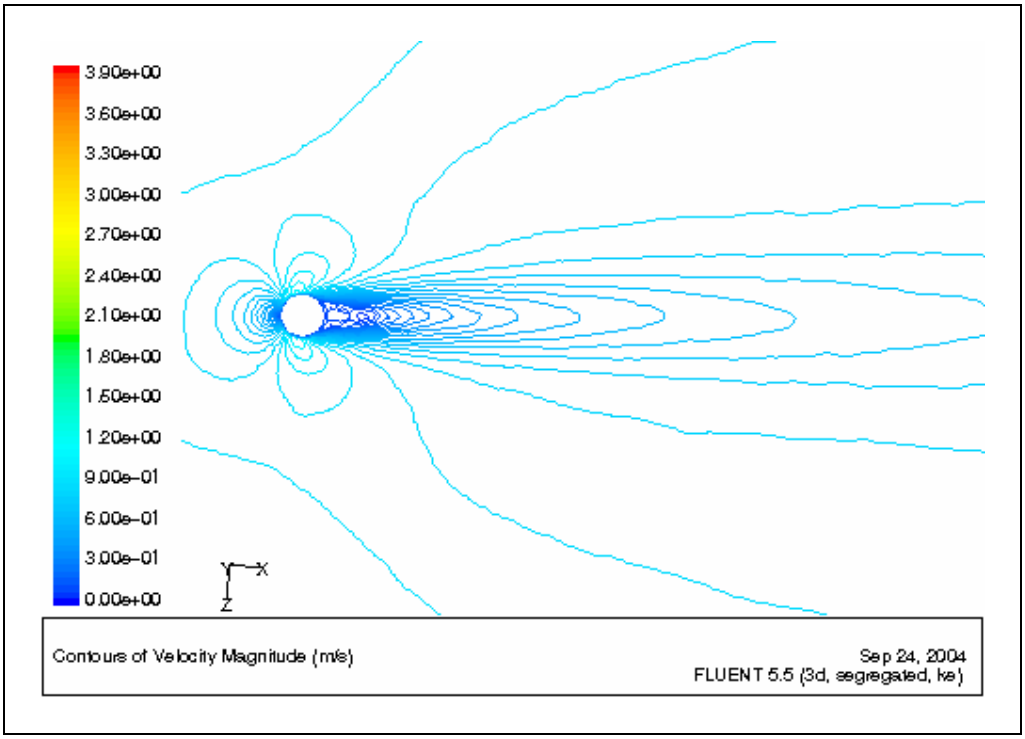

Figure 5.36 Close up plan view of Turbine 1 showing formation of vortices and wake

5.3.2.2 Front View of Turbine 1 in Channel

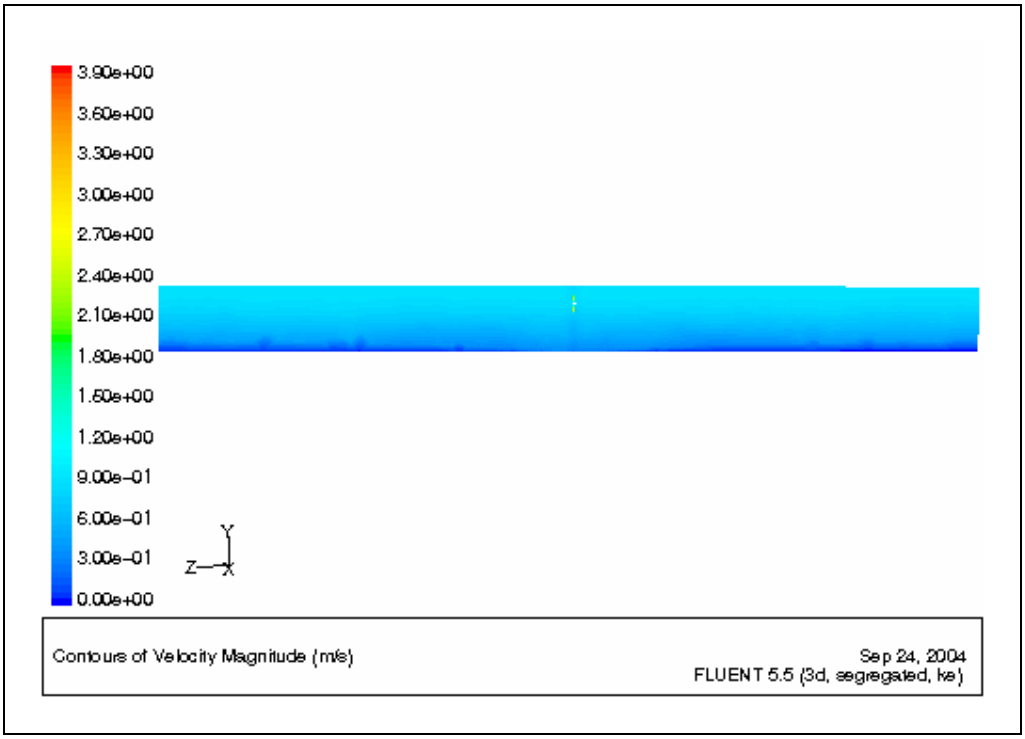

Figure 5. 37 Front view of Turbine 1 in channel showing wavy velocity beneath rotor blades

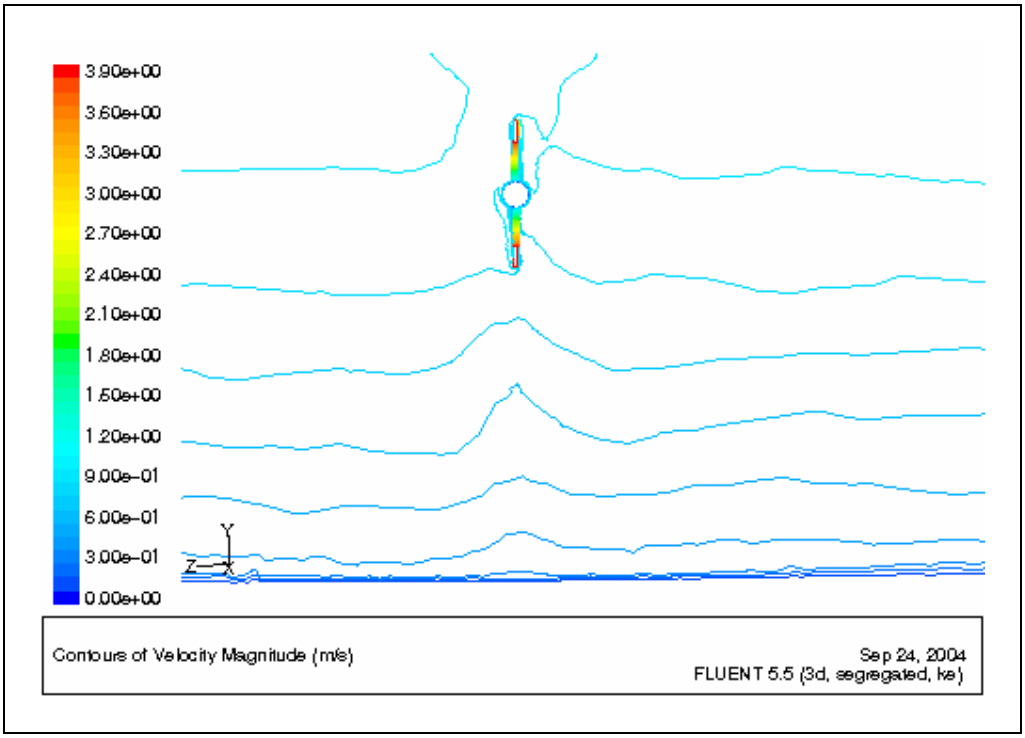

Figure 5.38 Close up front view of Turbine1 showing upwelling beneath rotor blades

5.3.2.3 Side View of Turbine 1 in Channel

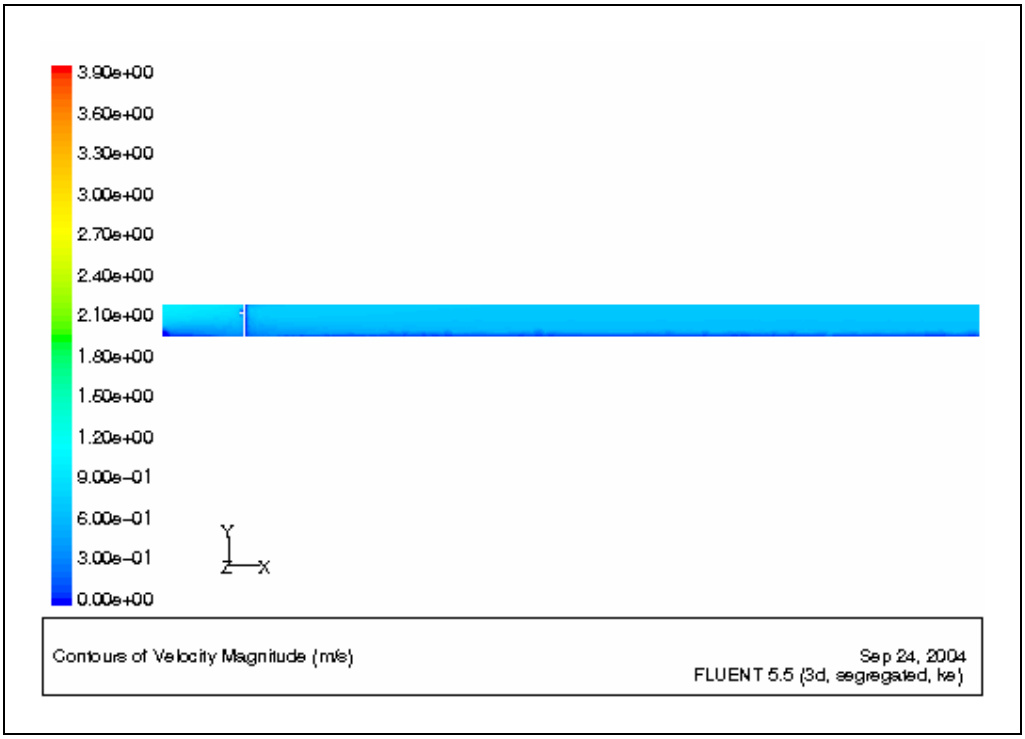

Figure 5.39 Side view of Turbine 1 showing the velocity distribution across the length of the channel

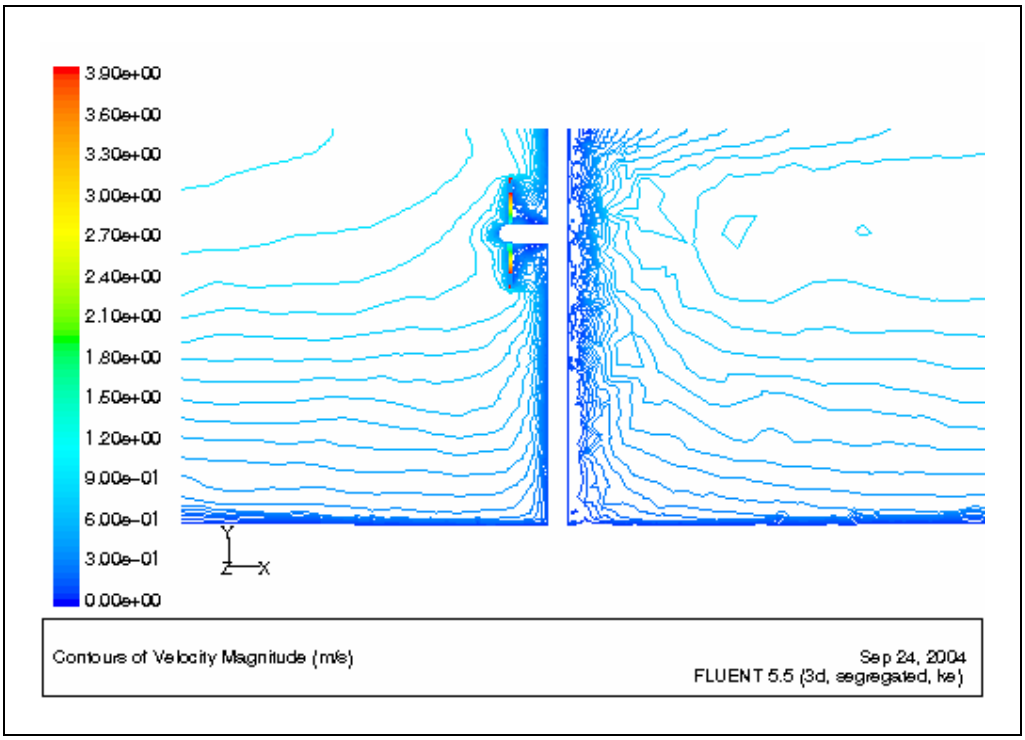

Figure 5.40 Close up view of Turbine 1 showing increased turbulence around the structure

5.3.3 Turbine 2

5.3.3.1 Plan View of Turbine 2 in Channel

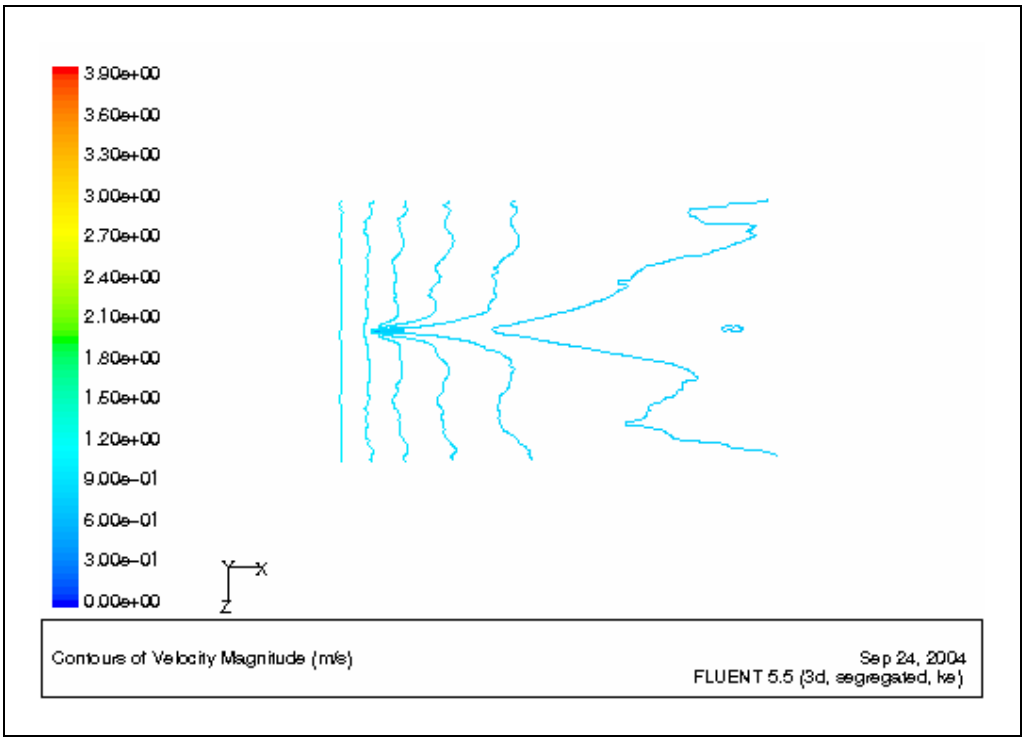

Figure 5.41 Plan view of Turbine 2 in channel showing deformation of the surface velocity

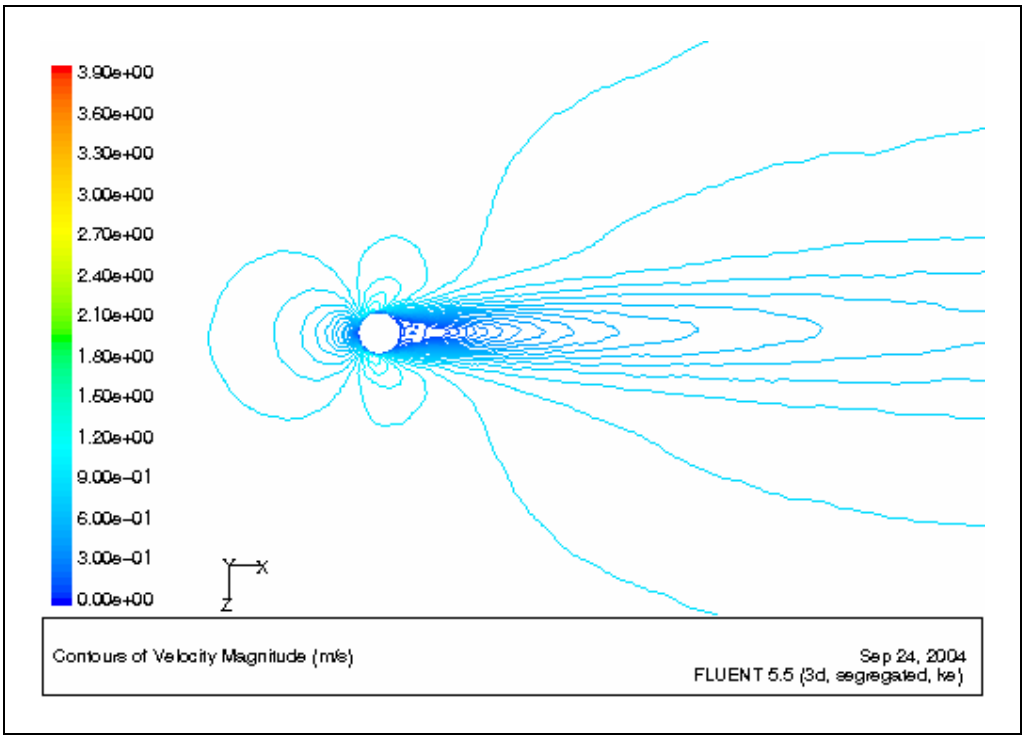

Figure 5.42 Close up plan view of Turbine 2 showing formation of vortices and wake

5.3.3.2 Front View of Turbine 2 in Channel

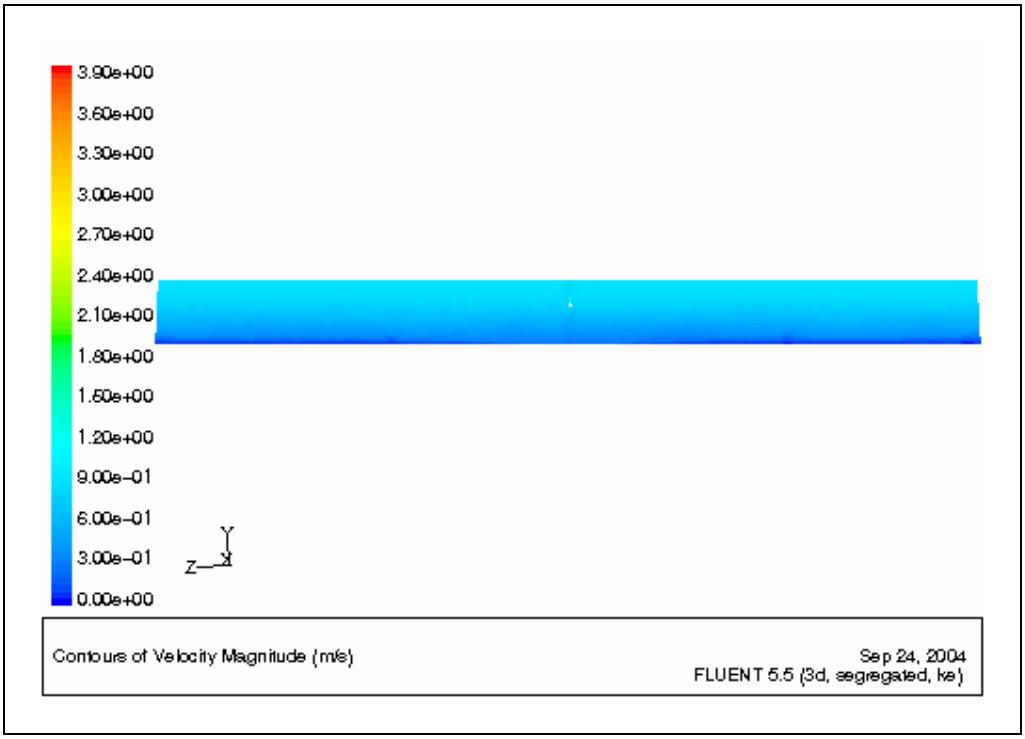

Figure 5.43 Front view of Turbine 2 in channel showing wavy velocity beneath rotor blades

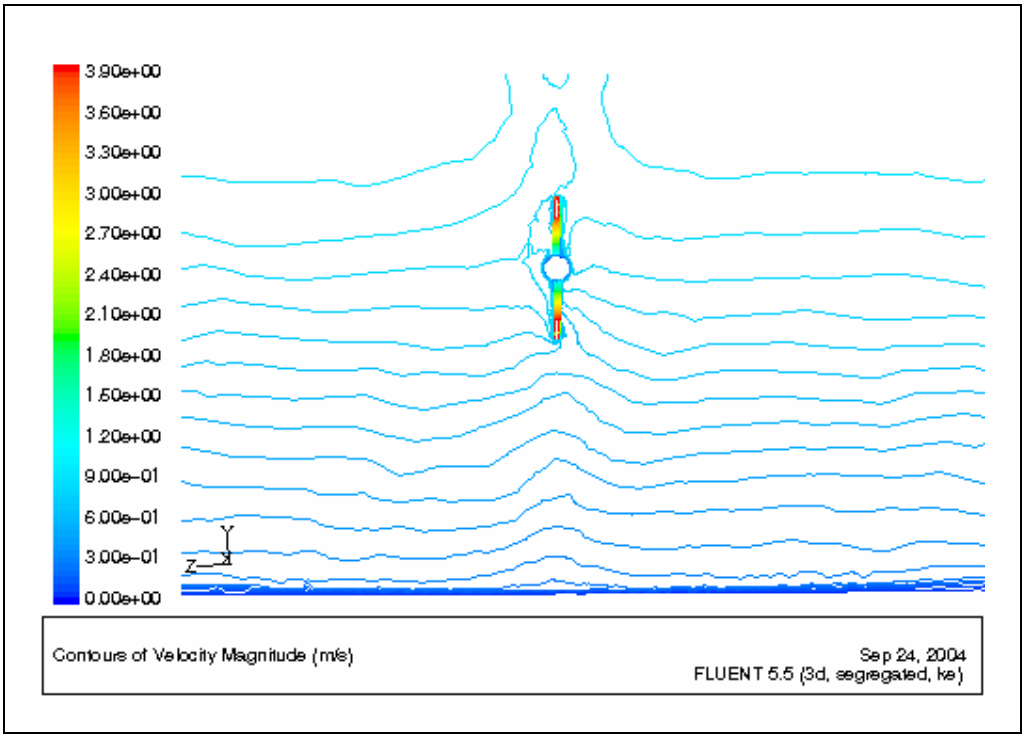

Figure 5.44 Close up front view of Turbine 2 showing upwelling beneath rotor blades

5.3.3.3 Side View of Turbine 2 in Channel

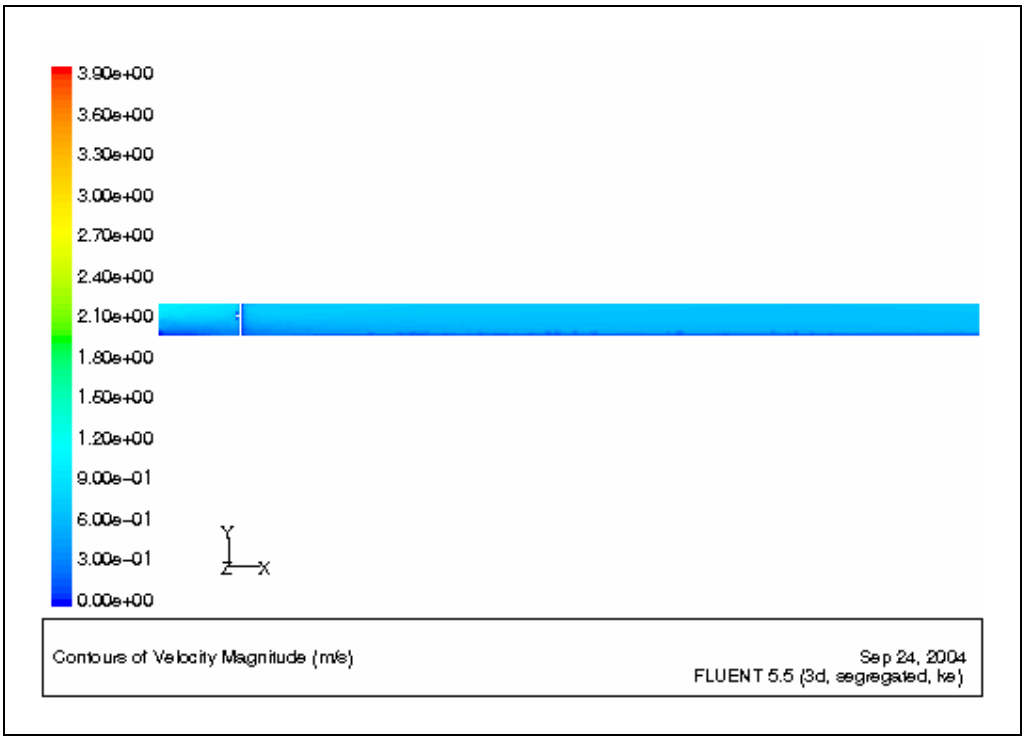

Figure 5.45 Side view of Turbine 2 showing the velocity distribution across the length of the channel

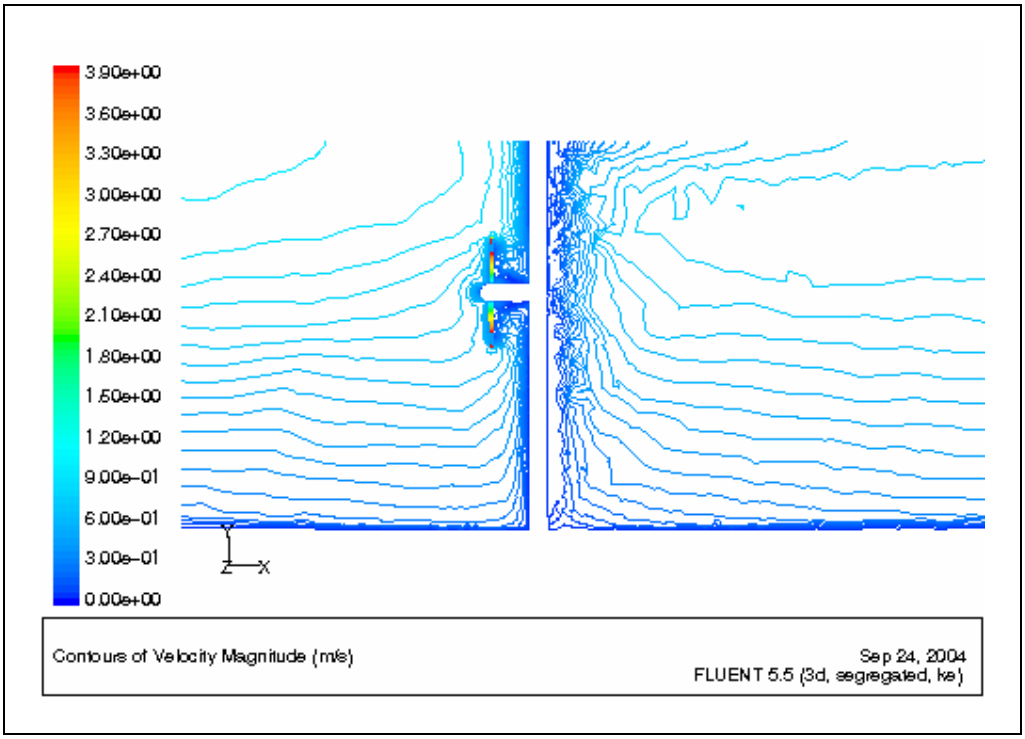

Figure 5.46 Close up view of Turbine 2 showing increased turbulence around the structure

5.3.4 Comparison of Results

In this case the wake behind the turbines is broader as a result of the low speed of the currents. The upwelling of the flow beneath the rotor blades is not as profound as that for the higher velocities. In addition the distortion in the velocity profile across the rotor blades and along the channel from inlet to outlet is lower compared to the higher velocities.

CHAPTER SIX – CONCLUSION AND FUTURE WORK

6.1 Conclusion

The flow in the channel with and without energy extraction has been analysed. For the case of energy extraction two turbine models, with different depths of deployment of rotor blades, were analysed. The flow was presented in three views; plan, front and side views comparing them to the no-energy extraction case. Further more, different velocity regimes were applied to determine their influence on the nature of the flow in the channel. Within the limits of simplifying assumptions and the accuracy of the CFD programme the following conclusions are made.

6.1.1 Depth of Deployment

The nature of the vertical velocity profile of flow in high marine current sites indicates that to maximise energy generation by use of turbines the rotor blades should be as close as possible to the free water surface. The analyses have shown that locating the blades close to the free surface leads to two main effects:

- Distortion of the velocity profile past the rotor blades and support structure leading to a reduction in the surface velocities and an increase in the sea bed velocities.

- Increased upwelling of the flow directly below the rotor blades.

The first effect is likely to affect adjacent aquatic environments. This is because reduction in surface velocities will lead to increased stratification at near by estuaries. The second effect will lead to scouring of the sea bed which will intend affect sediment transport and also increase turbidity as well as threaten the strength of the support structure. Locating the rotor blades further below the free surface (10 m for 40 m depth) will minimise these effects.

6.1.2 Changing Current Speed

The study has shown that the nature of the flow past the turbines is not very different for different current speeds, however some observations are worth mentioning:

- Increased speeds lead to formation of a narrower wake and quicker recovery of the wake.

- Increased speeds leads to less upwelling of the flow below the rotor blades.

This means that the process of energy extraction is likely to modify the underlying hydraulic nature of the marine environment however this is will be minimal in high speed areas.

6.2 Recommendation

The observations made in this study should be taken into consideration in planning marine current farms. Issues like depth of deployment have a role to play in optimising the output of the farms while minimising the effects on the marine environment. The severity of the environmental impacts will also vary according to the changing current speeds and this needs to be taken into consideration when conducting environmental impact assessment studies. These observations however need to be substantiated by comparing them to that of real life developments.

Secondly potential developers must assess the nature of the marine environment to be exploited in its entirety. Variation of temperature and salinity, sediment transport characteristics, and production, distribution and diversity of species of the specific site must also be determined before and after exploitation to assess the impacts on them.

REFERENCE

1. Alber, M. (2002), A conceptual model of estuarine freshwater inflow management, Estuaries 25 (6B), 1246-1261

2. Bahaj, A.S. and Myers, L.E, *Fundamentals applicable to the utilisation of marine current turbines for energy production*, Renewable Energy 28 (2003) pp 2205-2211

3. Brian, K, *Development in ducted water current turbines*, School of Engineering, Griffith University, Australia

4. Bryden I, *Energy extraction from tidal flows*, Hydraulic aspects of renewable energy, 16th Annual Seminar, Scottish Hydraulics Study Group, Glasgow, March 2004

5. Bryden, I.G., Naik, S, Fraenkel, P and Bullen, C.R, *Matching tidal current plants to local flow conditions*, Energy Vol 23 No. 9 pp 699-709

6. Chanson, H, *The Hydraulics of open channels flow: An introduction*, 2nd Edition (2004), Elsevier Butterworth-Heinemann, Oxford, chpt 1

7. Chow, Ven Te, *Open channel hydraulics*, 1959, McGraw Hill,

8. Duarte, C M (1995), Submerged aquatic vegetation in relation to different nutrient regimes, Ophelia 41, 87-112

9. Douglas, J F, Gasiorek, J M and Swafield, J A, *Fluid Mechanics*, 4th Edition 2001, Prentice Hall, London, New York etc

10. Fraenkel P L, *Marine Current Turbines: An emerging technology*, Hydraulic aspects of renewable energy, 16th Annual Seminar, Scottish Hydraulics Study Group, Glasgow, March 2004

11. French, R H, *Open channel hydraulics* 1994, McGraw Hill Inc, New York, Singapore etc, chpt 1- 5, 10

12. Hoegh-Guldberg, O. (1999), Climate *change, coral bleaching and the future of the world's coral reefs*, Marine and Freshwater Research 50, 839-866

13. Jennings, J S, *Future sustainable energy supply*, Energy World, February 1996 pp 8-10

14. Lange, B, Waldl, H P, Barthelmie, R, Guerrero, A G and Hienemann D, *Modelling of offshore wind turbine wakes with the wind farm program FLaP*, Science Direct

15. Mathieu, J and Scott, J, *An introduction to turbulent flow*, Cambridge University Press (2000), Cambridge

16. Pontes, M. T. and Falcao, A, *Ocean Enegies: Resources and Utilisation*, 18th World Energy Confernce, Argentina (2001), DS6 Research and development and Information Technology, Paper 01-06-02

17. Singer, S, *PowerSwitch! Climate change and the power sector*, Renewable Energy World July-August 2003 vol 6, no 4 2003, James and James (Science Publishers) Ltd. London

18. Small A D, *Tidal stream power from the Gulf of Corryvreckan: A Preliminary Report,* Glasgow College of Nautical Studies

19. Souders, D T and Hirt, C W, *Modelling roughness effects in open channel flows*, Flow Science Inc.

20. Vanoni, V. A., Brooks, N.H., Kennedy J. F., *Sediment transport and channel stability,* Agricultural Research Science 1961

21. Whitefield, A K (1994), *Abundance of larval and juvenile marine fishes in the lower reaches of three southern African estuaries with differing freshwater input*, Marine Ecology Progress Series 105, 257-267.

22. Isaacs, J.D. and Seymour R.J. *The oceans as a power resource*, Int. Journal of environmental Studies. 1973.

23. *A scoping study for an environmental impact field programme in tidal energy,* (2002) Centre for Environmental Engineering and Sustainable Energy, RGU, Published by ETSU for DTI (T/04/00213/REP)

24. *The Exploitation of tidal marine currents*, Summary Report, EU-JOULE II (JOU2-CT94-0355), Authored by Tecnomare SpA and IT Power Ltd. in partnership with Ponti di Archimede nello Stretto di Messina SpA, Tecnomare UK Ltd and University of Patras

25. *Tidal stream energy review*, Prepared by Engineering & Power Development Consultants Ltd., Binnie & Partners, Sir Robert McAlpine & Sons Ltd and IT Power Ltd. for ETSU, UK Dept. of Energy, Report No. ETSU T/05/00155/REP, Crown Copyright 1993

26. *Green Energy Study for British Columbia Phase 2: Mainland, Tidal current energy*, Prepared by Triton Consultants Ltd. For BC Hydro, Engineering, 2002

27. Vermeer, L. J., Sorensen, J. N. and Crespo, A., *Wind turbine wake aerodynamics*, Progress in Aerospace Sciences 39 (2003) 467-510, Pergamon (Available online at http://www.sciencedirect.com)

28. ANZECC/ARMCANZ (Oct 2000), *Australian guidelines for water quality monitoring and reporting* (http://www.ea.gov.au/water/quality/nwqms)

29. Marine Current Turbine Limited (http://ww.marineturbines.com)

30. Engineering Business Limited (http://www.engb.com)

31. Blue Energy (www.bluenergy.com)

32. SMD Hydrovision (www.smdhydrovision.com)

33. Hammerfest Strøm AS (www.e-tidevannsenergi.com

BIBLIOGRAPHY

1. Beyer, H G, Lange, B and Waldl, H P, *Modelling tools for wind farm upgrading*, Section Energy and Semiconductor Research, Carl von Ossietzky Universitat Oldenburg.

2. Katul, G, *A mixing layer theory for flow resistance in shallow streams*, Water Resources Research, Vol 38 No 11, 1250, 2002

3. Massey, B, *Fluid Mechanics*, 7th Edition 1998, Stanley Thornes (Publishers) Ltd. London

4. *Training manual on design and development of management plans for marine protected areas (2003),* Coastal Resoureces Multi-conplex Building

5. US Environmental Protection Agency (http://ww.epa.gov)

6. Practical Ocean Energy Management Systems, Inc (www.poemsinc.org)